



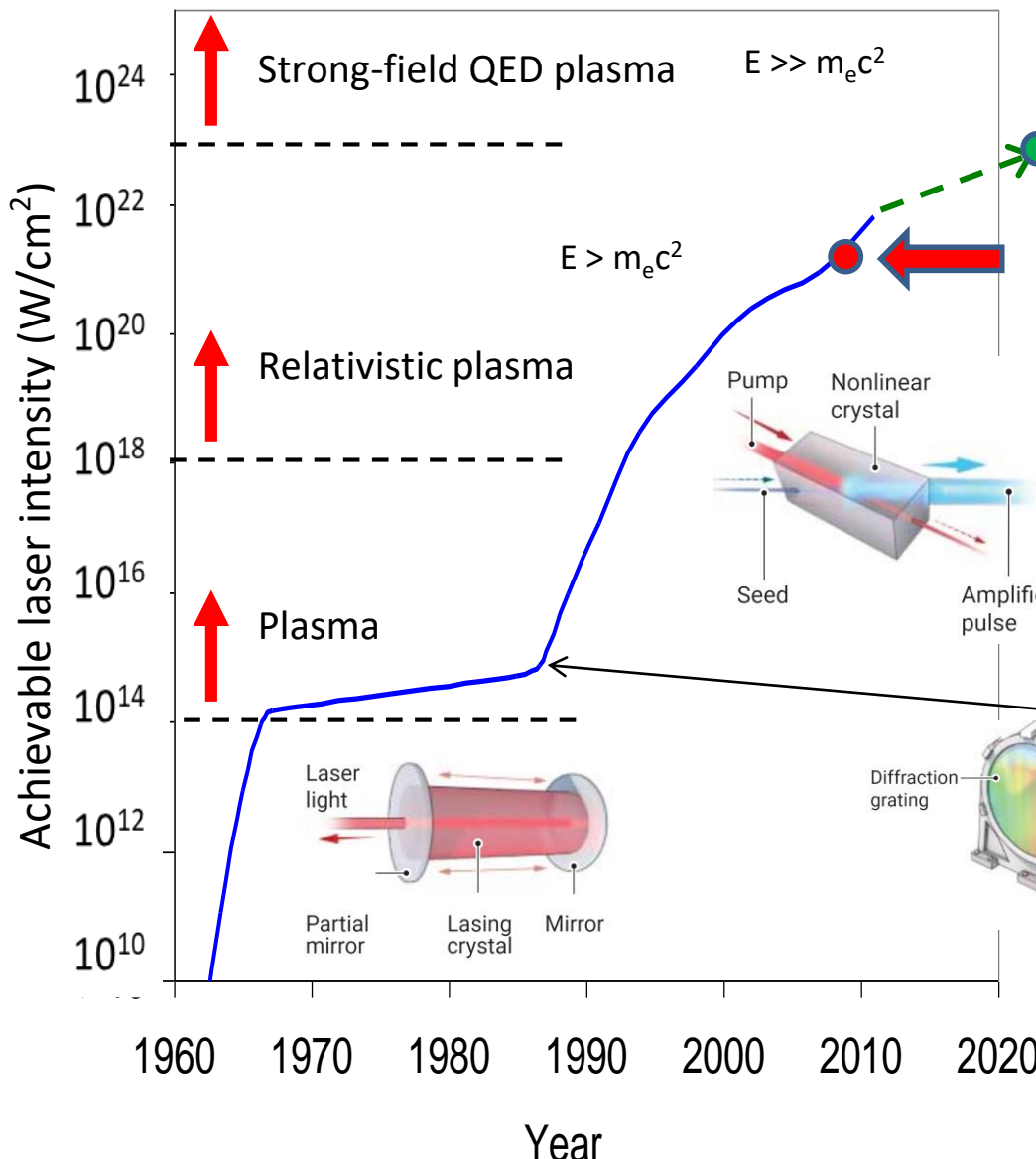
Relativistic optics and strong field QED phenomena in near critical density plasma

Paul McKenna
University of Strathclyde, Scotland, UK

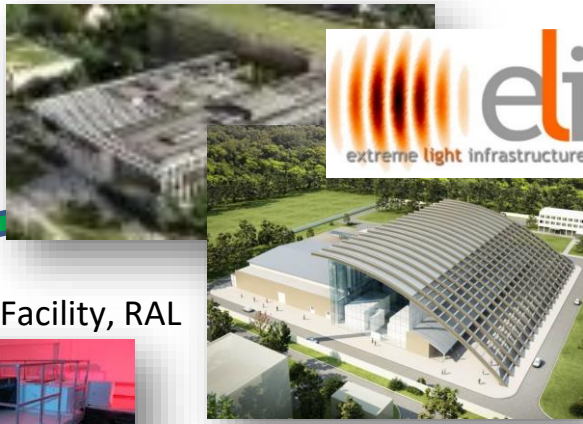
Lecture overview:

1. Introduction to high power lasers
2. Near critical density (NCD) plasma generation
3. Relativistic optics effects in NCD plasma
4. Relativistic plasma aperture
5. Electron and ion acceleration in NCD plasma
6. Strong-field QED phenomena
7. [Experimental considerations and methodology – if time permits]

Achievable laser intensity...



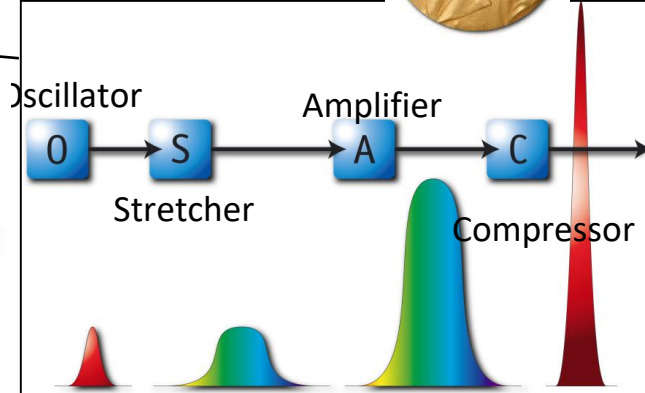
Extreme Light Infrastructure (ELI)



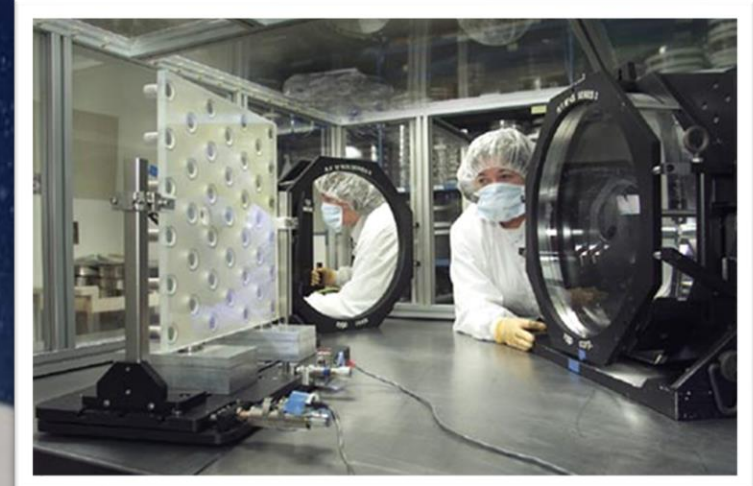
Chirped pulse amplification (CPA)



Nobel
2018



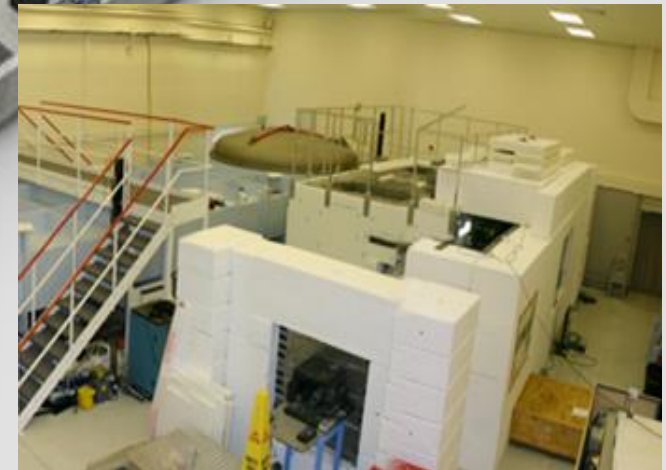
Laser systems: High energy drivers, e.g. NIF



National Ignition Facility – 192 laser beams delivering 2 MJ in UV ($0.35\text{ }\mu\text{m}$)
0.2 petawatts (13x global energy consumption rate); 10 ns pulses

Laser systems: High intensity, PW-class

e.g. Vulcan at the Rutherford Appleton Laboratory



Power	1 PW
Energy	>500 J
Wavelength	1.05 μm
Pulse duration	0.5 ps (+ 6 x 5ns beams)
Intensity	~ 10^{21} Wcm ⁻²
Repetition	8 to 10 shots / day

Laser systems: Ultra-short pulse, PW-class

Gemini at the Rutherford Appleton Laboratory



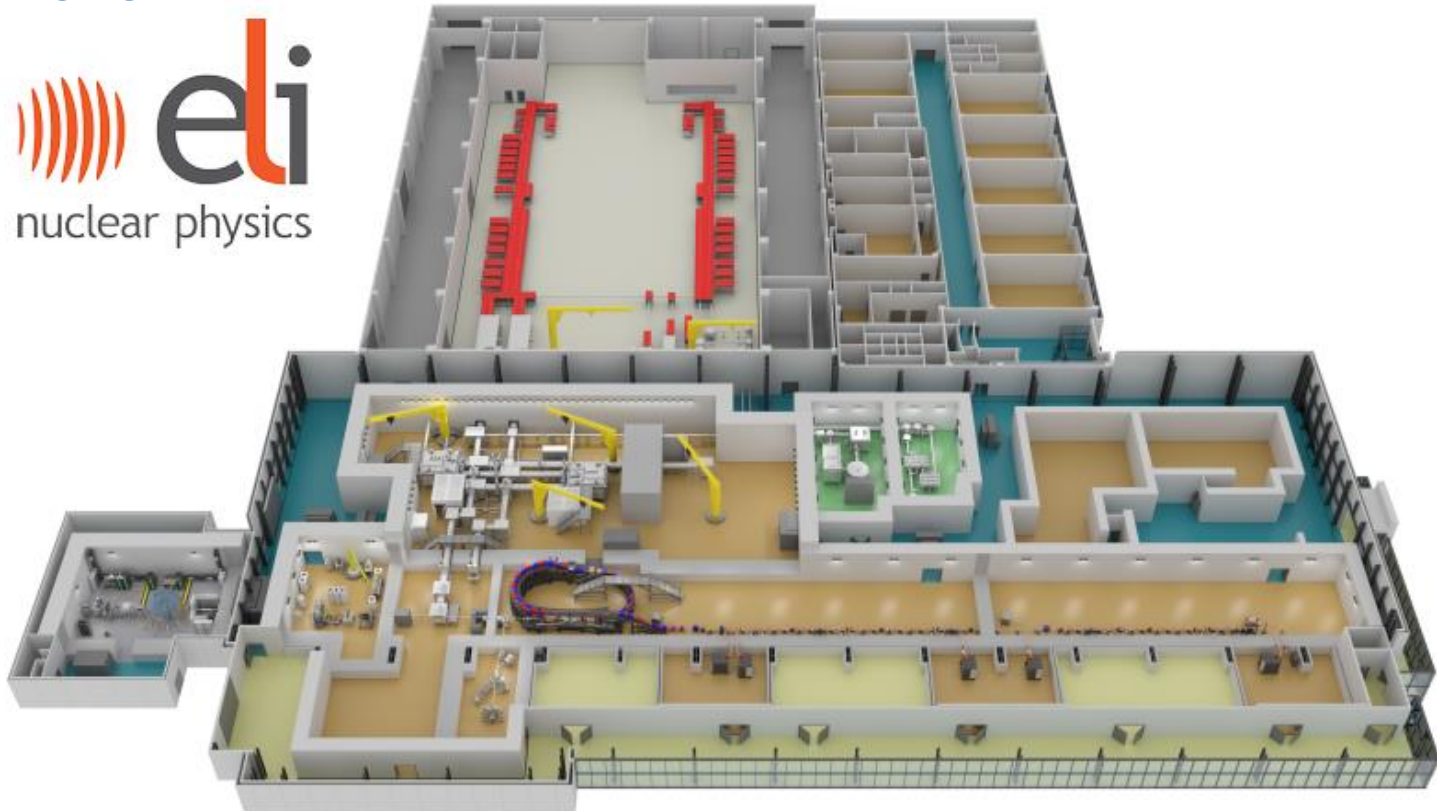
Power	0.5 PW in each beam (x2)
Energy	>6 J (on target)
Wavelength	0.8 μm
Pulse duration	35 fs
Intensity	$\sim 10^{21} \text{ Wcm}^{-2}$
Repetition	3 shots / minute

SCAPA at Strathclyde



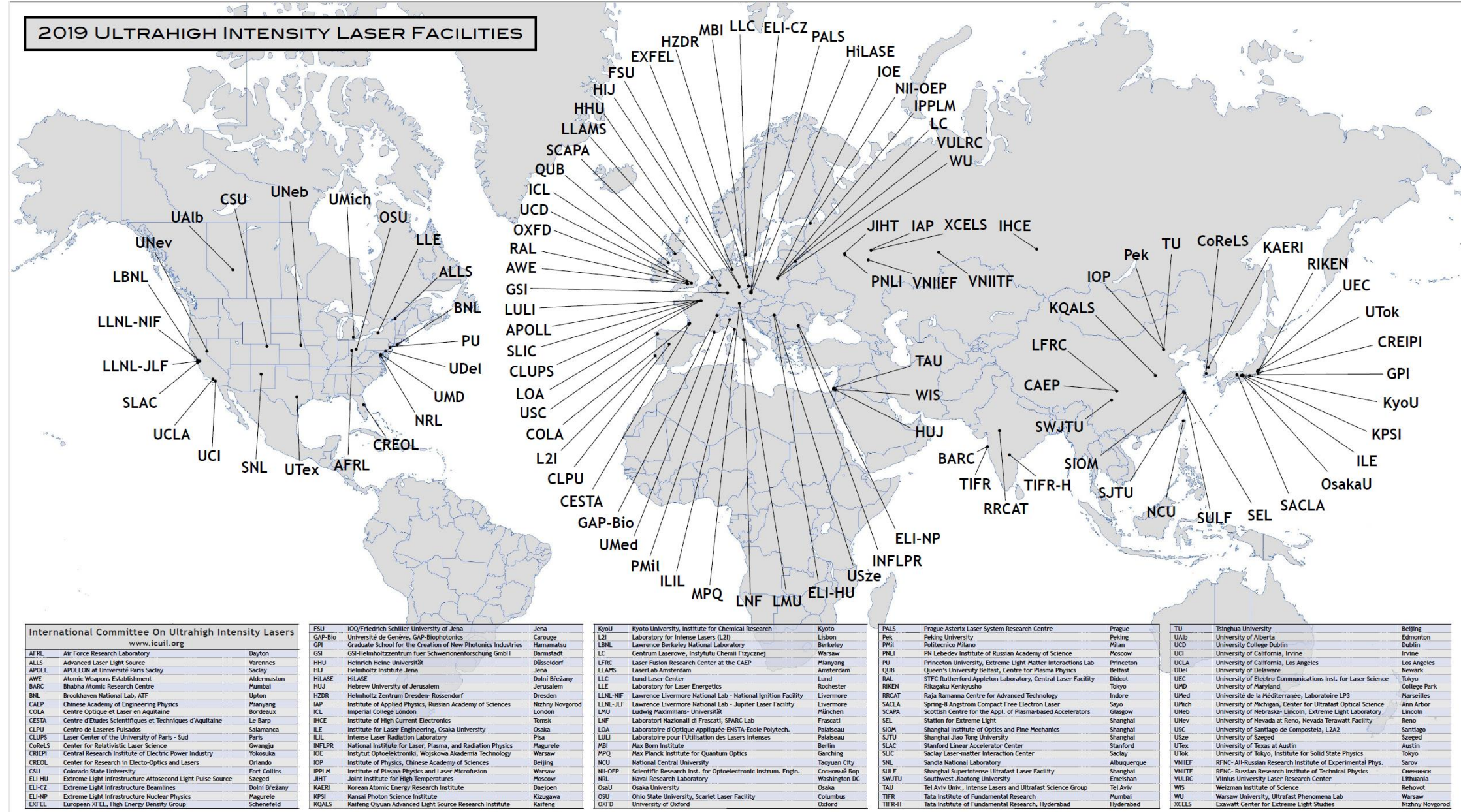
Power	0.35 PW
Energy	>4 J (on target)
Wavelength	0.8 μm
Pulse duration	25 fs
Intensity	$\sim 10^{20} \text{ Wcm}^{-2}$
Repetition	few Hz

Laser systems: Multi-PW-class, High intensity at high repetition rate



Power	2 x 10 PW @ 1 shot/minute 1 x 1 PW @ 1 Hz
Energy	>250 J (on target)
Wavelength	0.8 μm
Pulse duration	22 fs
Intensity	10^{21} - 10^{23} Wcm ⁻²

High power laser facilities worldwide



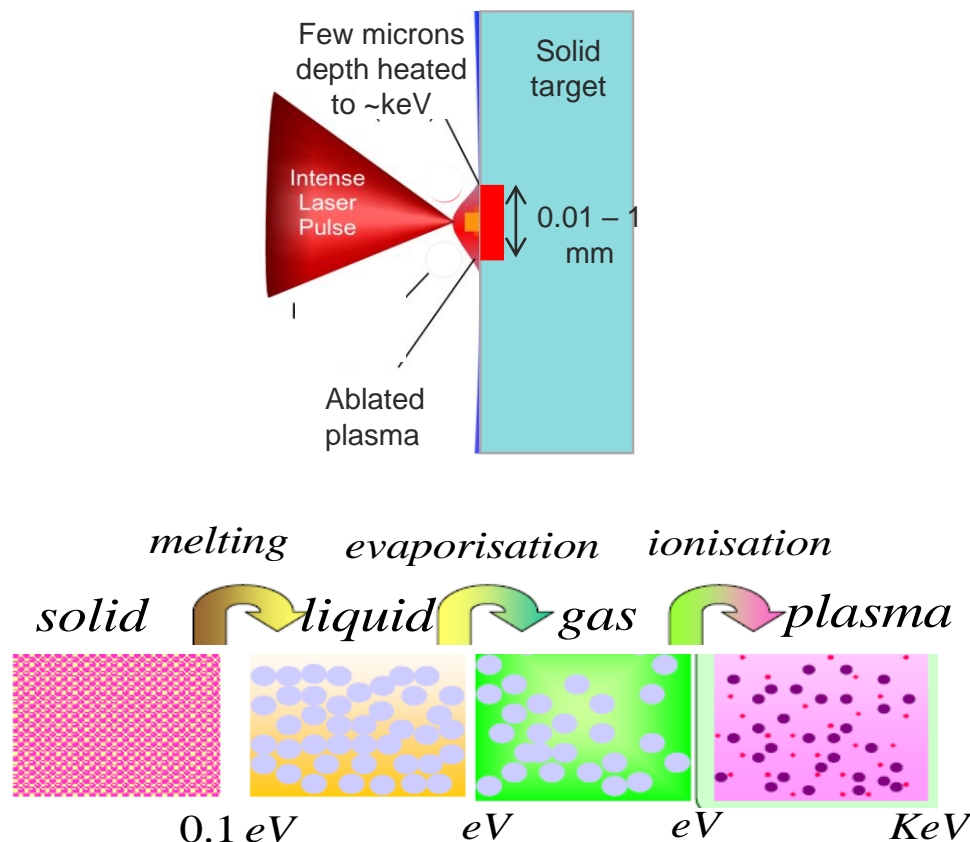
Lecture overview:

1. Introduction to high power lasers
2. **Near critical density (NCD) plasma generation**
3. Relativistic optics effects in NCD plasma
4. Relativistic plasma aperture
5. Electron and ion acceleration in NCD plasma
6. Strong-field QED phenomena
7. [Experimental considerations and methodology – if time permits]

Ionisation – Basic considerations

Let's consider some approximate values:

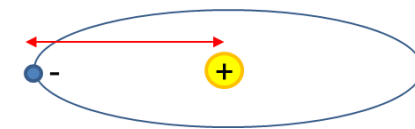
- High power laser → 1 kJ energy
- Enough to ionise 6×10^{20} atoms (10eV into each) – 1mm cube of solid density
- Plasma is typically many keV and highly ionised



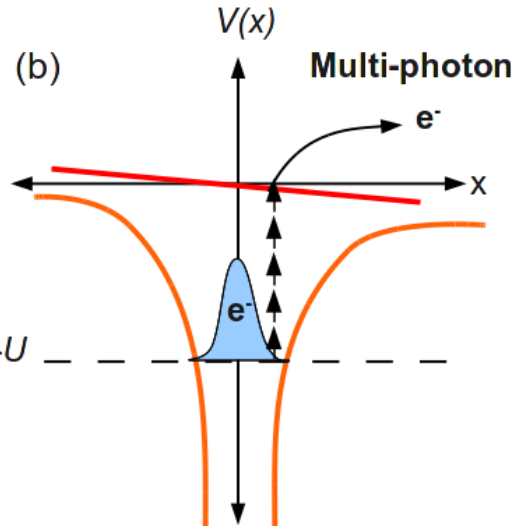
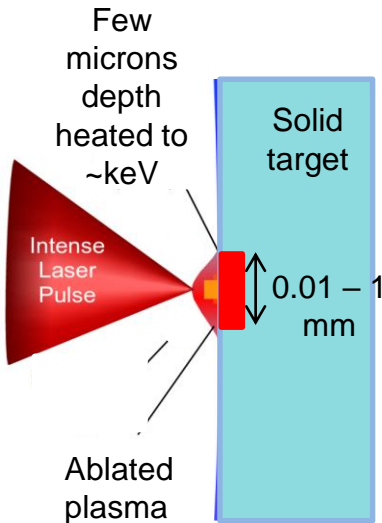
Bohr radius: $a_B = \frac{\hbar^2}{m_e e^2} = 5.3 \times 10^{-9} \text{ cm}$

Binding E-field: $E_a = \frac{e}{4\pi\epsilon_0 a_B^2} = 5.1 \times 10^9 \text{ Vm}^{-1}$

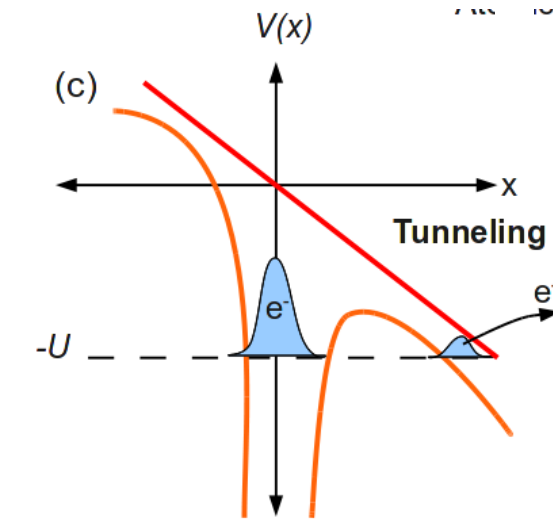
Intensity required: $I_a = \frac{\epsilon_0 c E_a^2}{2} = 3.5 \times 10^{16} \text{ Wcm}^{-2}$



Ionisation



$K \gg 1$ – multiphoton ionisation
– high frequency, low field



$K \ll 1$ – tunnelling ionisation
– low frequency, high field

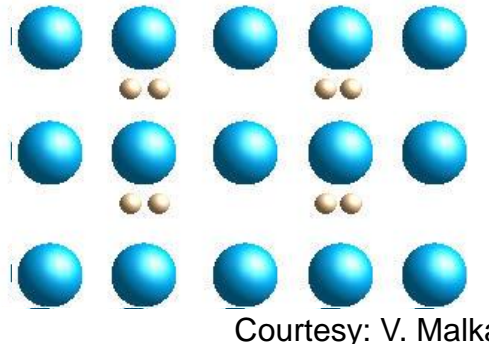
Keldysh adiabaticity parameter K determines whether ionisation is predominately via multiphoton or tunnelling ionisation / over-the-barrier ionisation

$$K = \omega_L \sqrt{\frac{2U}{I_L}}$$

Barrier suppression lowers the minimum intensity required for ionisation. For the ground state of hydrogen $\sim 10^{14} \text{ W/cm}^2$

Charged particle motion

In the interaction of a laser pulse with plasma, electrons collectively quiver around the (almost) stationary ions \Rightarrow plasma oscillations



If $\omega_p > \omega_{\text{Laser}}$ the plasma electrons can follow the light oscillations and therefore cancel the light propagation.

Electron plasma frequency:

$$\omega_p = \sqrt{\frac{e^2 n_e}{\epsilon_0 m_e}}$$

← Electron density ← Electron mass (increases in the relativistic regime)

The maximum plasma electron density in which light can still propagate is called the **critical density**: $n_c = \frac{\omega_L^2 \epsilon_0 m_e}{e^2}$

$n_e > n_c$ Overdense – opaque plasma

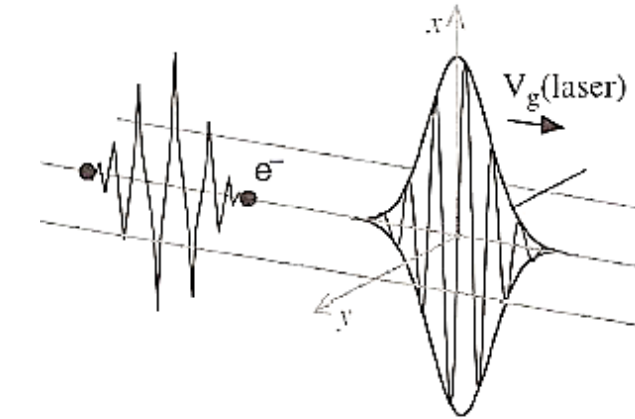
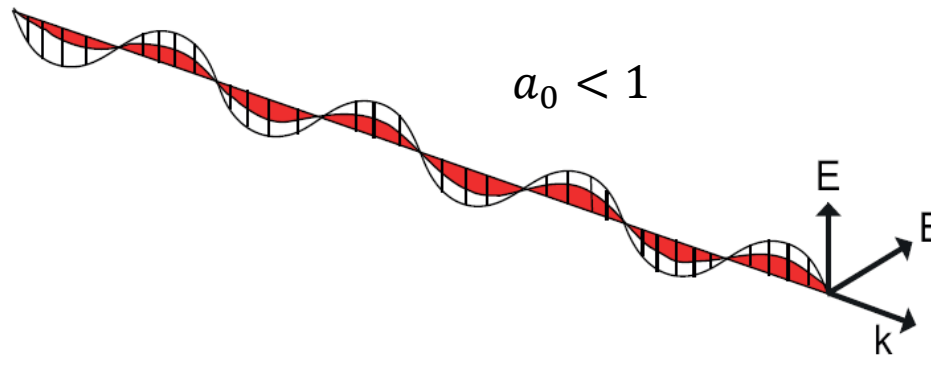
$n_e < n_c$ Underdense – transparent plasma

- Ions respond on a time scale $\omega_{pi}^{-1} = (m_i/m_e)^{1/2} \omega_p^{-1}$ to slowly varying electric fields generated by large charge separations

E-field driven electron oscillations

Electron equation of motion in a laser field is governed by the Lorentz force

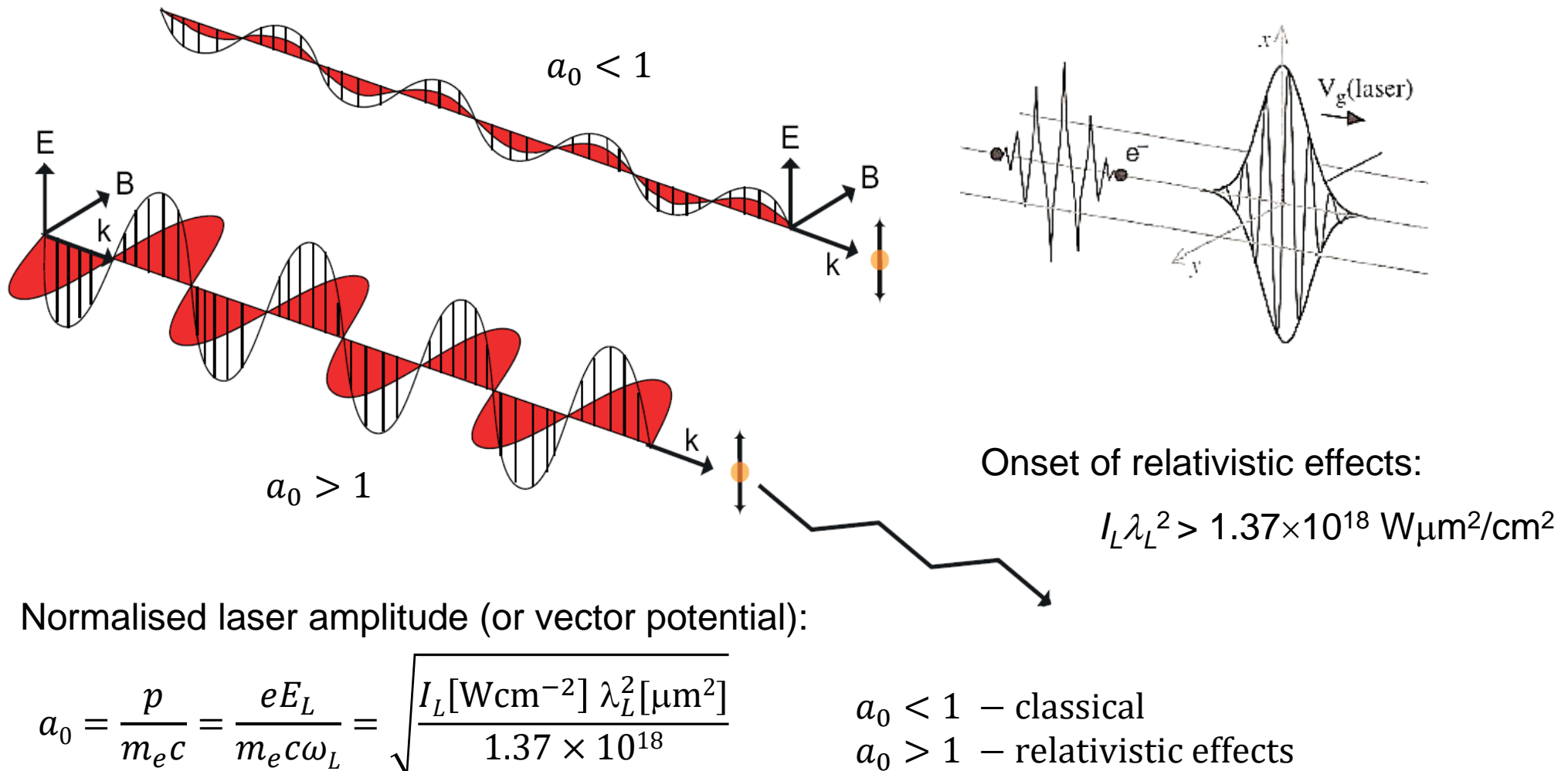
$$\frac{d\mathbf{p}}{dt} = -e \cdot (\mathbf{E} + \mathbf{v} \times \mathbf{B})$$



Relativistic effects: Influence of the B-field

Electron equation of motion in a laser field is governed by the Lorentz force

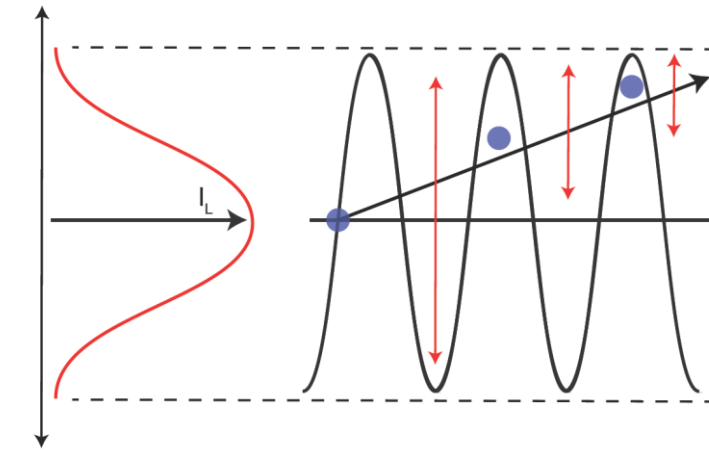
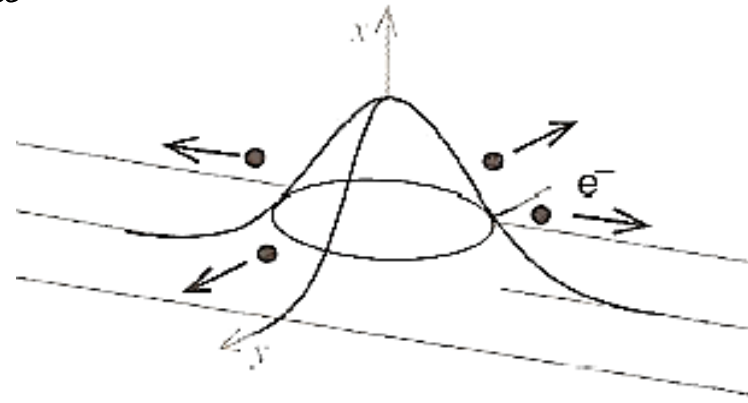
$$\frac{d\mathbf{p}}{dt} = -e \cdot (\mathbf{E} + \mathbf{v} \times \mathbf{B})$$



The ponderomotive force

- The laser beam has a transverse spatial intensity profile
- The duration of the laser pulse is much longer than the e.m. wave period
- Results in a force along the gradient of the intensity - the **ponderomotive force**

$$F_p = -\frac{e^2}{4m_e\omega^2} \nabla E^2$$



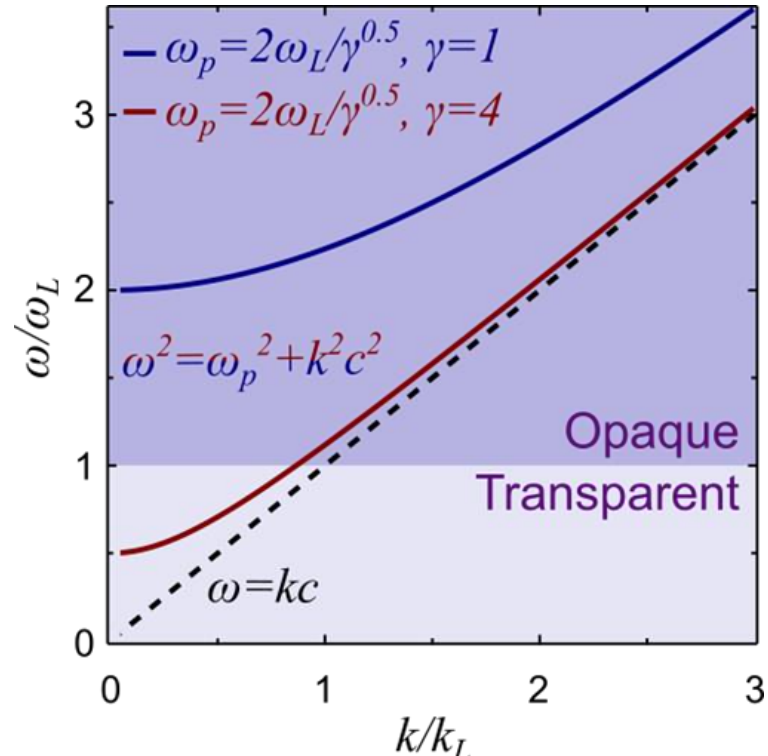
The force derives from the spatial gradient in the E-field and pushes electrons out to lower field regions with velocity v_\perp

Laser light propagation in plasma

Electromagnetic wave: $E(\omega, t) = E_0 e^{-i(kz - \omega t)}$

Dispersion relationship: $\omega^2 = \omega_p^2 + k^2 c^2$

Phase velocity: $v_{ph} = \frac{\omega}{k}$ Group velocity: $v_g = \frac{d\omega}{dk}$

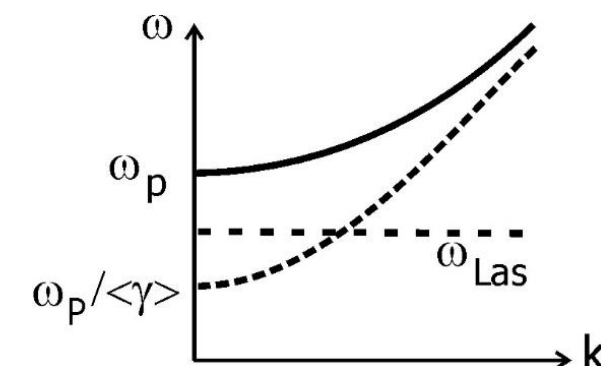


$$\omega_p = \sqrt{\frac{e^2}{\epsilon_0} \frac{n_e}{m_e}}$$

Electron density
Electron mass (increases in the relativistic regime)

$n_e > n_c$ Overdense - opaque

$n_e < n_c$ Underdense - transparent

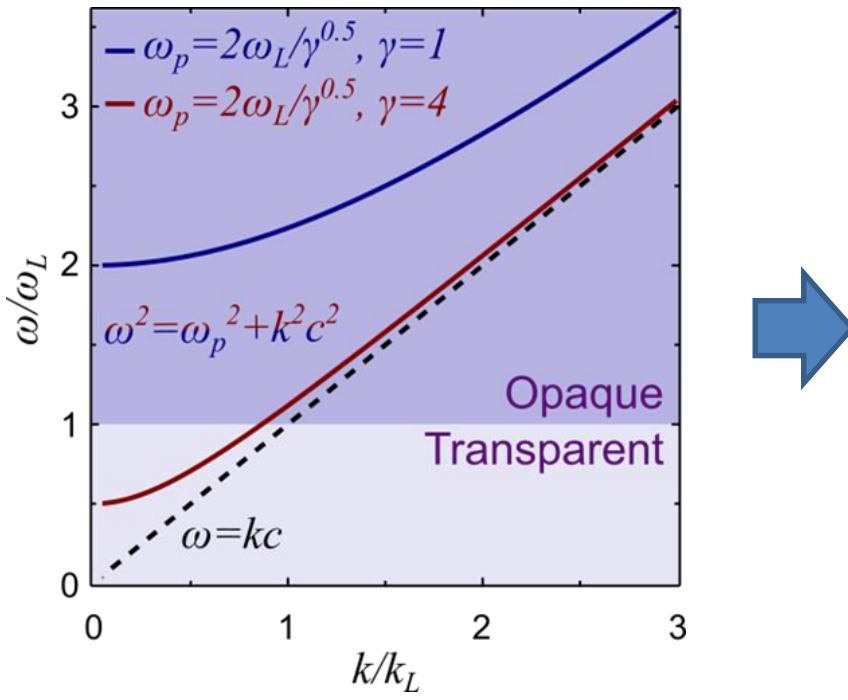


Lorentz factor: $\gamma = \frac{1}{\sqrt{1 - v^2/c^2}}$

$$\gamma = \sqrt{(1 + a_0^2)} \text{ for circular polarisation}$$

$$\gamma = \sqrt{(1 + a_0^2/2)} \text{ for linear polarisation}$$

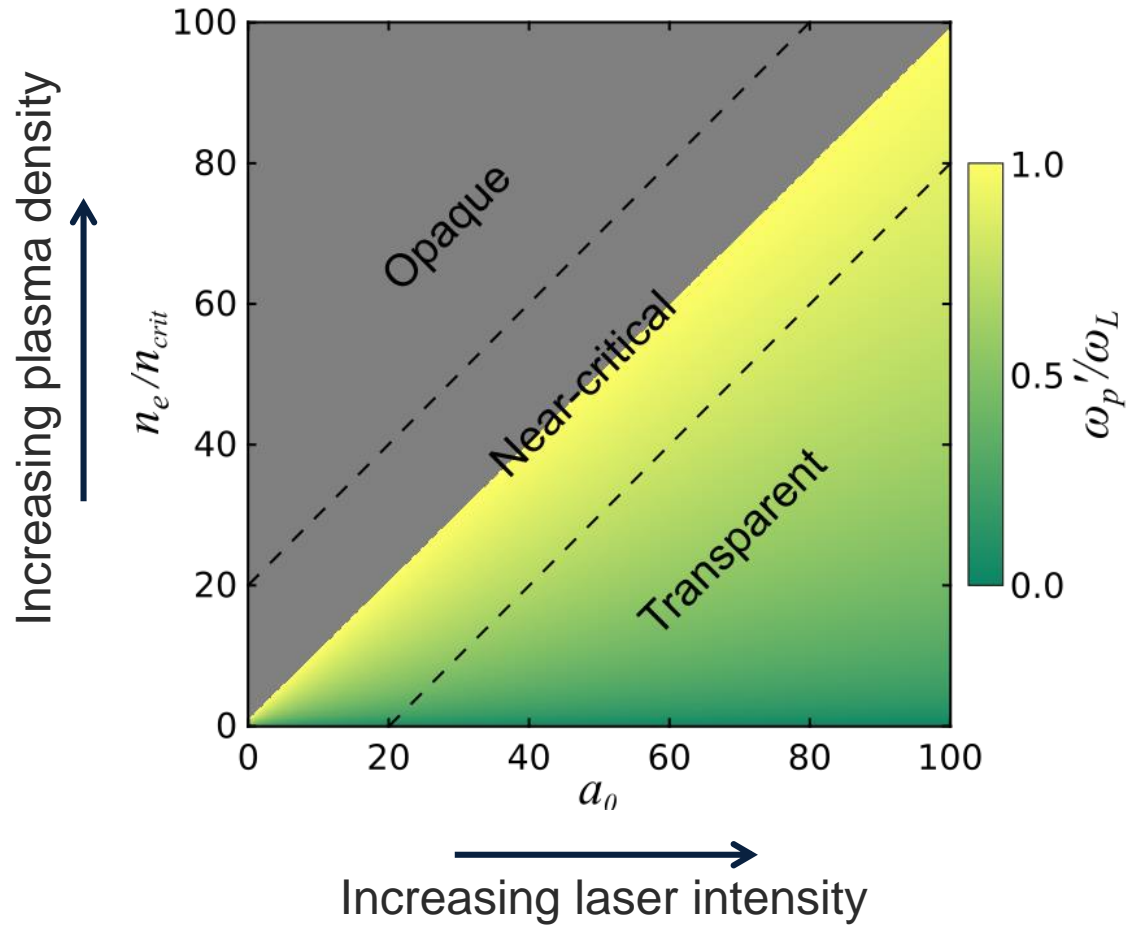
Near-critical density plasma



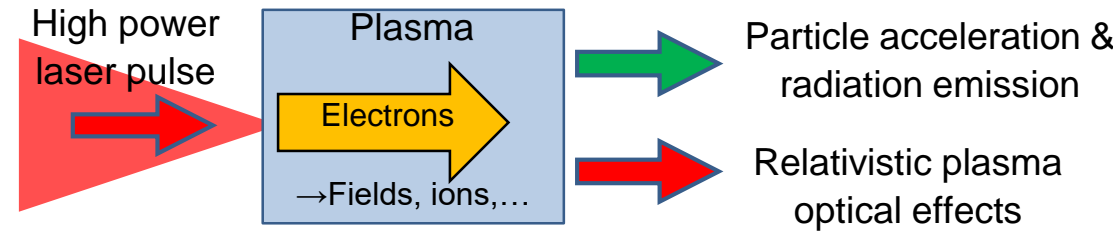
Increasing plasma density ↑

Threshold density for transparency increases with laser intensity

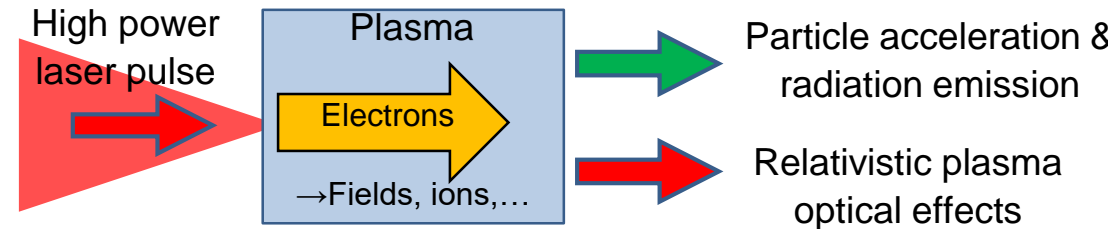
Region around the threshold density is the near-critical density regime



Collective electron dynamics in laser-plasma



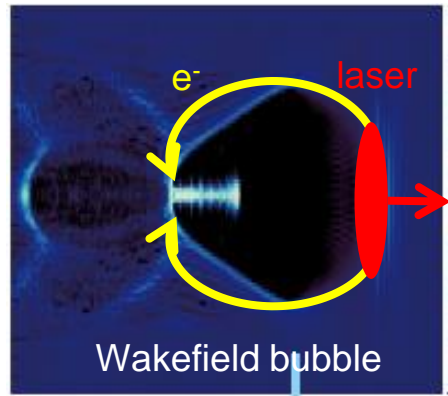
Collective electron dynamics in laser-plasma



Gas —————→ Solid

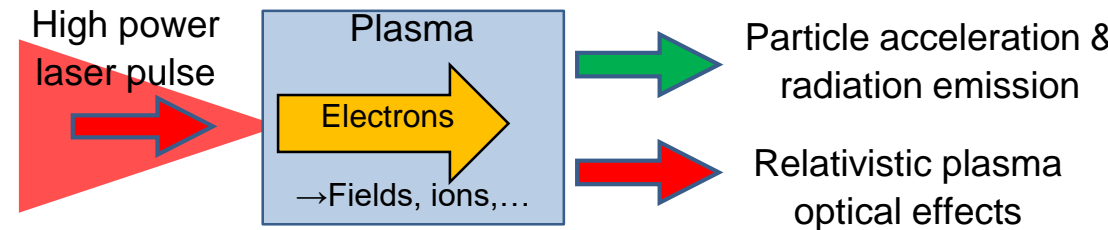
$$\omega_{\text{plasma}} < \omega_{\text{Laser}}$$

Underdense plasma



Wakefield electron
acceleration

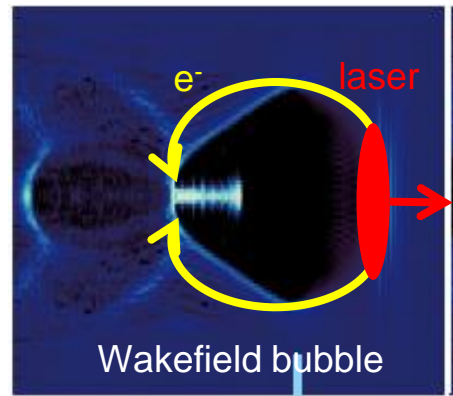
Collective electron dynamics in laser-plasma



Gas → Solid

$$\omega_{\text{plasma}} < \omega_{\text{Laser}}$$

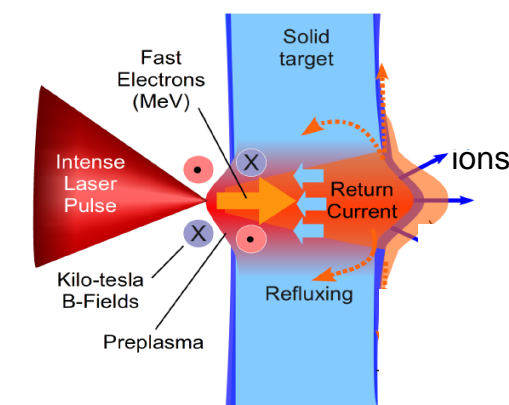
Underdense plasma



Wakefield electron acceleration

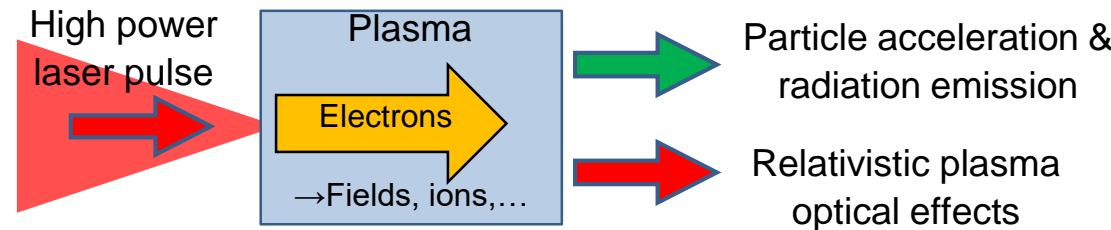
$$\omega_{\text{plasma}} > \omega_{\text{Laser}}$$

Ondense plasma



Ion acceleration and energy transport

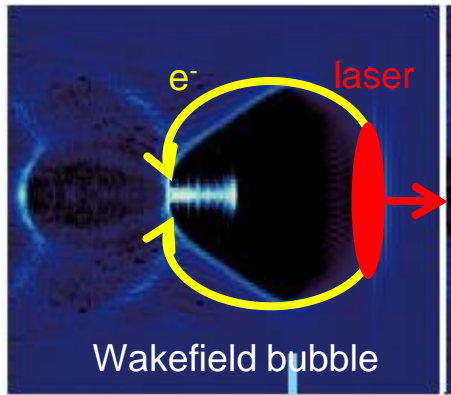
Collective electron dynamics in laser-plasma



Gas → Solid

$$\omega_{\text{plasma}} < \omega_{\text{Laser}}$$

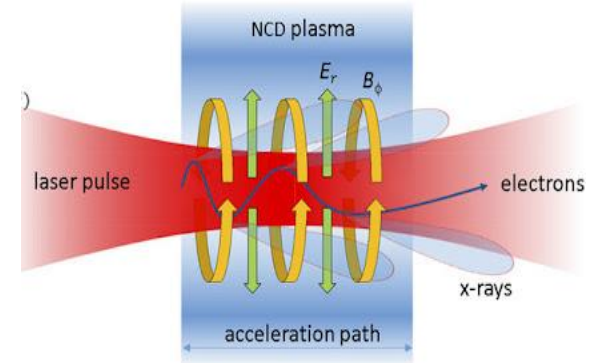
Underdense plasma



Wakefield electron acceleration

$$\omega_{\text{plasma}} \sim \omega_{\text{Laser}}$$

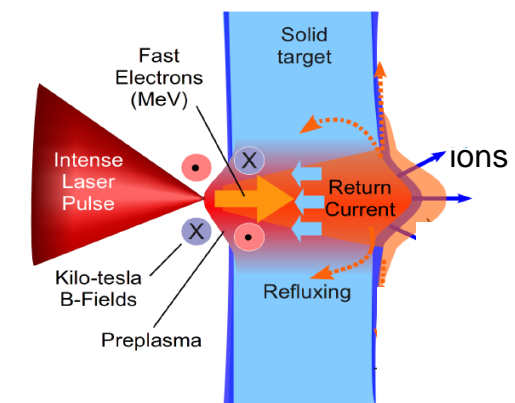
Near critical density plasma



Bright betatron radiation from direct-laser-accelerated electrons

$$\omega_{\text{plasma}} > \omega_{\text{Laser}}$$

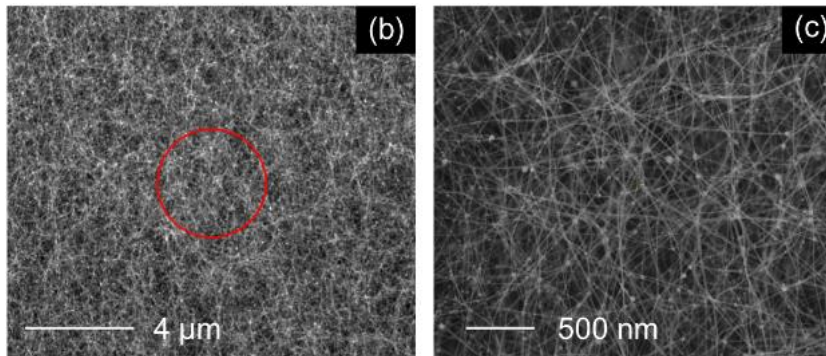
Overdense plasma



Ion acceleration and energy transport

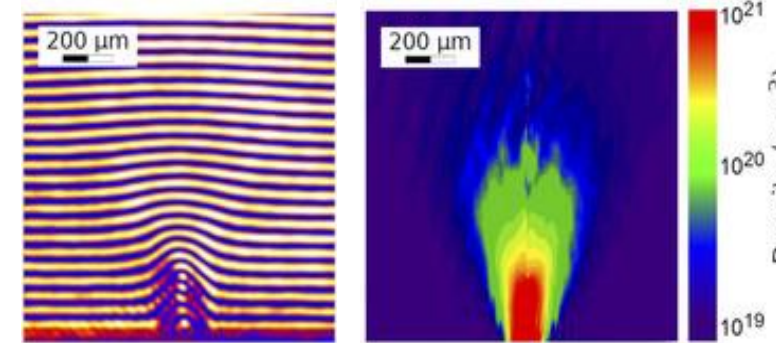
Generating near critical density plasma

Foams, aerogels and carbon nanotubes

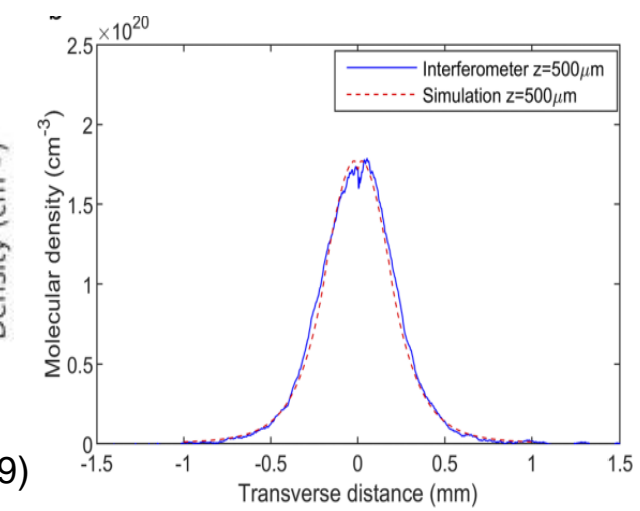


Wang et al., HPLSE 9, e29 (2021)

High pressure gas jets

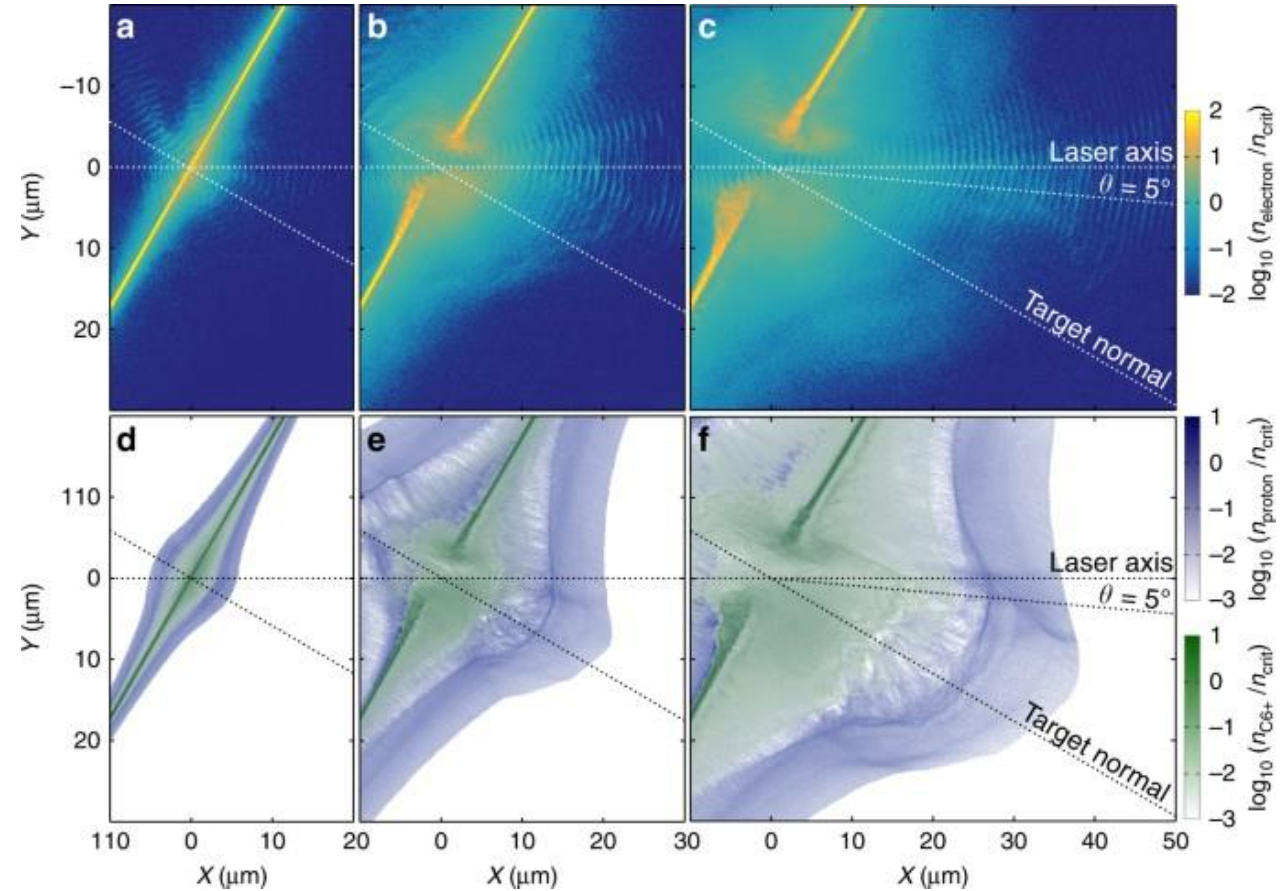
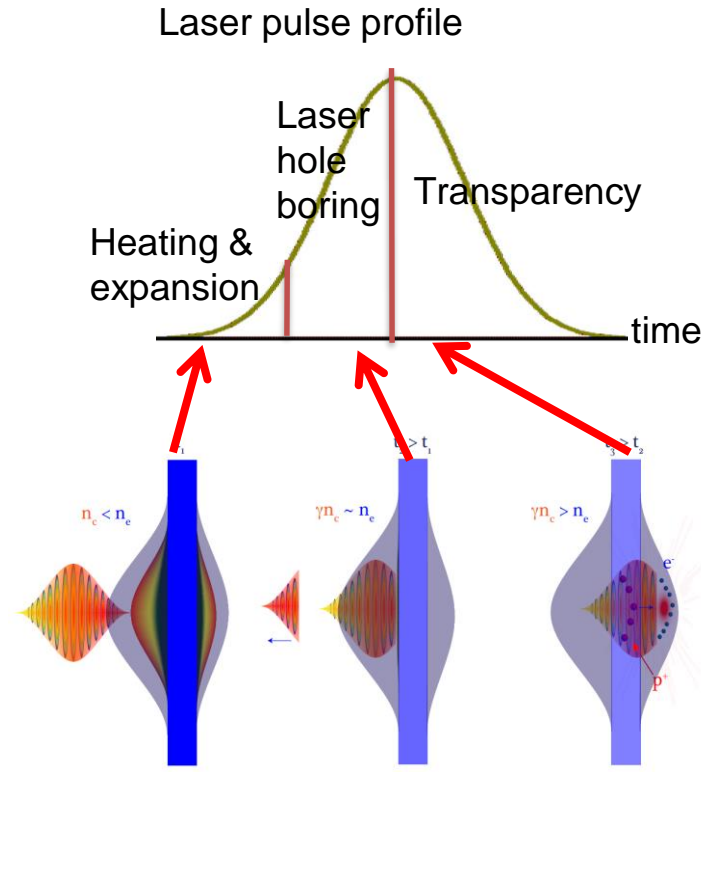


Henares et al., Rev. Sci. Inst. 90, 063302 (2019)



NCD plasma generated by foil expansion

Expanding ultrathin foils driven by single or double laser pulse

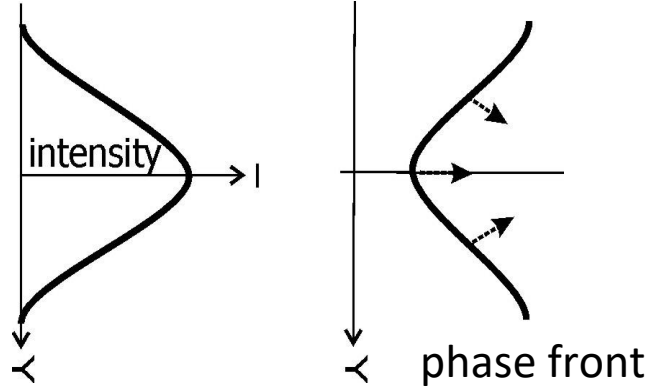
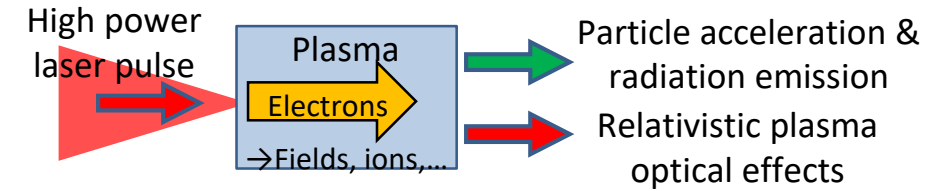


Higginson *et al*, Nature Comms, 9, 724 (2018)

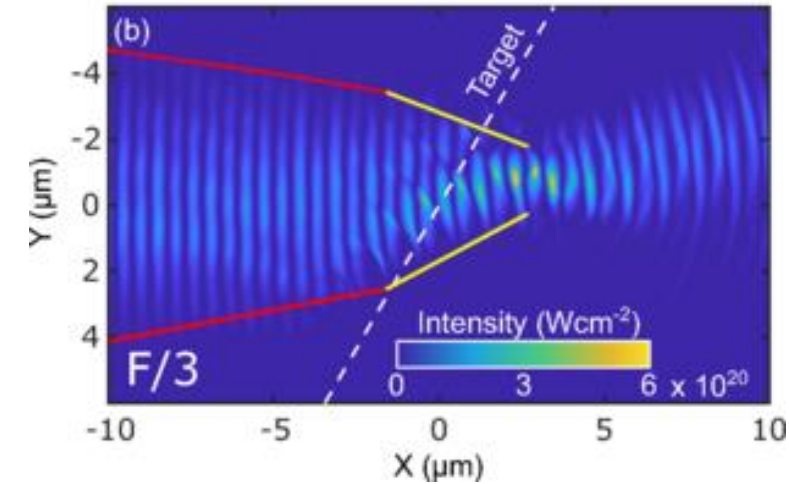
Lecture overview:

1. Introduction to high power lasers
2. Near critical density (NCD) plasma generation
3. **Relativistic optics effects in NCD plasma**
4. Relativistic plasma aperture
5. Electron and ion acceleration in NCD plasma
6. Strong-field QED phenomena
7. [Experimental considerations and methodology – if time permits]

Relativistic self-focusing



- Refractive index $n = \sqrt{1 - \frac{\omega_p^2 / \langle \gamma \rangle}{\omega_L^2}}$
- phase velocity $v_{ph} = c/n$ is smaller on-axis
- plasma acts like a positive lens - self-focusing for powers beyond critical level.



Frazer et al., Phys. Rev. Res. **2**, 042015 (2020)

Temporal pulse compression

Time/space laser profile of a propagating laser pulse is modified by plasma, which can lead to processes such as pulse compression and collapse.

Complex interaction dynamics – the laser ponderomotive expels electrons, changing the density. The moving pulse creates a spatiotemporally varying refractive index, that can increase the group velocity at the back of the pulse, compressing the pulse and increasing the spectral bandwidth.

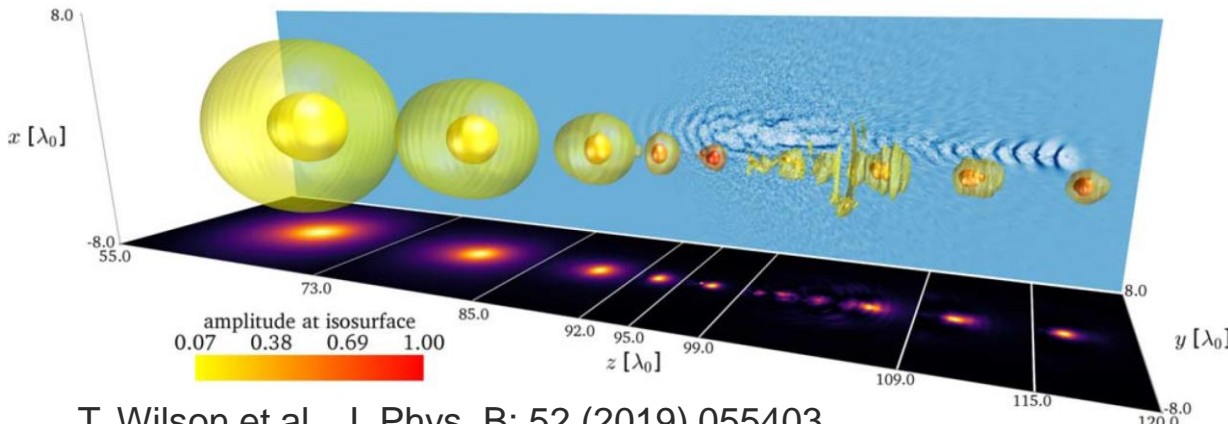
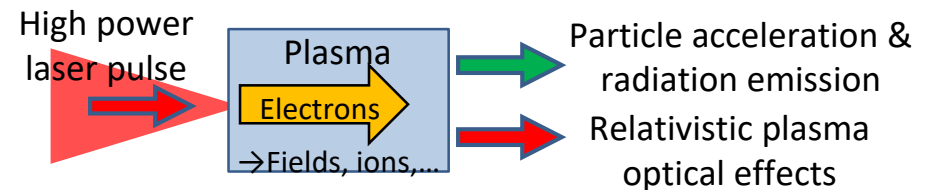
Pulse width is a function of plasma frequency

This leads to pulse compression for both:

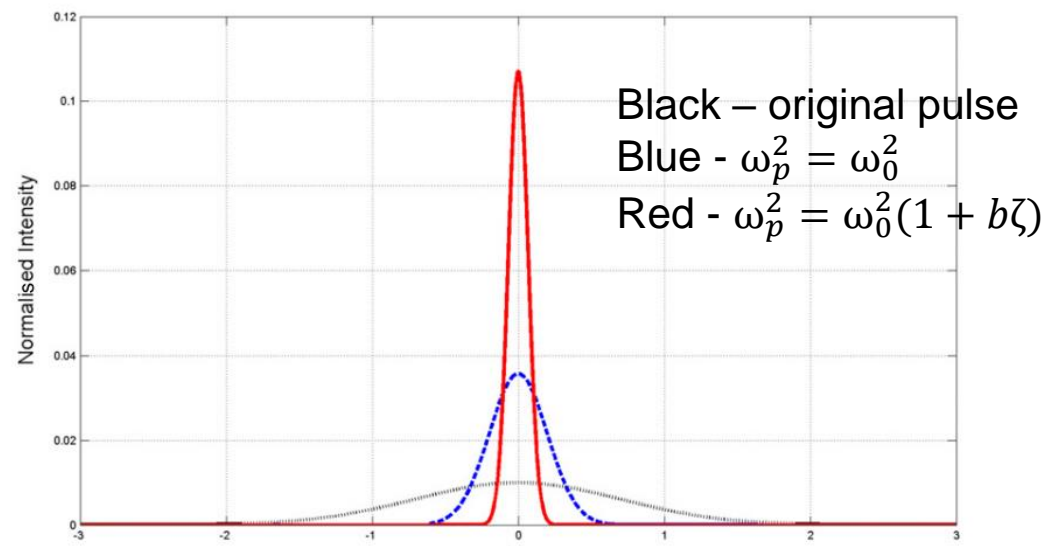
$$\text{Homogeneous plasma } \omega_p^2 = \omega_0^2$$

$$\text{Inhomogeneous plasma } \omega_p^2 = \omega_0^2(1 + b\zeta)$$

Inhomogeneous plasma with a longitudinal density gradient improves the degree of pulse compression

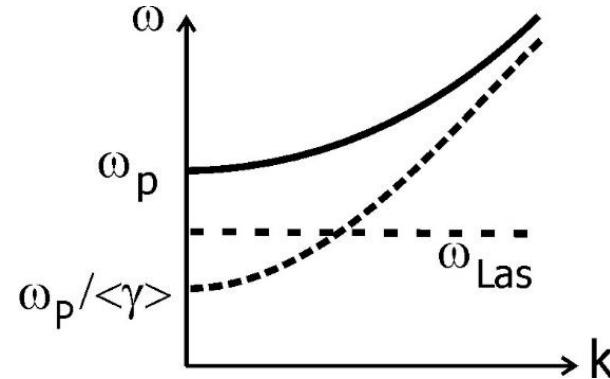
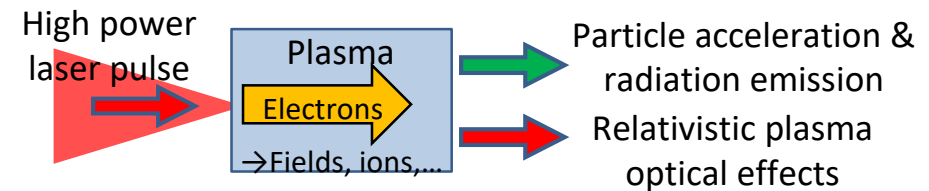


T. Wilson et al., J. Phys. B: 52 (2019) 055403

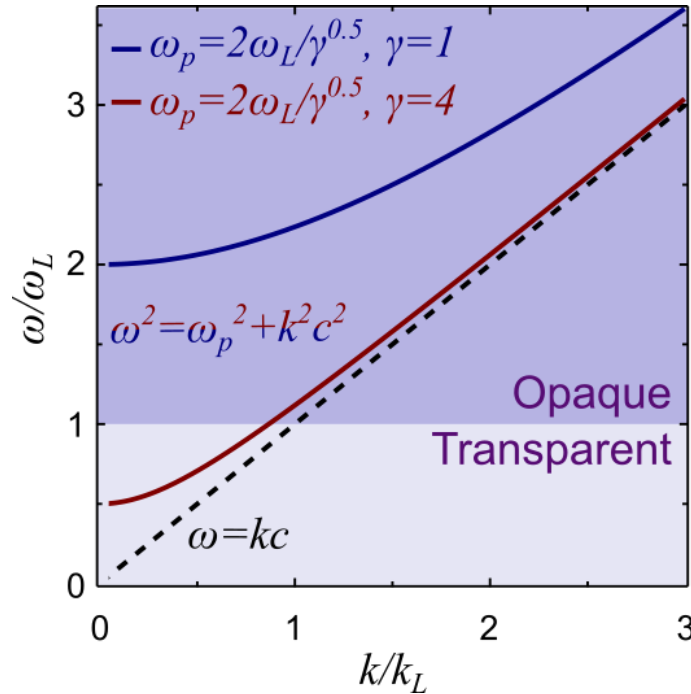


A. Sharma and I. Kourakis, PPCF (2010) 065002

Relativistic-induced transparency



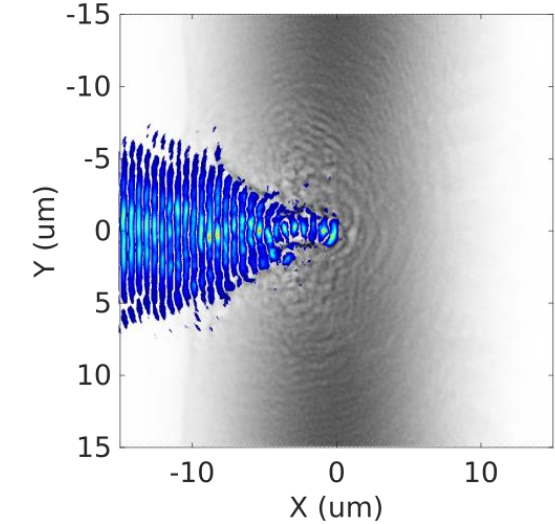
- In dense plasma with $\omega_p > \omega_{\text{Las}}$, light cannot propagate
- The dispersion relation governing laser light propagation depends on plasma frequency $\omega_p^2 = 4\pi e^2 n_e / m$ and the average $\langle \gamma \rangle$ -factor.
- Plasma becomes transparent for large $\langle \gamma \rangle$



Electron plasma frequency:

$$\omega_p = \sqrt{\frac{e^2}{\epsilon_0} \frac{n_e}{m_e}}$$

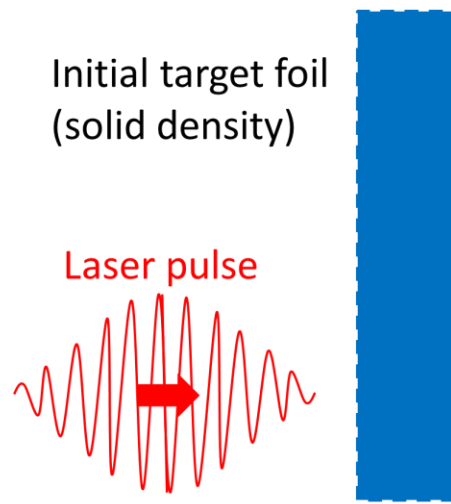
$$\gamma = \frac{1}{\sqrt{1 - v^2/c^2}}$$



Onset of relativistic induced transparency in thin foils

Transparency happens due to the combination of the relativistic increase in electron mass and the decrease in plasma density due to expansion – both act to reduce ω_p (effectively increase n_c)

$$\omega_p = \sqrt{\frac{e^2 n_e}{\epsilon_0 m_e}}$$



A laser pulse is propagated up to the relativistically corrected critical density:

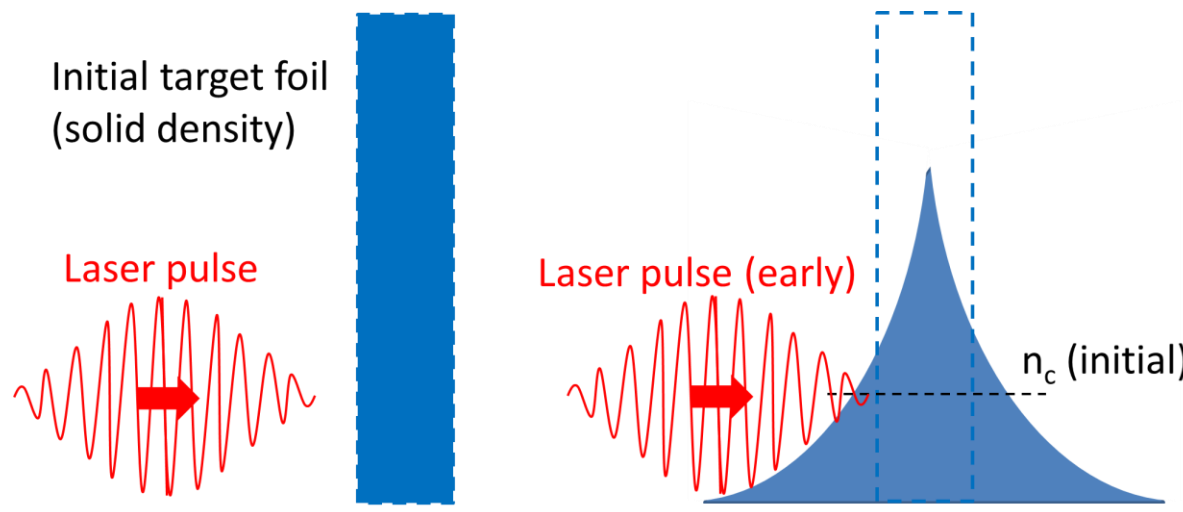
$$n'_c = \gamma n_c = \frac{\gamma m_e \epsilon_0 \omega_L^2}{e^2} \quad \frac{n_e \downarrow}{\gamma n_c \uparrow} \leq 1$$

plasma becomes transparent

Onset of relativistic induced transparency in thin foils

Transparency happens due to the combination of the relativistic increase in electron mass and the decrease in plasma density due to expansion – both act to reduce ω_p (effectively increase n_c)

$$\omega_p = \sqrt{\frac{e^2 n_e}{\epsilon_0 m_e}}$$



A laser pulse is propagated up to the relativistically corrected critical density:

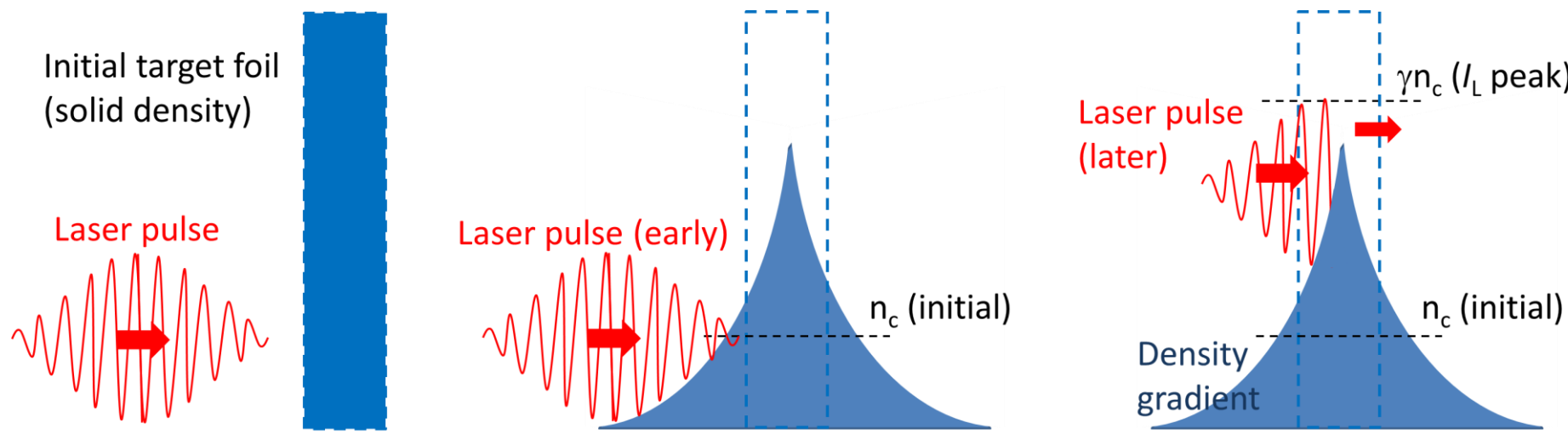
$$n'_c = \gamma n_c = \frac{\gamma m_e \epsilon_0 \omega_L^2}{e^2} \quad \frac{n_e \downarrow}{\gamma n_c \uparrow} \leq 1$$

plasma becomes transparent

Onset of relativistic induced transparency in thin foils

Transparency happens due to the combination of the relativistic increase in electron mass and the decrease in plasma density due to expansion – both act to reduce ω_p (effectively increase n_c)

$$\omega_p = \sqrt{\frac{e^2}{\epsilon_0} \frac{n_e}{m_e}}$$



A laser pulse is propagated up to the relativistically corrected critical density:

$$n'_c = \gamma n_c = \frac{\gamma m_e \epsilon_0 \omega_L^2}{e^2} \quad \frac{n_e \downarrow}{\gamma n_c \uparrow} \leq 1$$

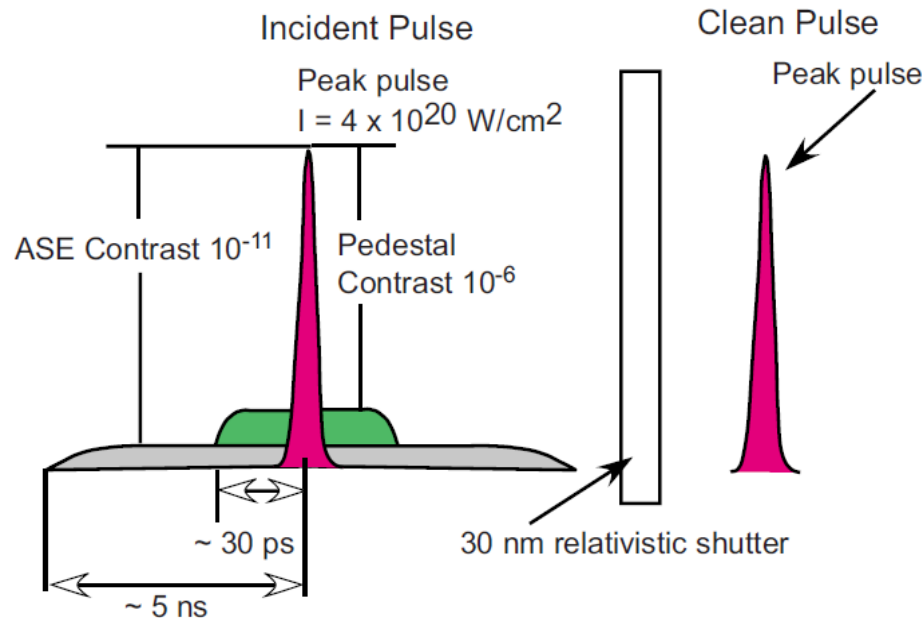
plasma becomes transparent

- The transmitted laser pulse:
- is temporally shorter
- has a sharper rise time

Plasma shutter!

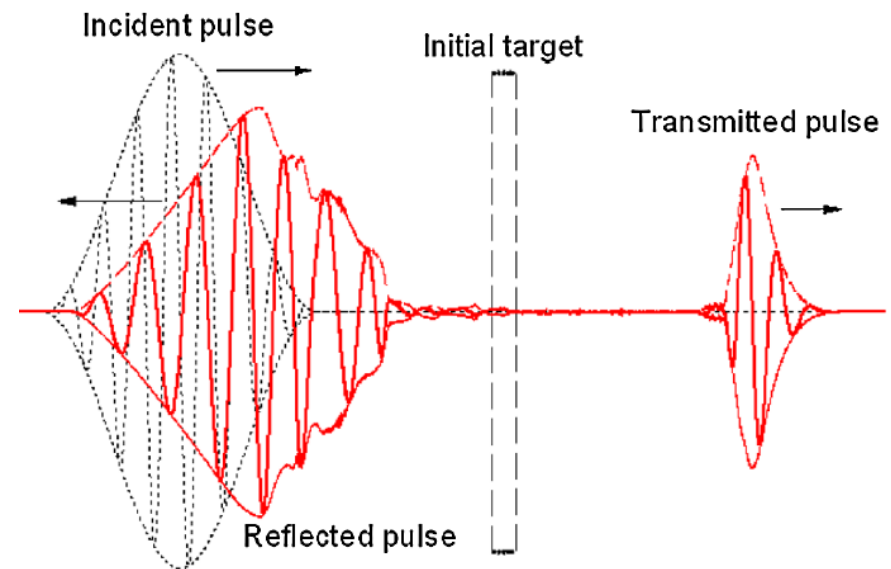
Plasma shutter based on relativistic induced transparency

A relativistic plasma shutter enhances the laser contrast removing the low level signal before and after the main pulse producing clean ultraintense pulses.



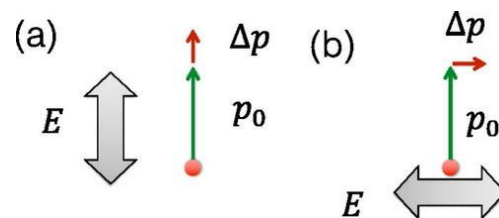
S. A. Reed et al., APL, 94, 201117 (2009)

Generates shorter relativistic pulses.



L. L. Ji et al., PRL, 103, 215005 (2009)

Plasma polariser



- (a) Laser electric field is collinear with the electron motion
- (b) Laser electric field is orthogonal with the electron motion

Assuming wave propagation transverse to two counter-streaming relativistic plasma flows of flow velocity u , leads to three distinct dispersion relations

$$\text{Longitudinal: } \omega^2 = \omega_p^2/\gamma$$

$$\text{Collinear: } \omega^2 = \frac{\omega_p^2}{\gamma^3} + k^2 c^2 \left(1 + \frac{1}{\gamma} \frac{\omega_p^2 u^2}{\omega^2 c^2}\right)$$

$$\text{Orthogonal: } \omega^2 = \omega_p^2/\gamma + k^2 c^2$$

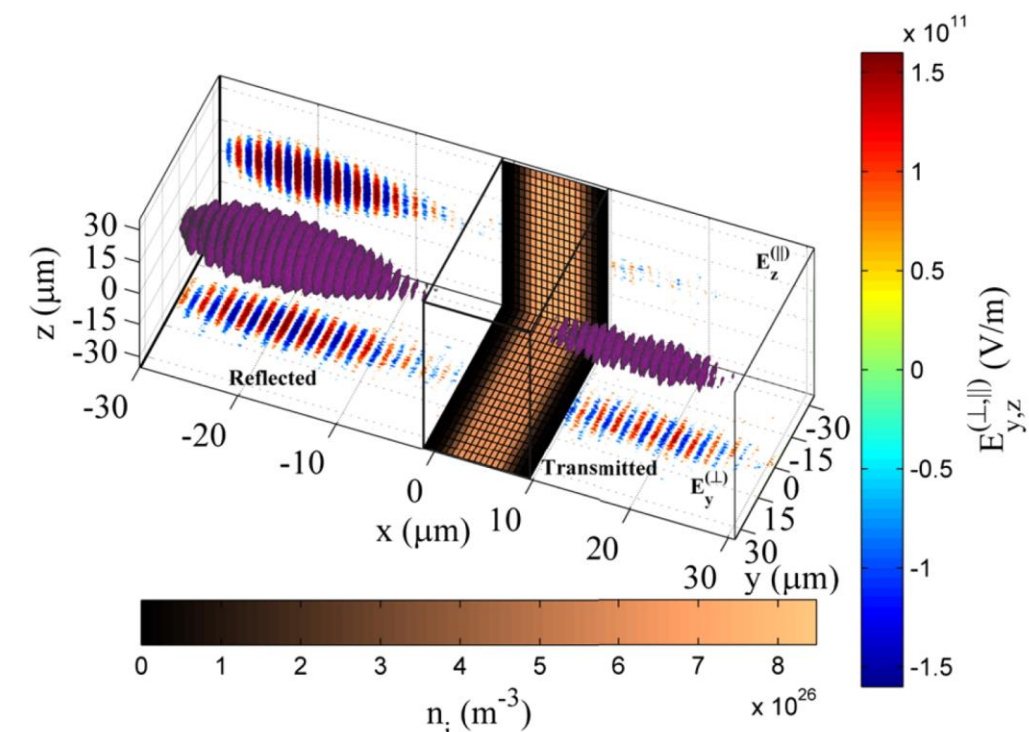
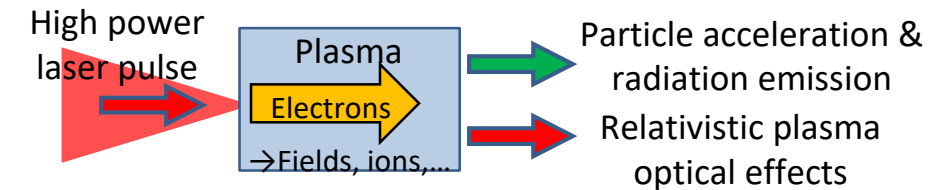
This leads to two different cut-off frequencies in the transverse directions

$$\text{Collinear: } n_c'^{(y)} = \gamma^3 n_c$$

$$\text{Orthogonal: } n_c'^{(z)} = \gamma n_c$$

where n_c is the non-relativistic critical density

A. V. Arefiev et al. Physics of Plasmas **27**, 063106 (2020)



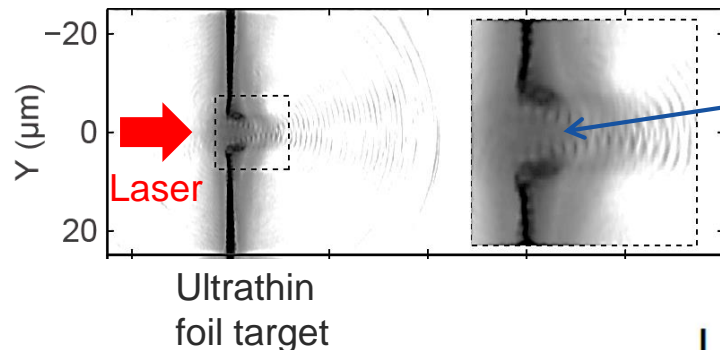
Stark et al., Phys. Rev. Lett. **115**, 025002 (2015)

Lecture overview:

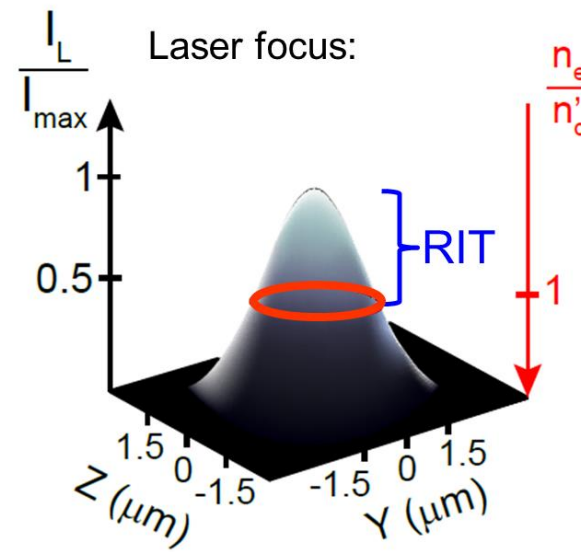
1. Introduction to high power lasers
2. Near critical density (NCD) plasma generation
3. Relativistic optics effects in NCD plasma
4. **Relativistic plasma aperture**
5. Electron and ion acceleration in NCD plasma
6. Strong-field QED phenomena
7. [Experimental considerations and methodology – if time permits]

Generation of a relativistic plasma aperture

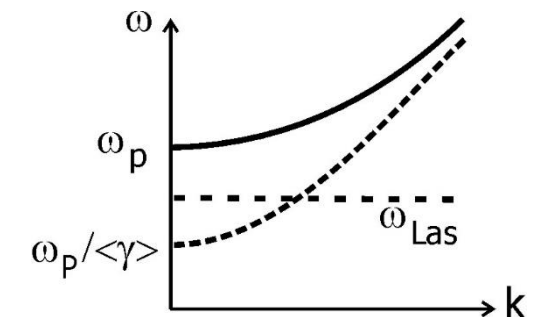
Electron density maps from 2D PIC simulations using
EPOCH code: $5 \times 10^{20} \text{ Wcm}^{-2}$; ultrathin Al foils



Short pulse – minimal expansion –
'relativistic plasma aperture'



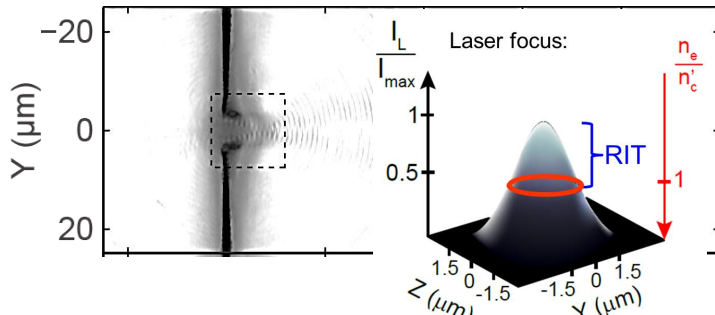
Plasma is locally relativistically transparent in the region in which the laser intensity is above the threshold
→ 'relativistic plasma aperture'



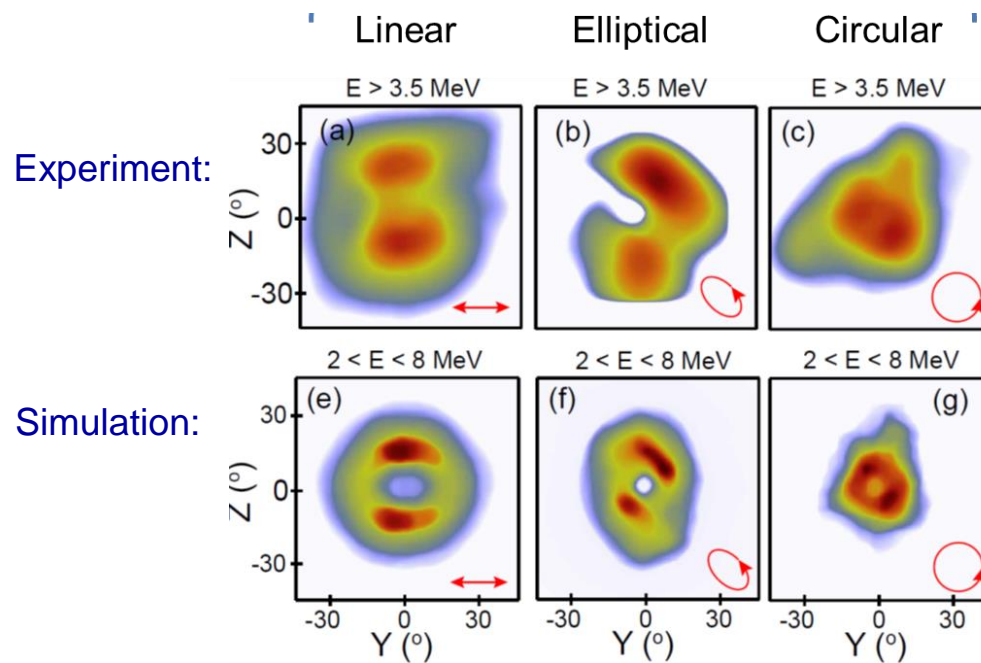
B. Gonzalez-Izquierdo *et al*, Nature Physics, 12, 505 (2016)

Collective plasma dynamics generated via the relativistic plasma aperture

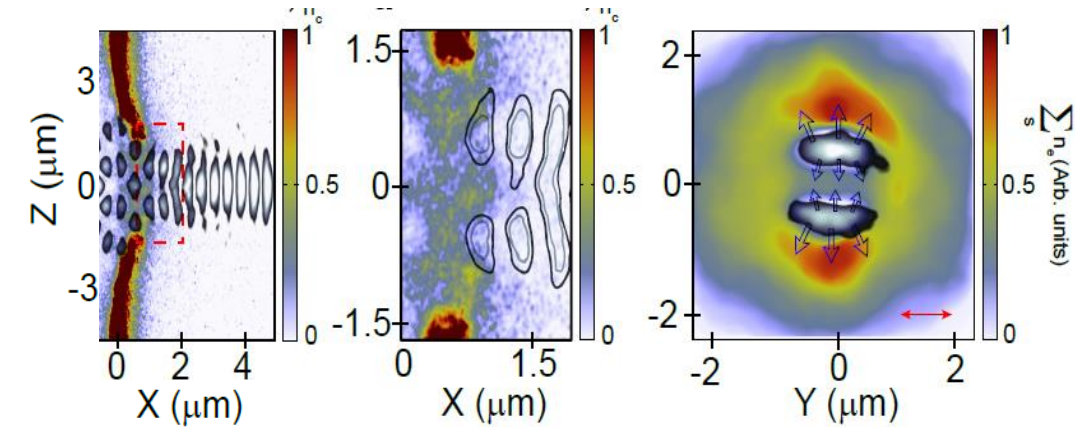
Electron density maps from 2D PIC simulations using
EPOCH code: $5 \times 10^{20} \text{ Wcm}^{-2}$; ultrathin Al foils



Short pulse – minimal expansion –
'relativistic plasma aperture'



Lobes of intense light in near field:



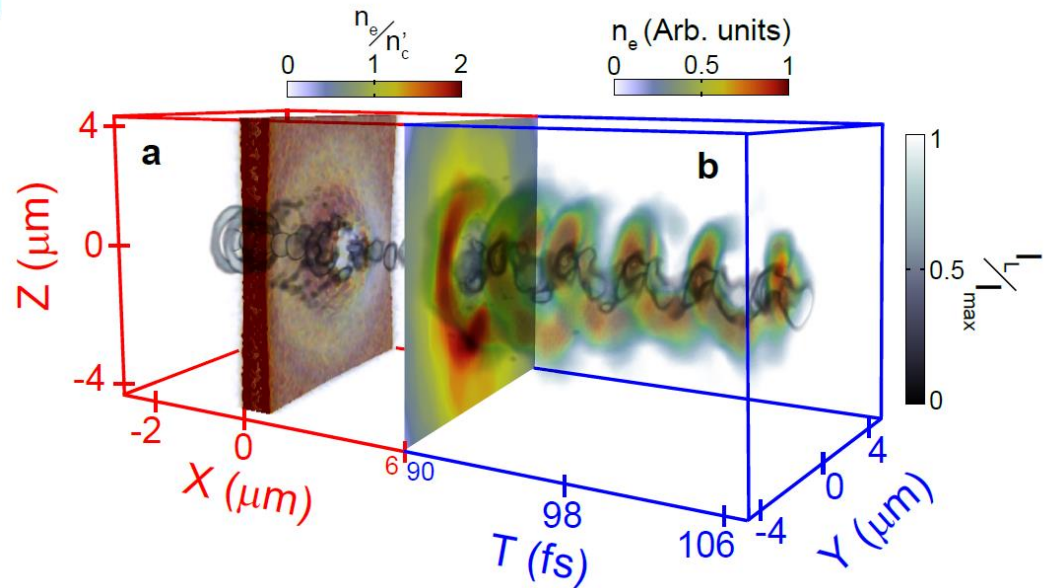
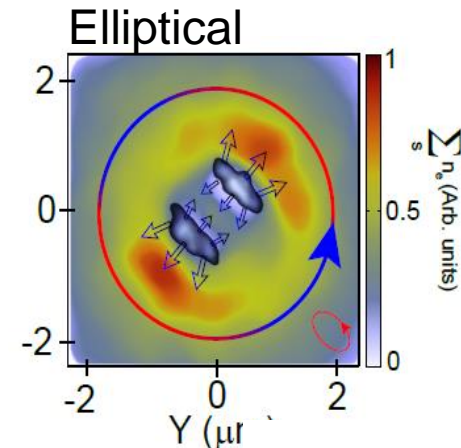
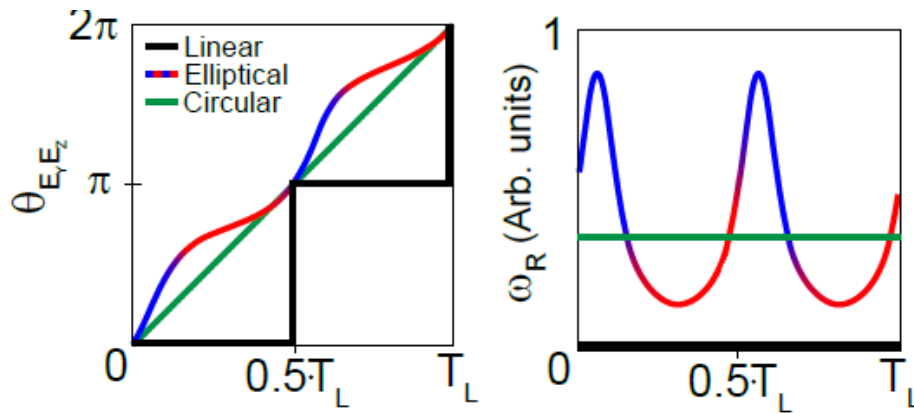
B. Gonzalez-Izquierdo *et al*,
Nature Physics, **12**, 505 (2016)

Collective plasma dynamics with tens of fs pulses

Linear – fixed diffraction pattern

Circular – rotating pattern at constant velocity

Elliptical – variable velocity of rotation



Can use laser polarisation to control the rotation of the lobes!

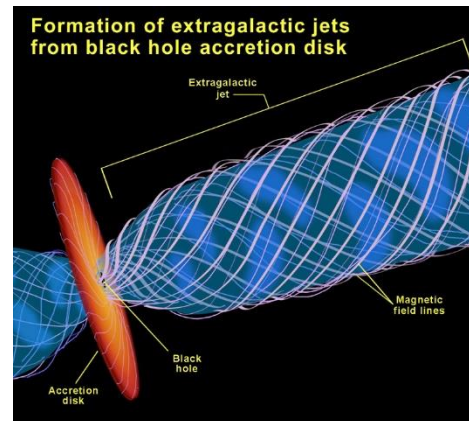
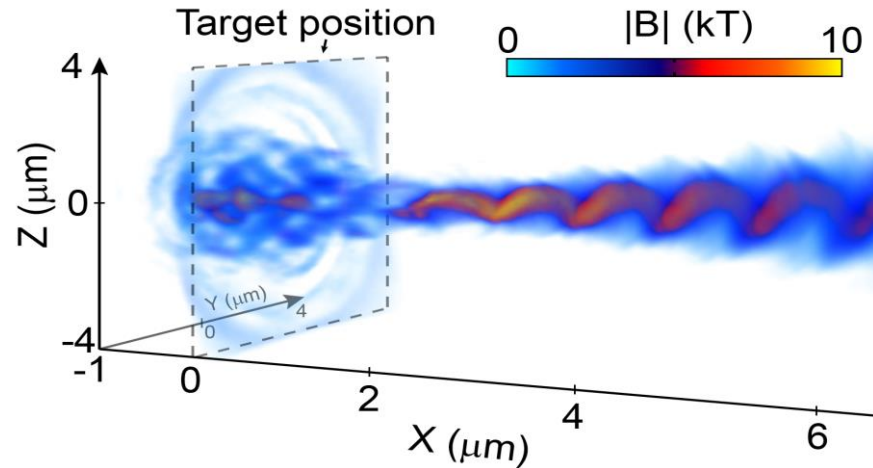
Can introduce variable velocity of rotation

B. Gonzalez-Izquierdo *et al*,
Nature Physics, 12, 505 (2016)

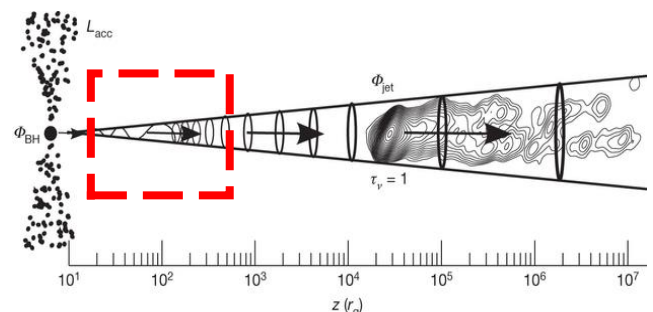
Laser-plasma produced helical magnetic field structures - Astrophysical jet analogue?

- Circular polarisation of the laser acts to drive a rotation in the diffraction lobes
- Helical magnetic fields – inverse Faraday rotation
- Pitch change due to density decrease from target
- Very strong magnetic fields up to 10kT
- Similar in behaviour to a jet created by an accretion disk rotating due to gravitational effects

Magnetic field map from 3D PIC simulations using EPOCH code: $5 \times 10^{20} \text{ Wcm}^{-2}$; ultrathin Al foil

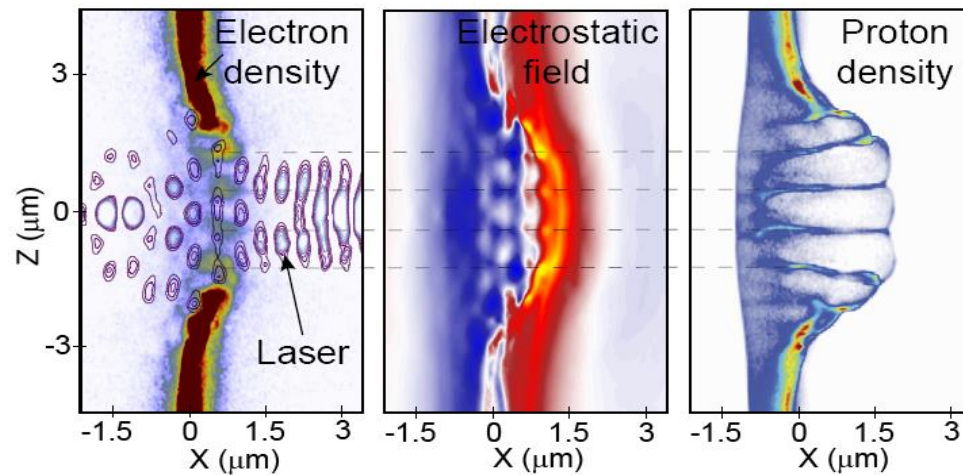


Credit: NASA and Ann Field (Space Telescope Science Institute)

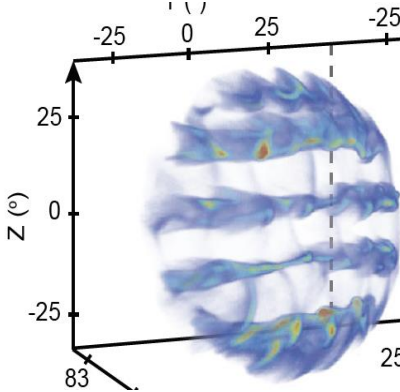


M. Zamaninasab et al., Nature 510, 126–128 (2014)

Structured ion beams generated using a relativistic plasma aperture



Proton beam profile:

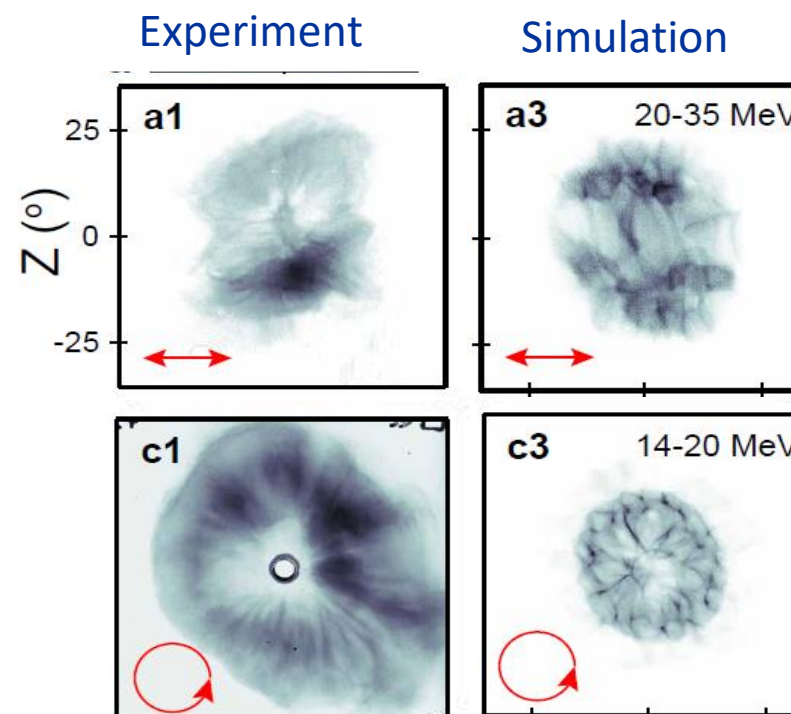


Lobe structure maps into the longitudinal electrostatic field!

Creates structure in the spatial-dose distribution of the electron and ion beams

B. Gonzalez-Izquierdo *et al*,
Nature Comms 7, 12891 (2016)

Linear pol.

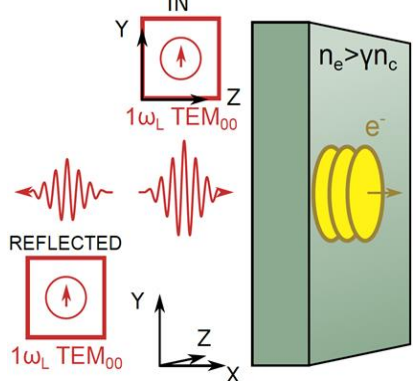


Circular pol.

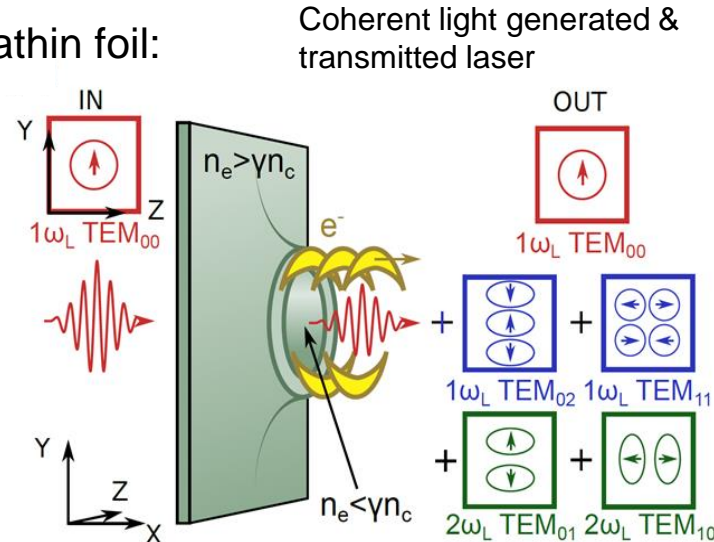
High order modes produced by asymmetric electron bunches accelerated from relativistic aperture

Electron bunches at ω_L (resonance absorption, Brunel,...) and $2\omega_L$ ($v \times B$) produce Coherent Transition Radiation (CTR)

Thick foil:



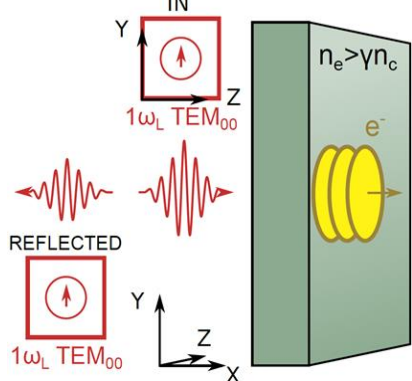
Ultrathin foil:



Duff *et al*, Scientific Reports 10, 105 (2020)

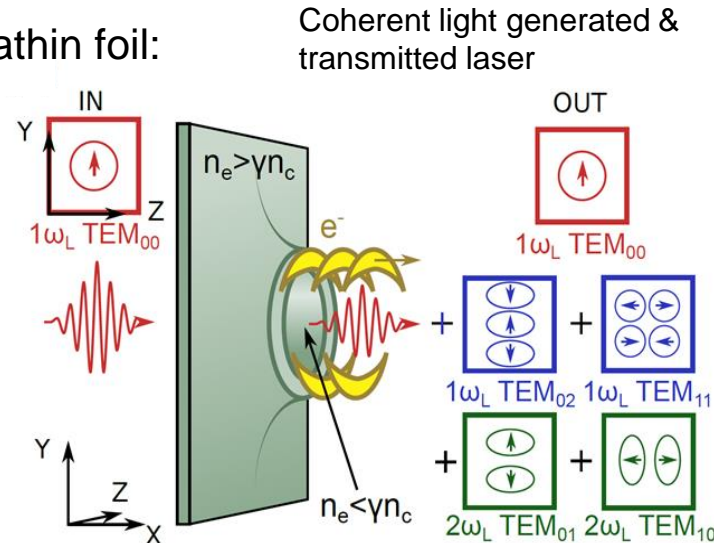
High order modes produced by asymmetric electron bunches accelerated from relativistic aperture

Thick foil:

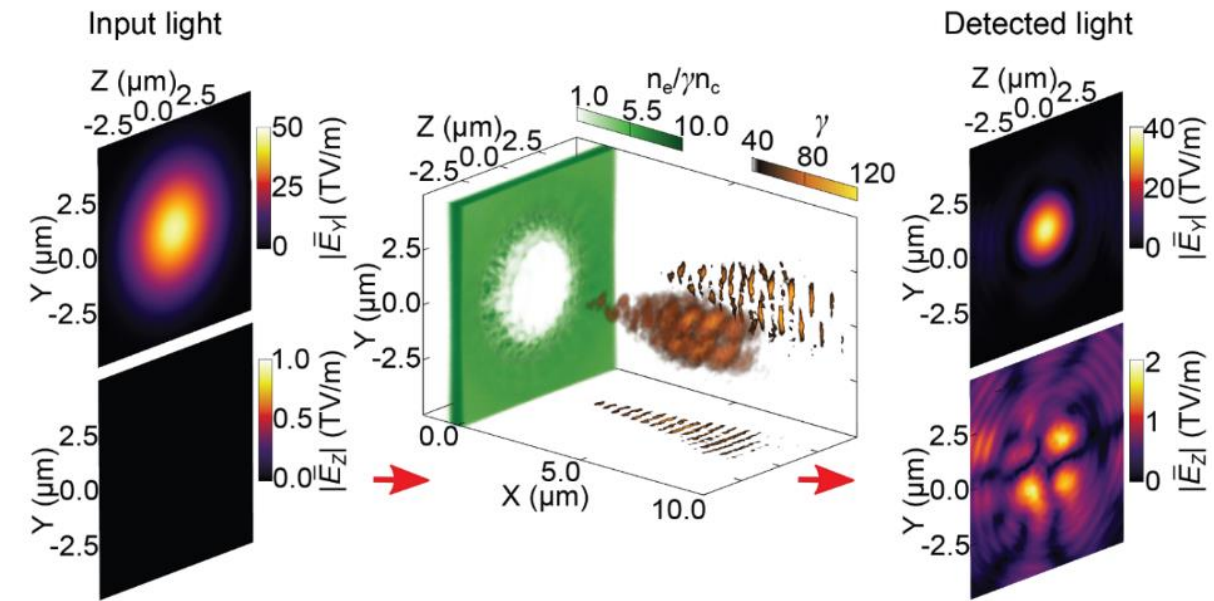


Electron bunches at ω_L (resonance absorption, Brunel,...) and $2\omega_L$ ($v \times B$) produce Coherent Transition Radiation (CTR)

Ultrathin foil:



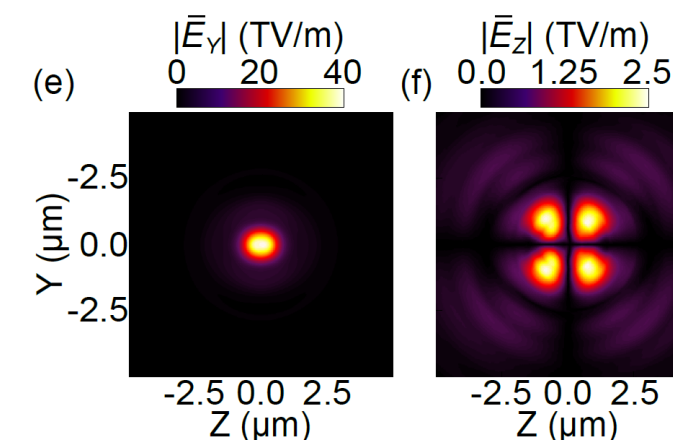
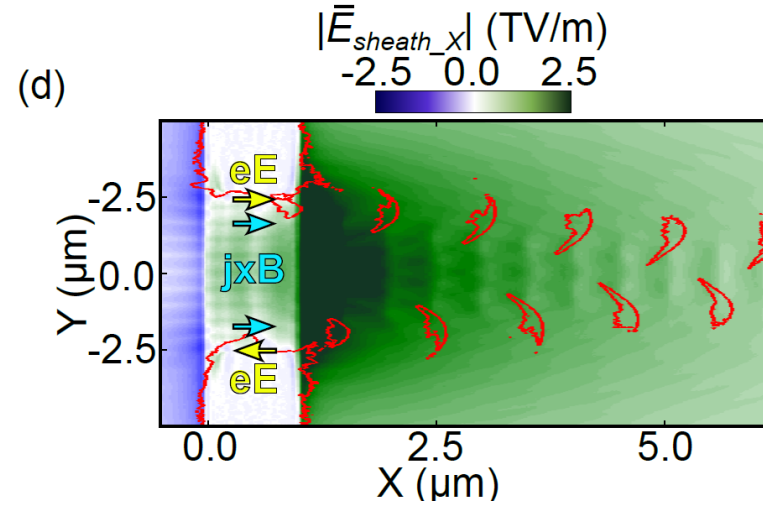
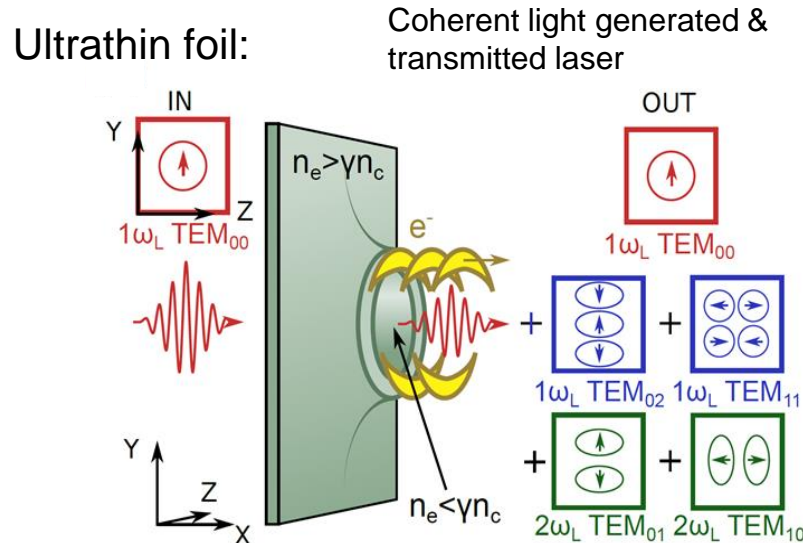
3D PIC (EPOCH) simulations of laser interaction with ultrathin foils show the generation of high order modes when relativistic transparency occurs



Duff et al, Scientific Reports 10, 105 (2020)

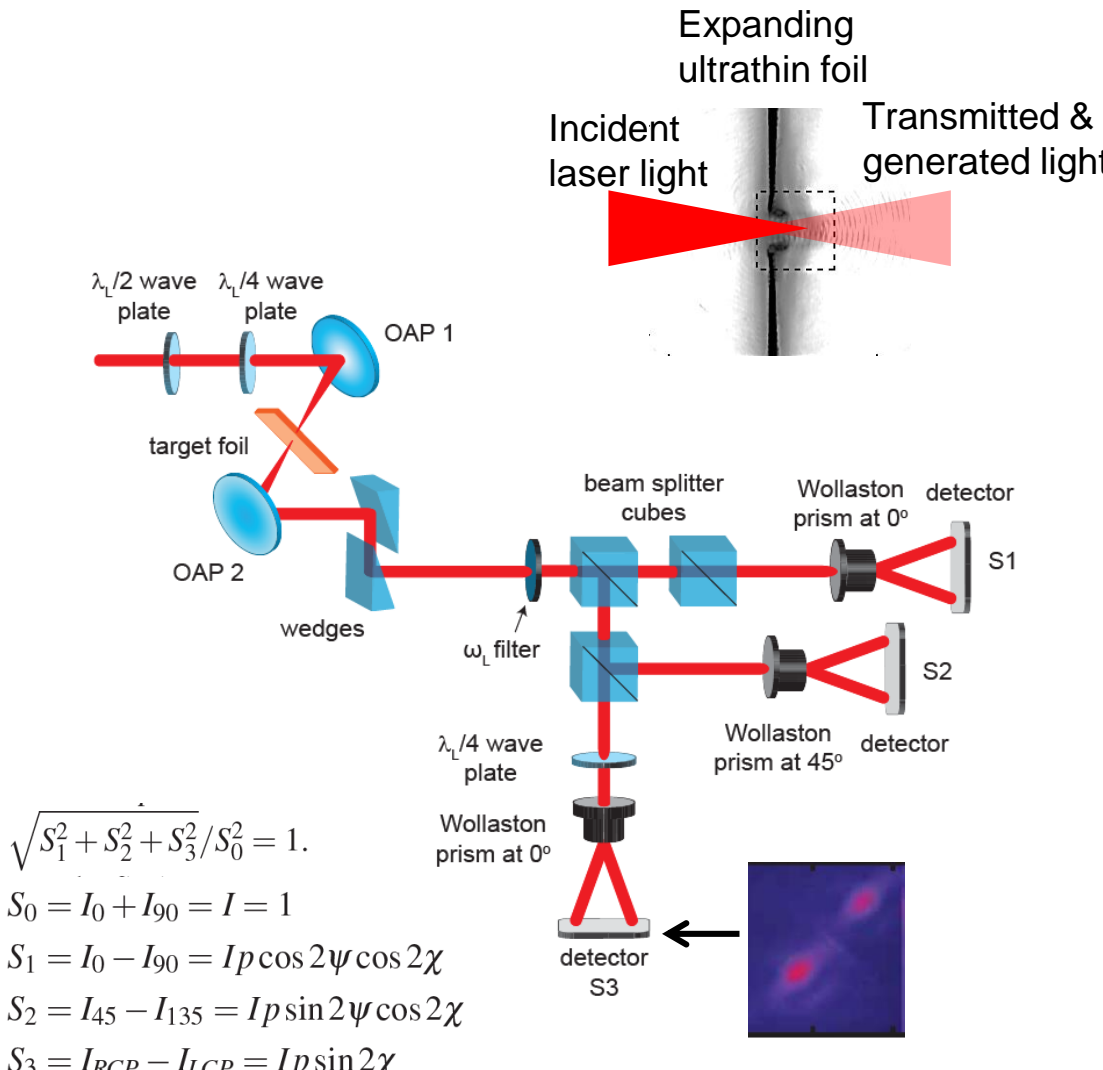
High order modes produced by asymmetric electron bunches accelerated from relativistic aperture

PIC (EPOCH) simulations of laser interaction with a fixed aperture (not a foil) show the generation of high order modes

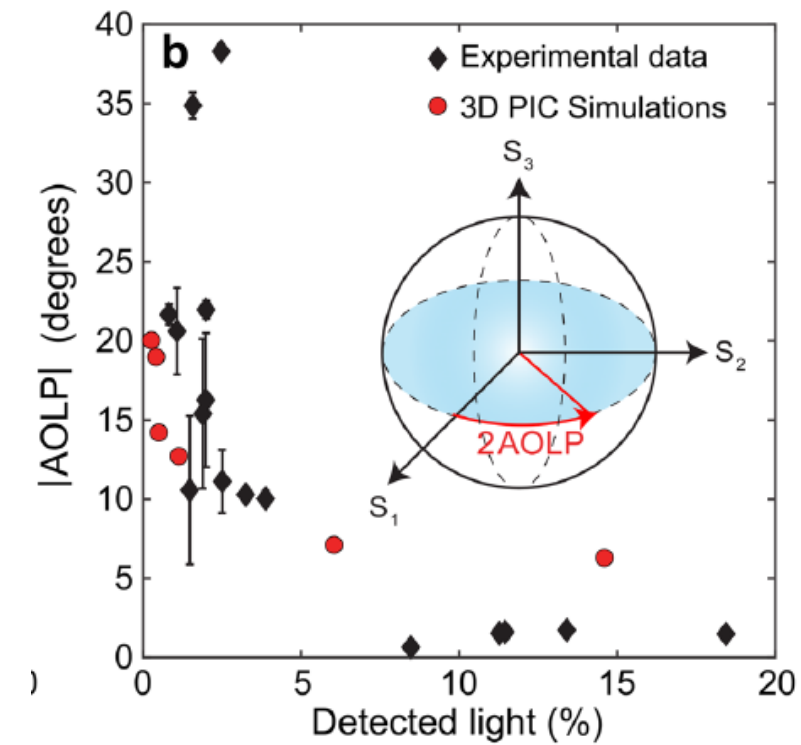


Summation of light from two modes results in an ‘effective’ polarisation shift

Measuring the polarisation of the transmitted light

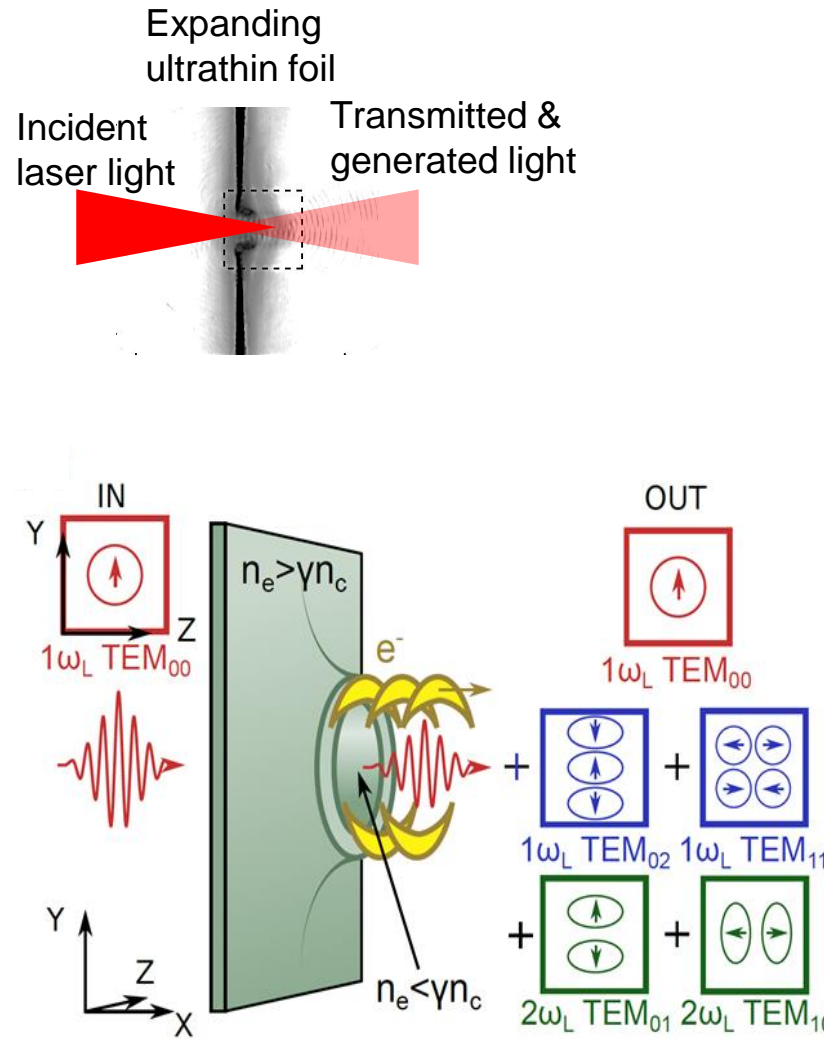


‘Effective’ polarisation shift highest with minimal laser transmission

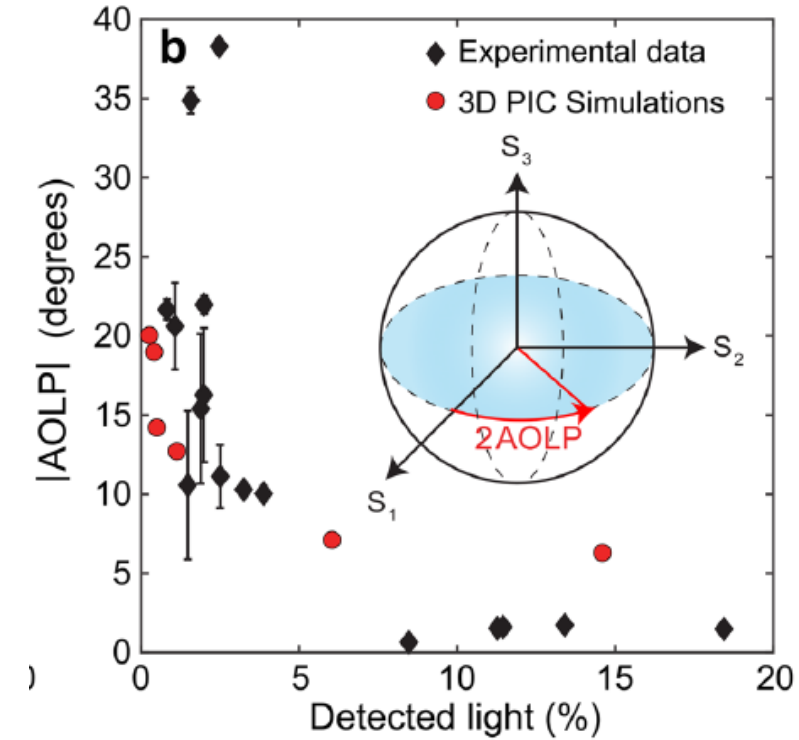


Duff *et al*, Scientific Reports 10, 105 (2020)

Summation of light from two modes results in an ‘effective’ polarisation shift



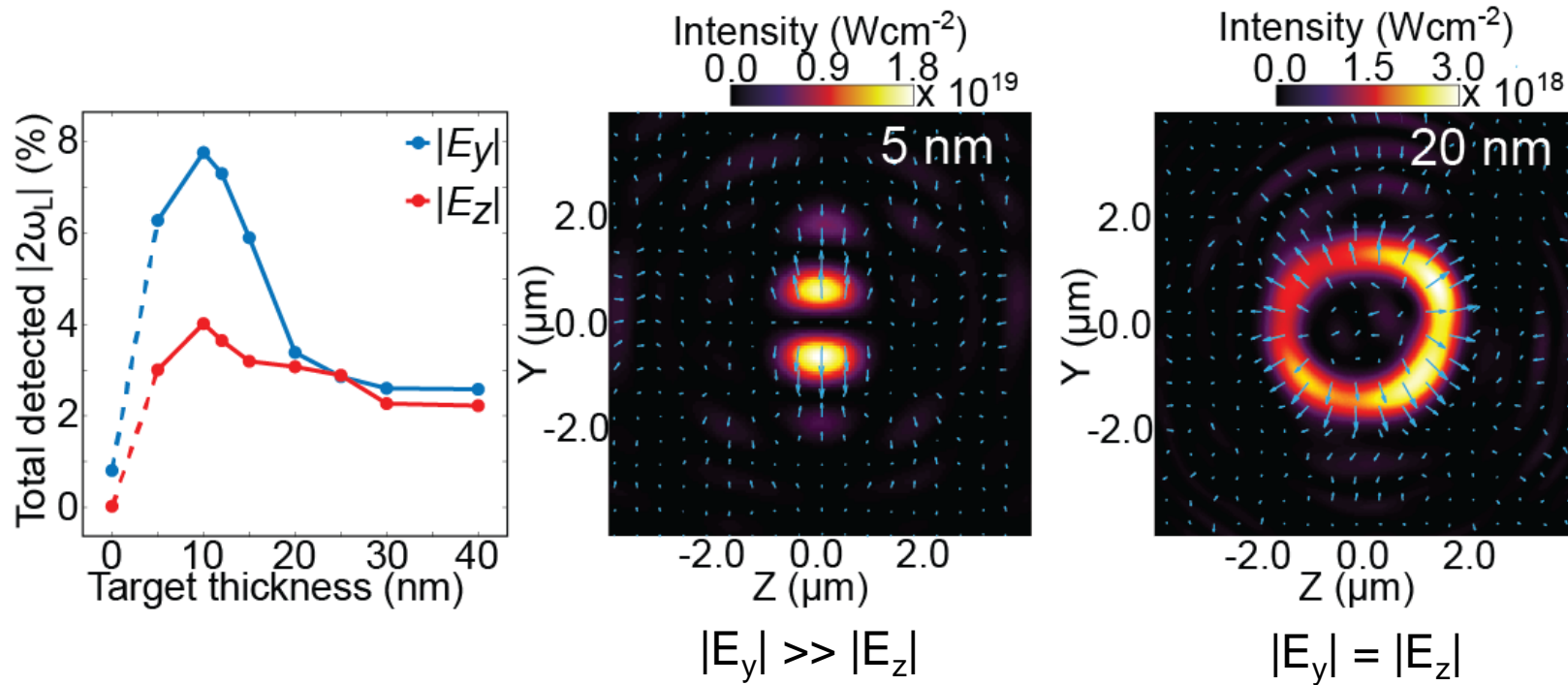
‘Effective’ polarisation shift highest with minimal laser transmission



Duff *et al*, Scientific Reports 10, 105 (2020)

High power light emission with tunable modes via a relativistic plasma aperture

Light emitted at the second harmonic is also in the form of TEMs



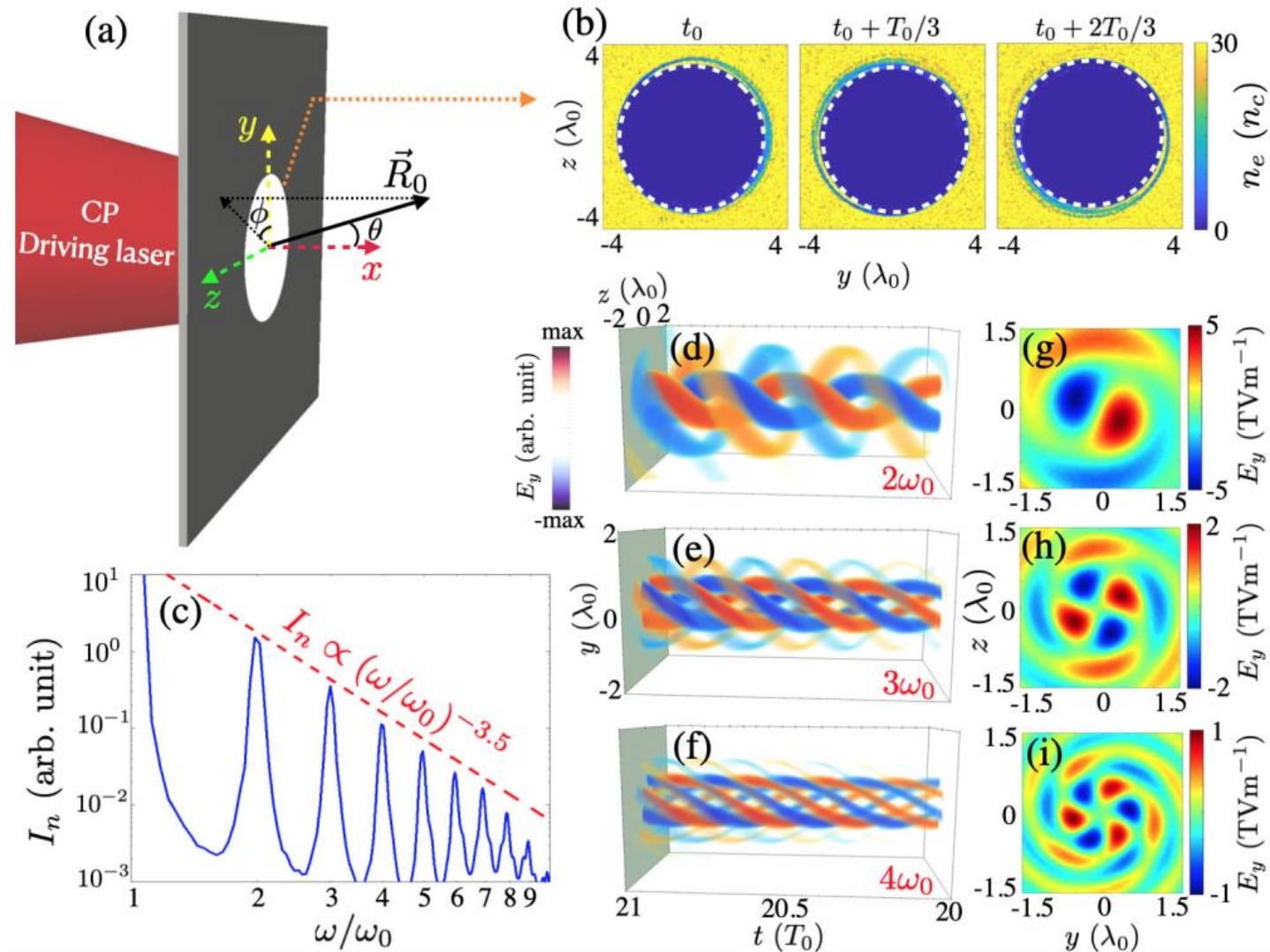
When the energy of the transmitted and self-generated light are approx. equal, a high intensity radially polarised mode is produced at $2\omega_L$

This process is tunable by varying any parameter which affects the onset of RSIT

High harmonic generation with relativistic oscillating aperture

Yi. Phys. Rev. Lett. **126**, 134801, 2021

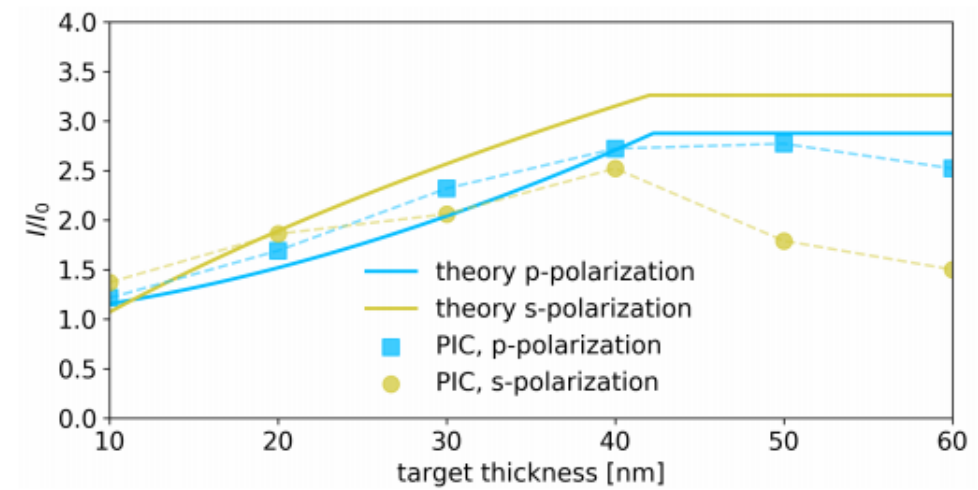
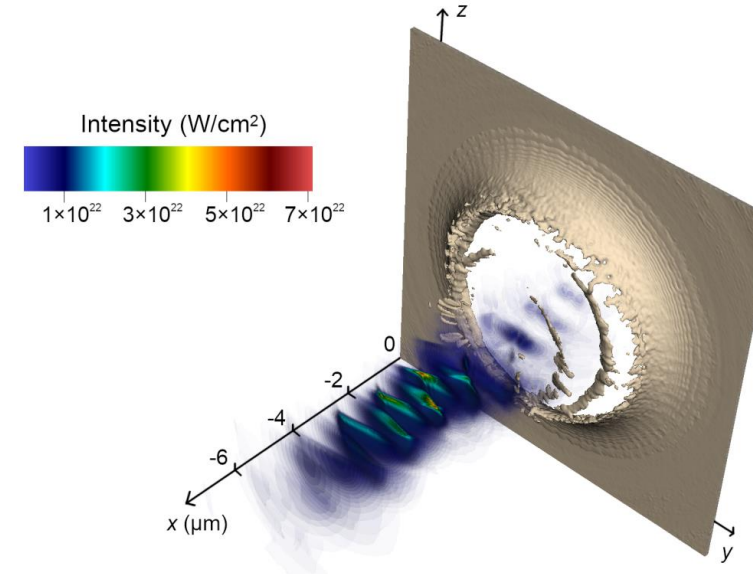
- Yi. reports that the relativistic oscillation of the critical surface in the laser field results in the generation of high harmonic radiation
- With circular polarisation the superposition of the diffracting harmonic radiation can yield beams with orbital angular momentum (OAM)



Relativistic plasma aperture for laser intensity enhancement

Jirka et al. Phys. Rev. Research 3, 033175 (2021)

- Jirka et al. reports that intensity enhancement can occur as the laser propagates through the formed relativistic plasma aperture in thin (nm) targets
- This occurs due to the superposition of generated harmonics from the aperture
- This can produce a localised intensity enhancement factor of >2.5 in 2D simulations – in 3D the intensity enhancement is a factor of >7



Lecture overview:

1. Introduction to high power lasers
2. Near critical density (NCD) plasma generation
3. Relativistic optics effects in NCD plasma
4. Relativistic plasma aperture
5. **Electron and ion acceleration in NCD plasma**
6. Strong-field QED phenomena
7. [Experimental considerations and methodology – if time permits]

Direct laser acceleration of electrons in NCD plasma

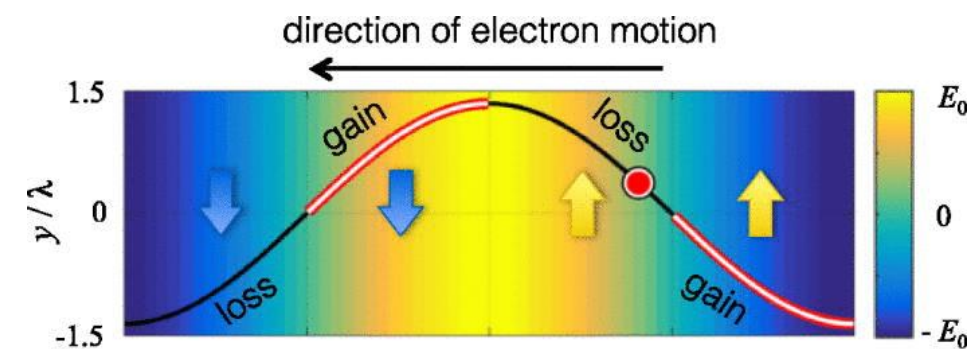
As relativistic electrons travel with a laser pulse they gain and lose energy (as they dephase).

If an accelerated electron leaves the finite spatial or temporal extent of the laser pulse, it will maintain the gained energy.

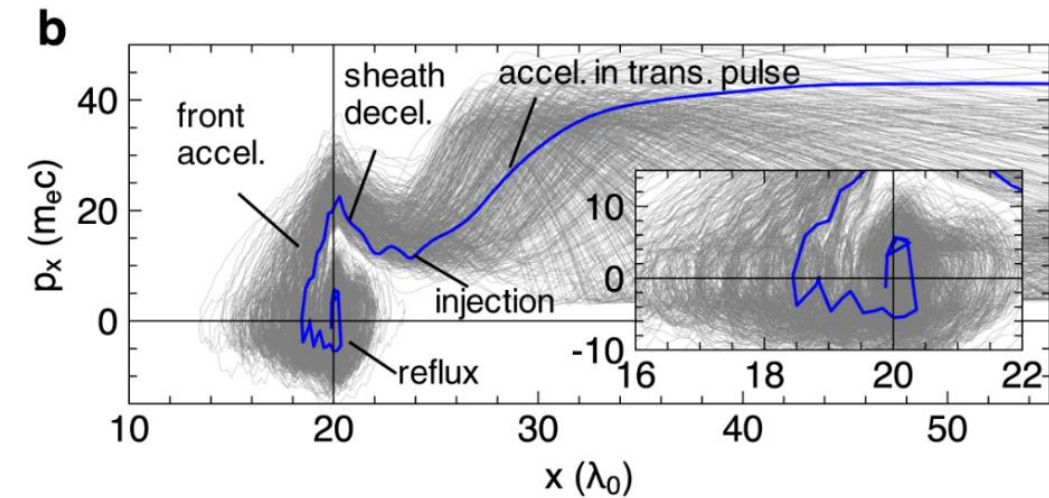
In the case of thin foil targets (and plasma channels), electrons are injected into the plasma at the front surface and propagate with the laser pulse

Electrostatic fields at the front and rear act to accelerate and decelerate the electrons which will affect the dephasing with the laser pulse

These electrons can then escape the finite extent of the laser pulse retaining their energy

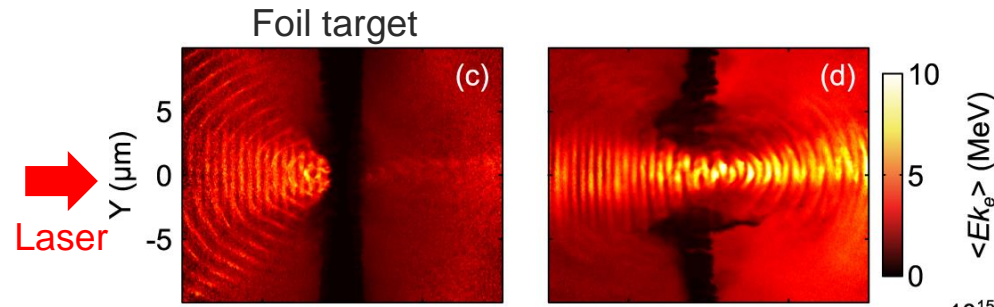


A. V. Arefiev et al. Physics of Plasmas 23, 056704 (2016)

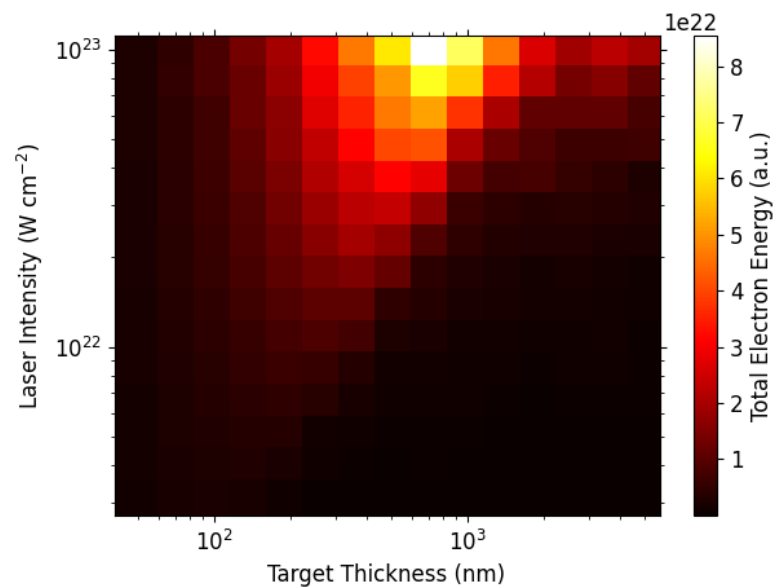


Singh et al, Nature Comms.13, 54 (2022)

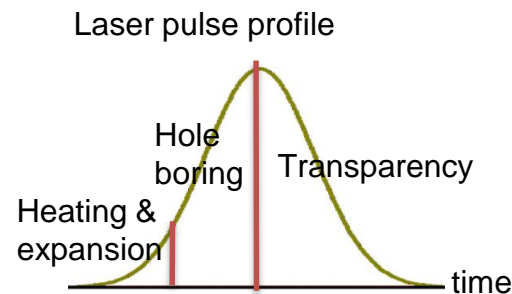
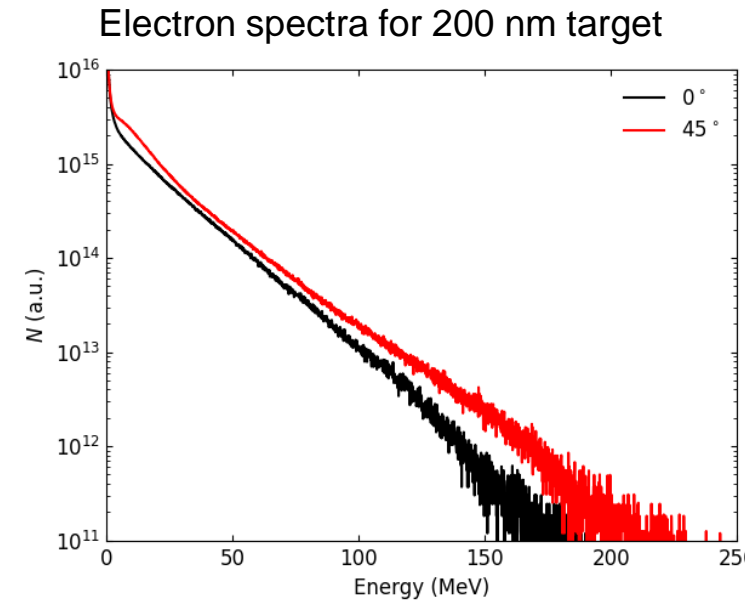
Direct laser acceleration of electrons in NCD plasma



The transition from opaque to relativistically transparent target enables direct laser acceleration of electrons



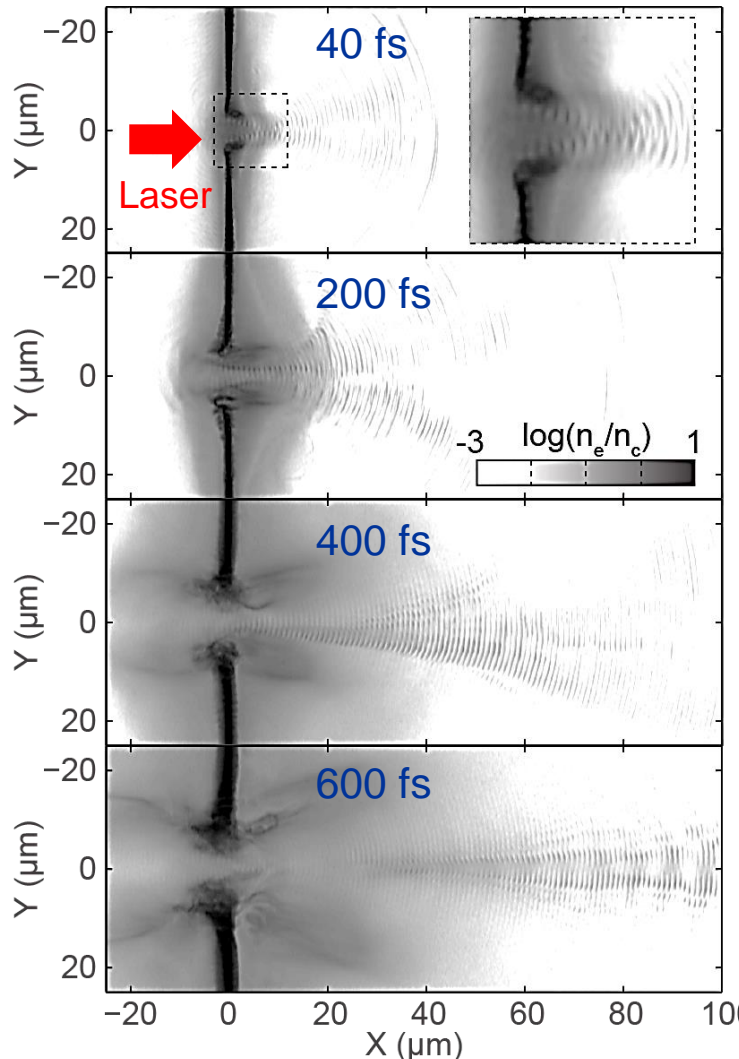
Optimum target thickness for direct laser acceleration of electrons increases with laser intensity



Optimum thickness when transparency occurs near the peak of the laser pulse interaction

Direct electron acceleration forms a modulated jet

Electron density maps from 2D PIC simulations using
EPOCH code: $5 \times 10^{20} \text{ Wcm}^{-2}$; ultrathin Al foils

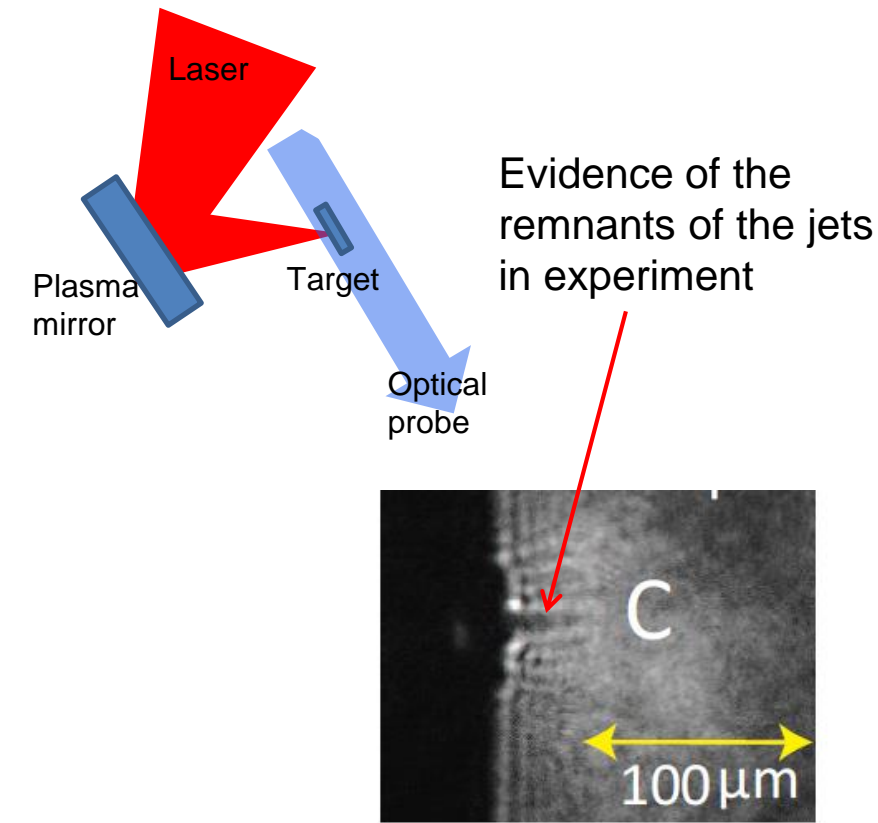
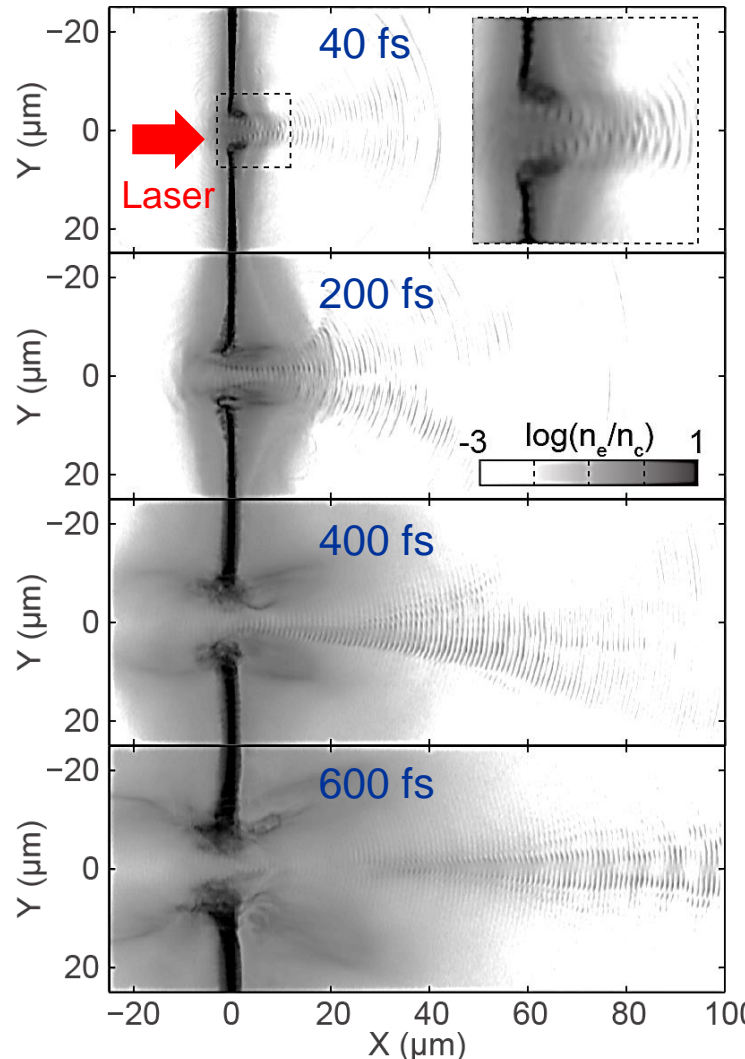


Short pulse – minimal expansion –
'relativistic plasma aperture'

Longer pulse – significant expansion –
plasma jet of directly accelerated electrons

Direct electron acceleration forms a modulated jet

Electron density maps from 2D PIC simulations using
EPOCH code: $5 \times 10^{20} \text{ Wcm}^{-2}$; ultrathin Al foils

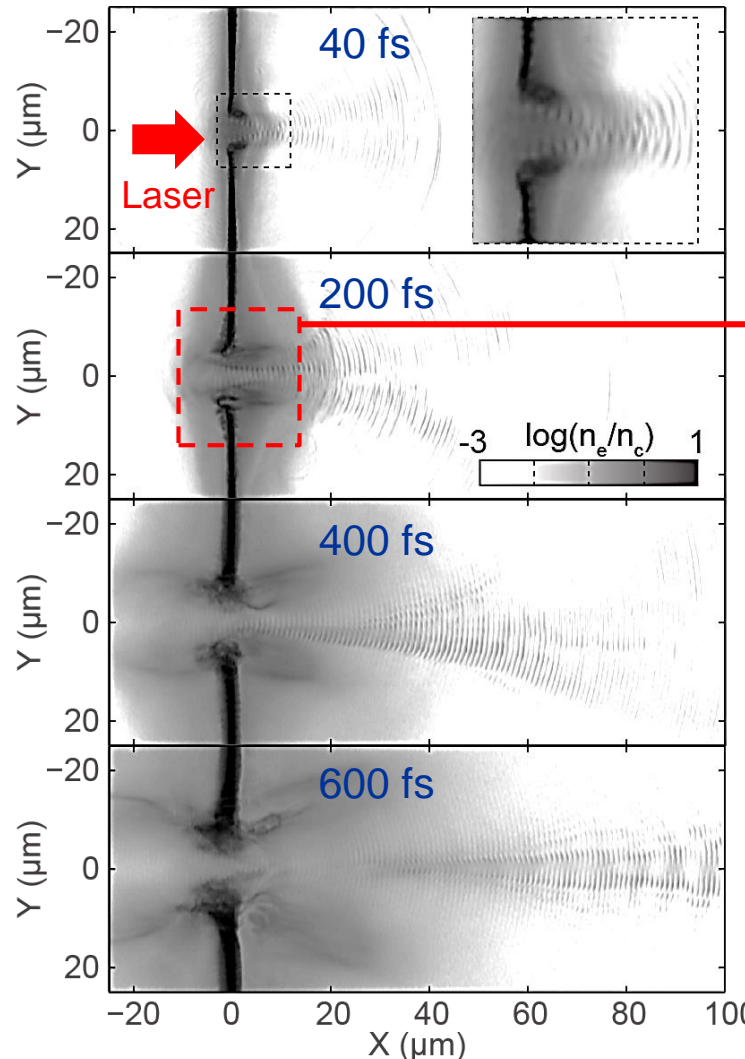


H. Powell et al, New J. Phys. 17, 103033 (2015)

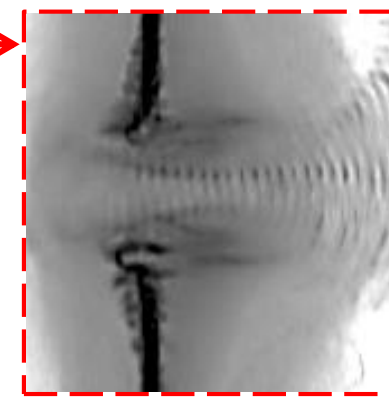
M. King et al, Nuc. Ins. Meth. A, 829, 163 (2016)

Direct electron acceleration forms a modulated jet

Electron density maps from 2D PIC simulations using
EPOCH code: $5 \times 10^{20} \text{ Wcm}^{-2}$; ultrathin Al foils



Short pulse – minimal expansion –
'relativistic plasma aperture'

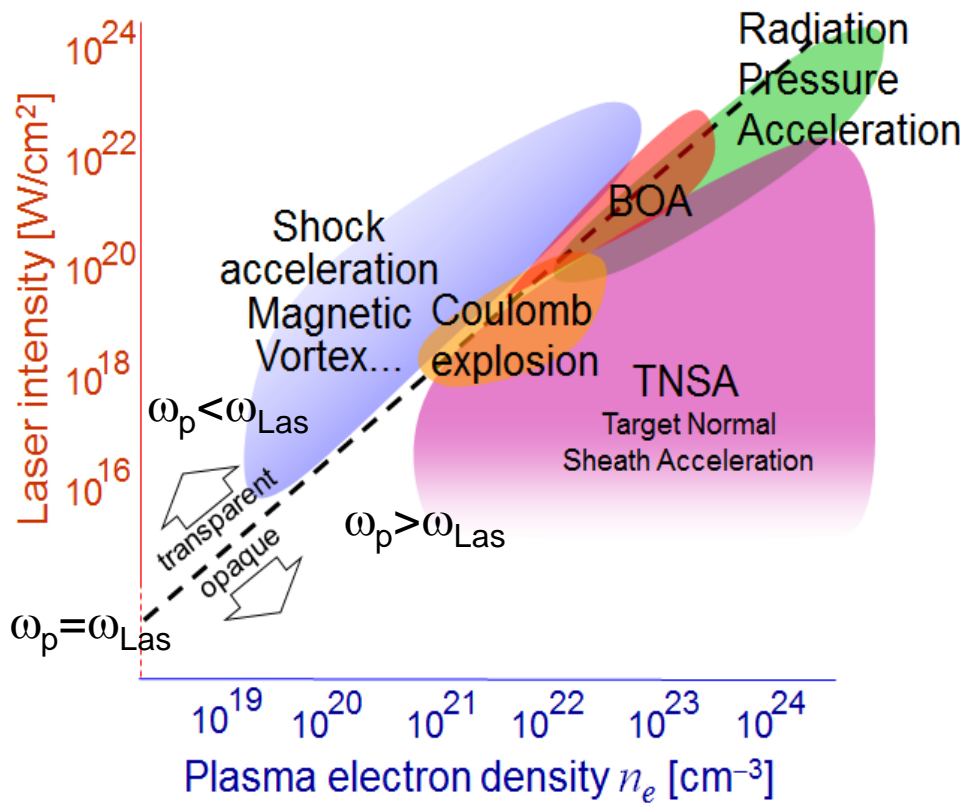


Self-focusing can occur,
enhancing laser
intensity

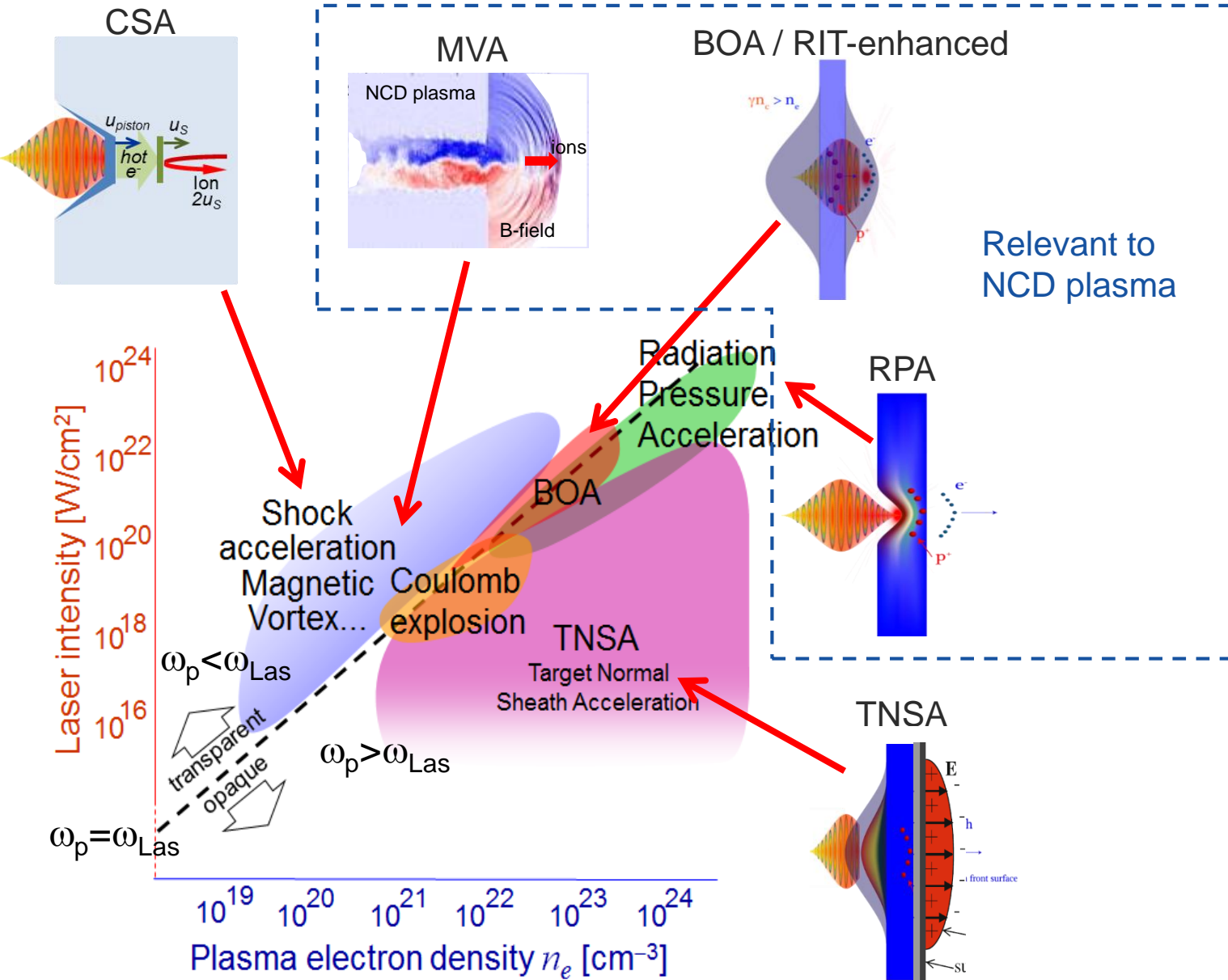
Longer pulse – significant expansion –
plasma jet of directly accelerated electrons

Laser-driven ion acceleration

Numerous acceleration mechanisms have been identified, in overdense, underdense and near critical density targets

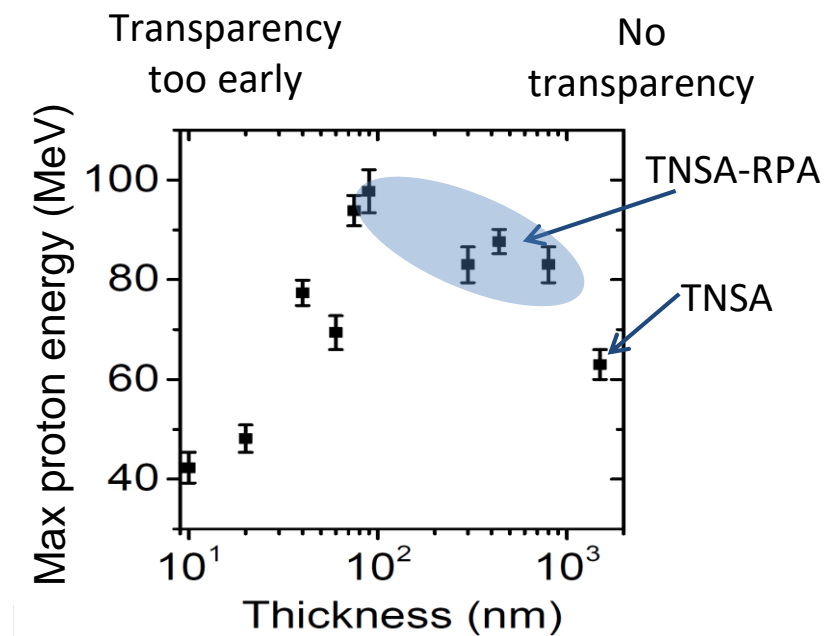
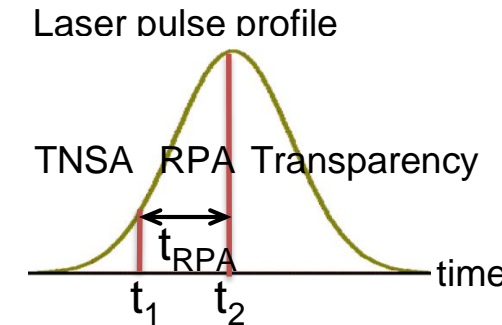
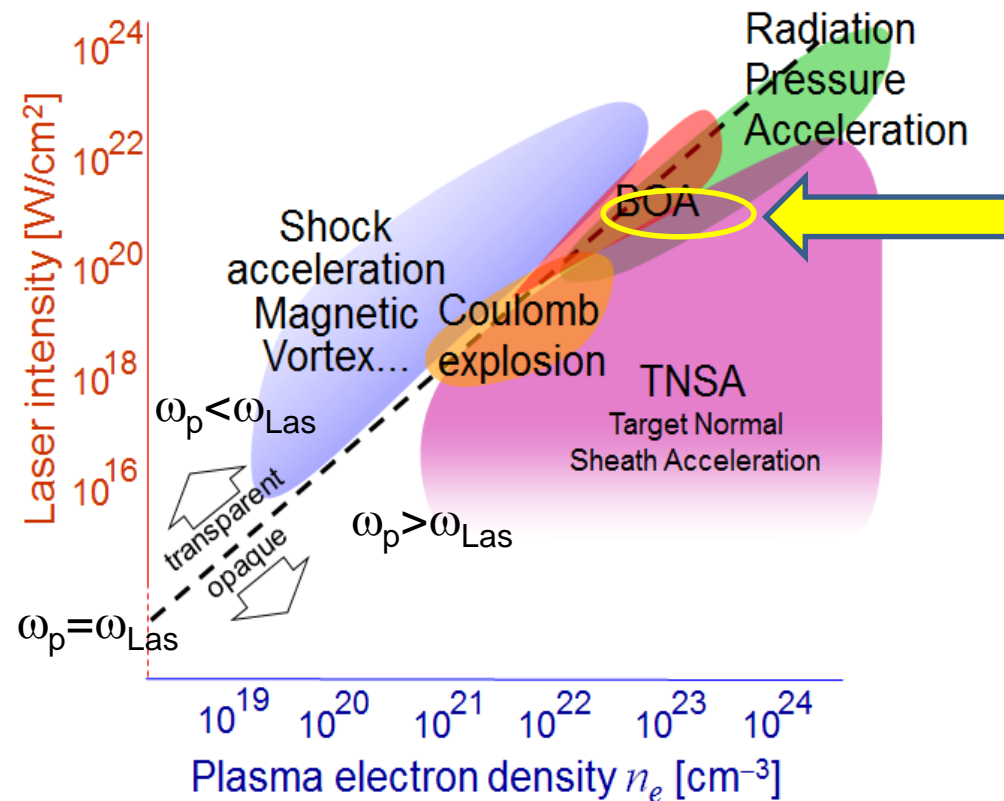


Laser-driven ion acceleration



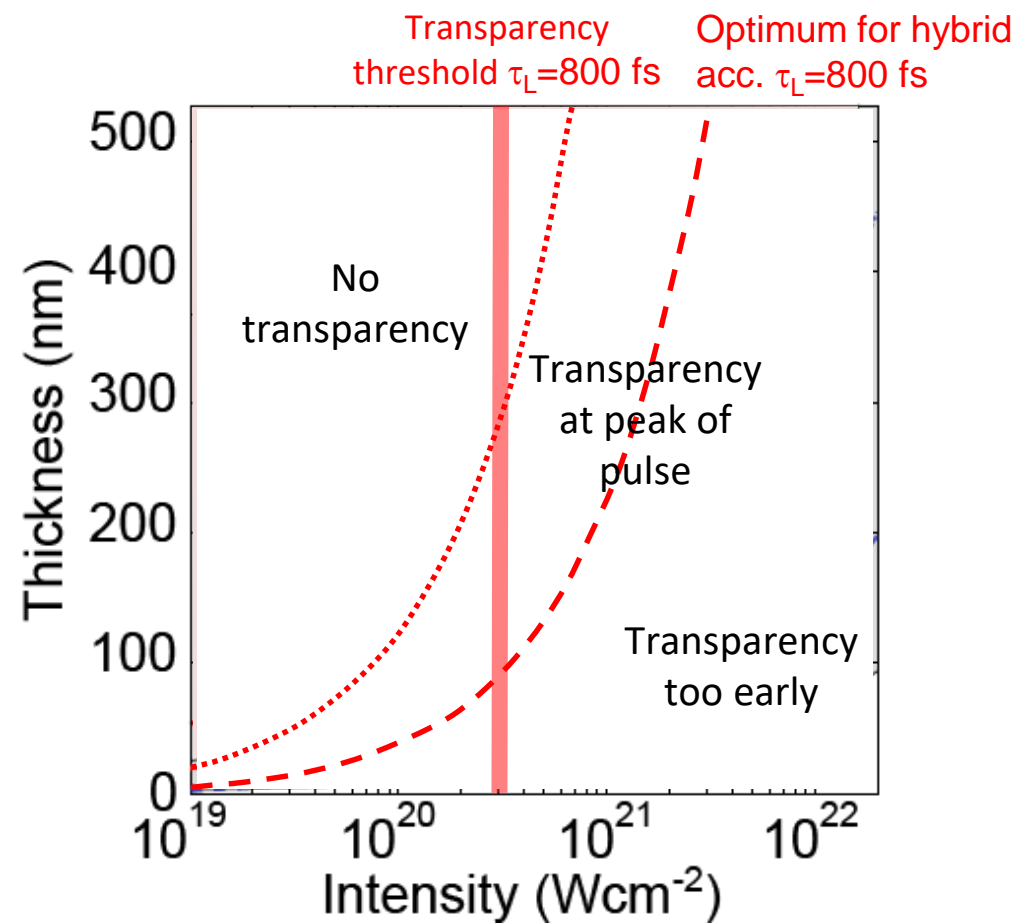
Laser-driven ion acceleration schemes

Highest energy protons measured achieved with ultrathin foils expanding to NCD and becoming relativistically transparent during the interaction



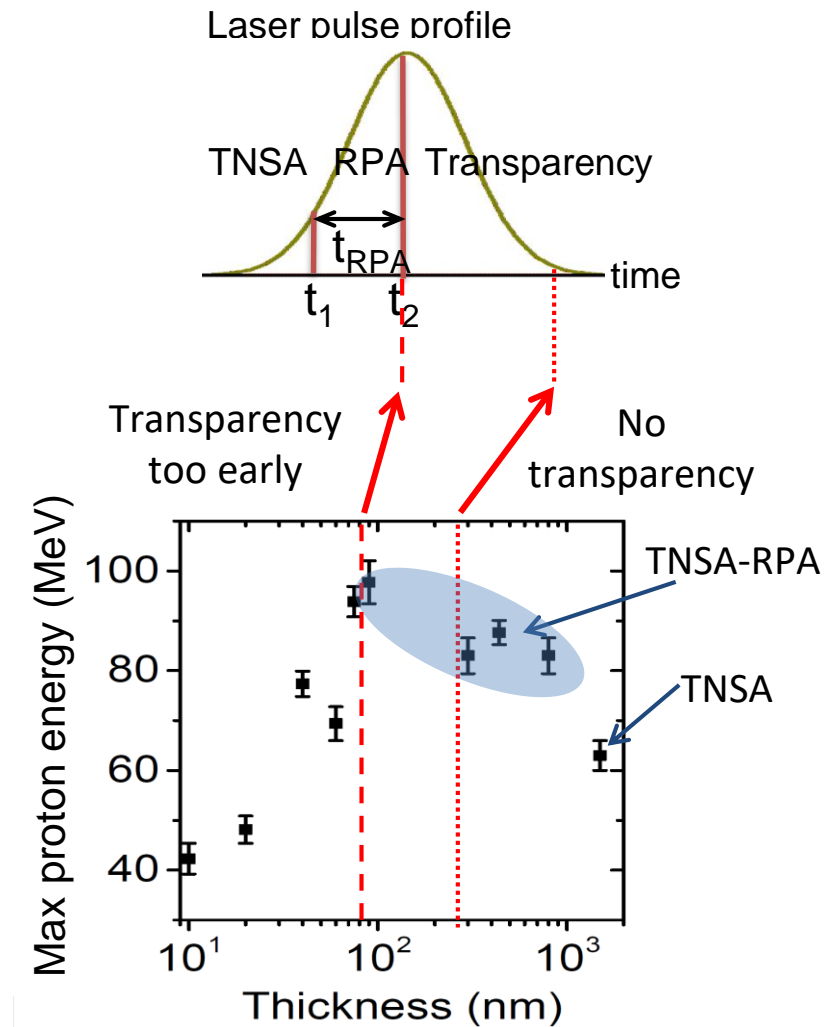
Higginson et al, Nature Communications, 9, 724 (2018)

Transparency-enhanced hybrid RPA-TNSA* parameter space



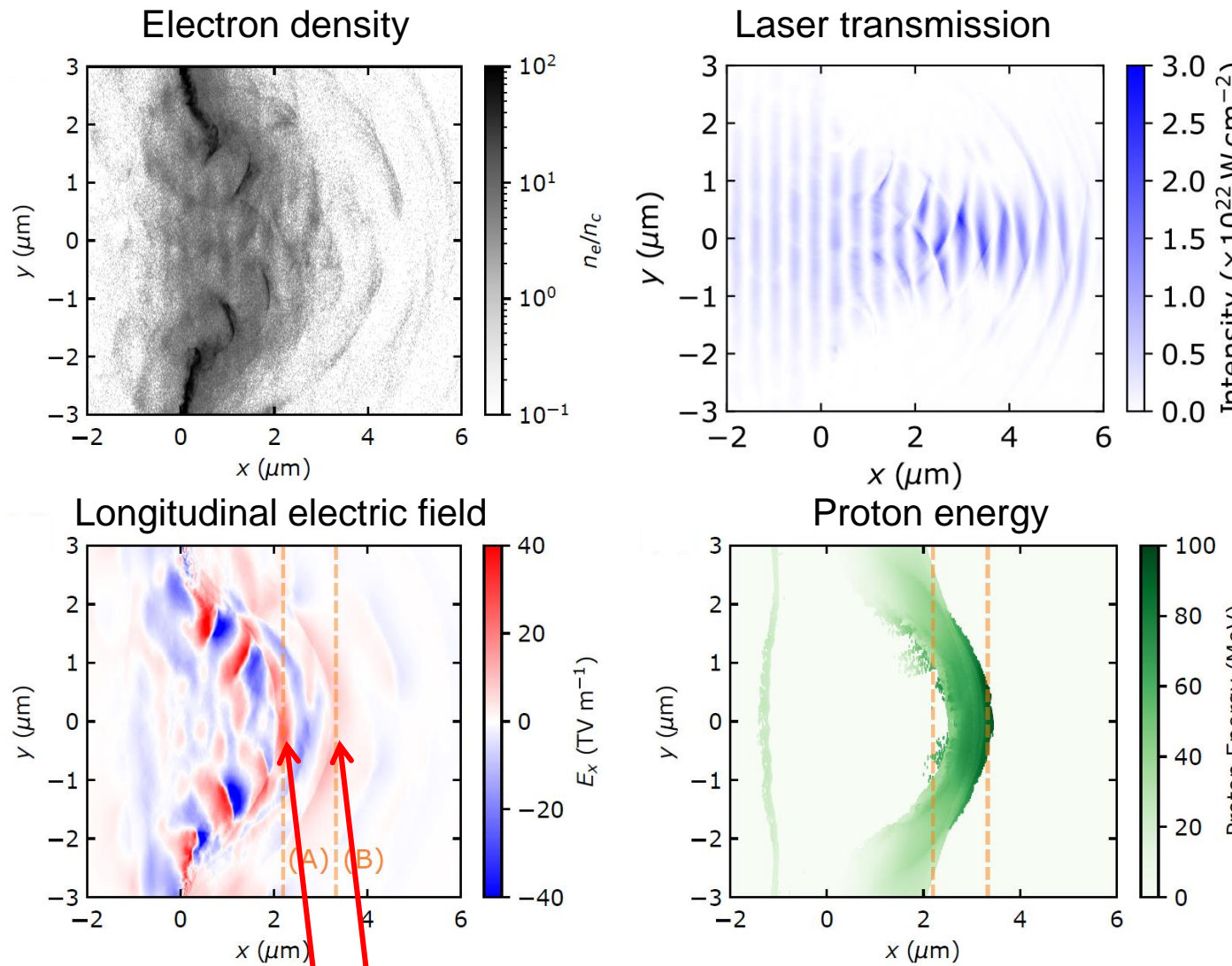
Semi-empirical model, based on plasma expansion model reported in X.Q. Yan et al., Appl Phys B, 98, 711 (2010)

*Hybrid RPA-TNSA scheme: B. Qiao et al., PRL108, 115002 (2012)



Higginson et al, Nature Communications, 9, 724 (2018)

Snapshots of the simulation grid after the onset of RSIT for thickness $l = 125\text{nm}$ and $a_0 = 50$

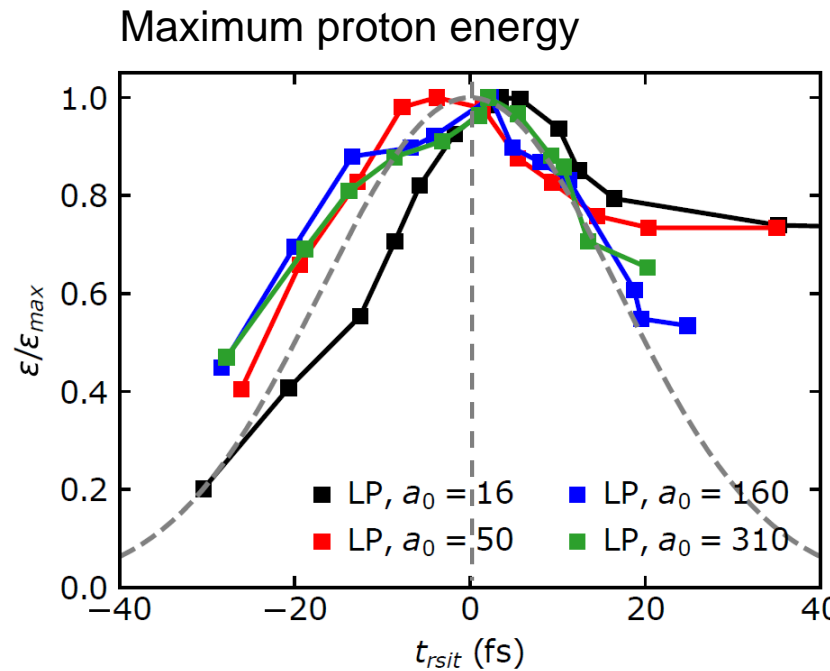
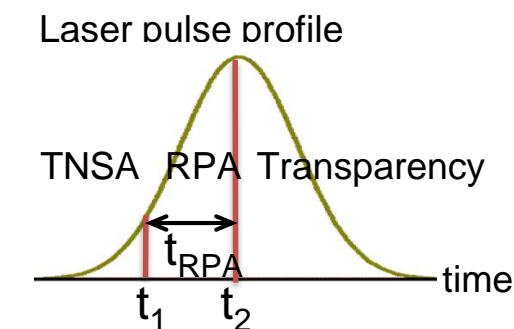


Dual-peaked electric field remains until laser pulse decays

2D EPOCH PIC code
 Pulse duration=40 fs (FWHM)
 focal spot = 3 μm (FWHM)
 wavelength = 0.82 μm
 5×10^{20} - $2 \times 10^{23} \text{ W cm}^{-2}$
 $(a_0=16-310$ for linear polarisation)

Proton beam properties as a function of relativistic transparency onset time: scaling to multi-PW lasers

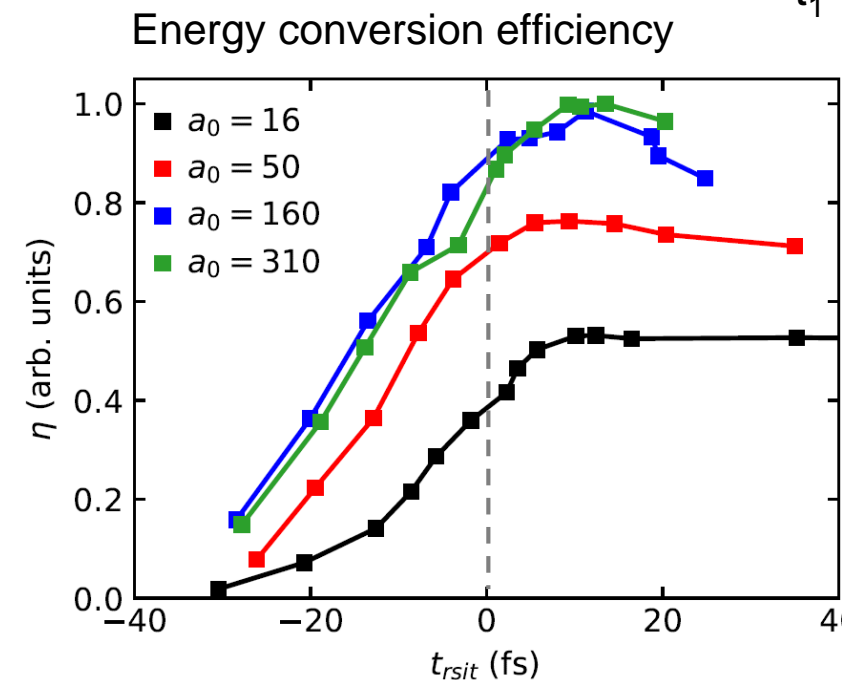
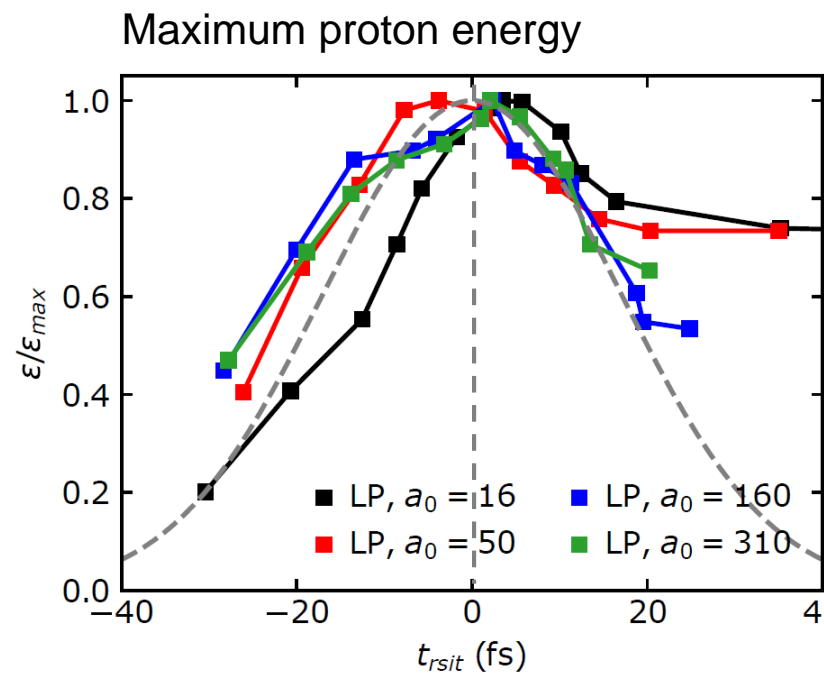
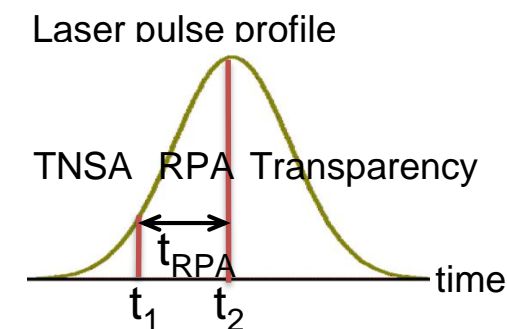
J Goodman *et al* New J. Phys. **24** 053016 (2022)



- Proton energy is maximised when transparency occurs at the peak of the laser pulse interaction

Proton beam properties as a function of relativistic transparency onset time: scaling to multi-PW lasers

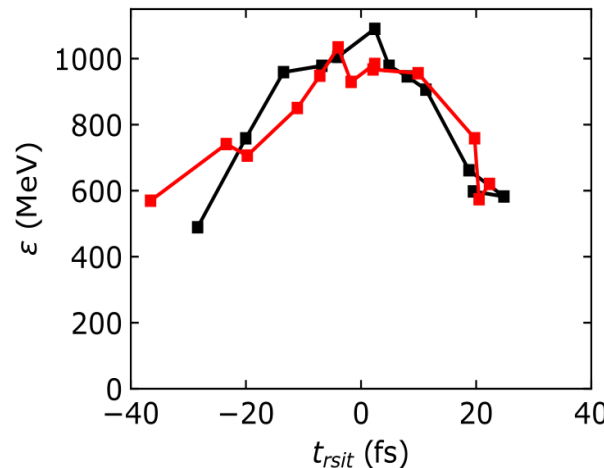
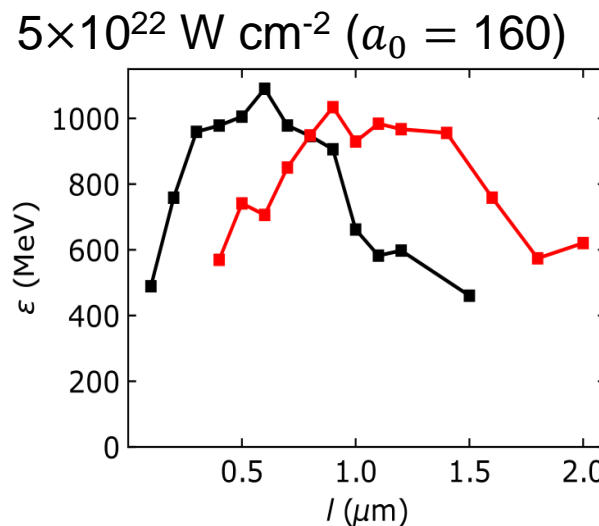
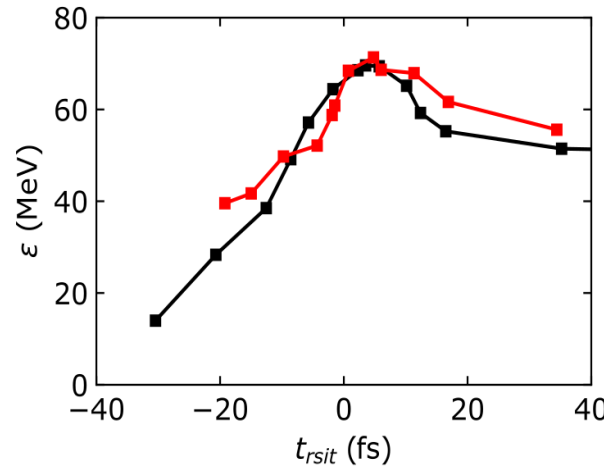
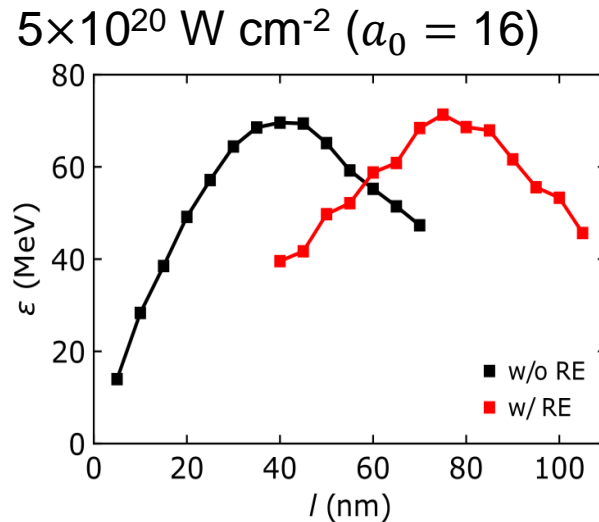
J Goodman *et al* New J. Phys. **24** 053016 (2022)



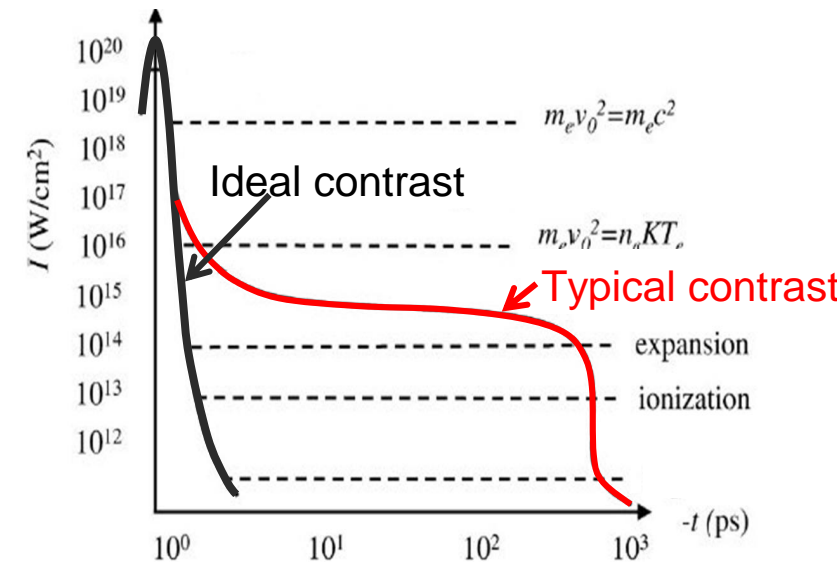
- Proton energy is maximised when transparency occurs at the peak of the laser pulse interaction
- Energy conversion efficiency saturates if transparency occurs later in time

Proton energy scaling to multi-PW lasers

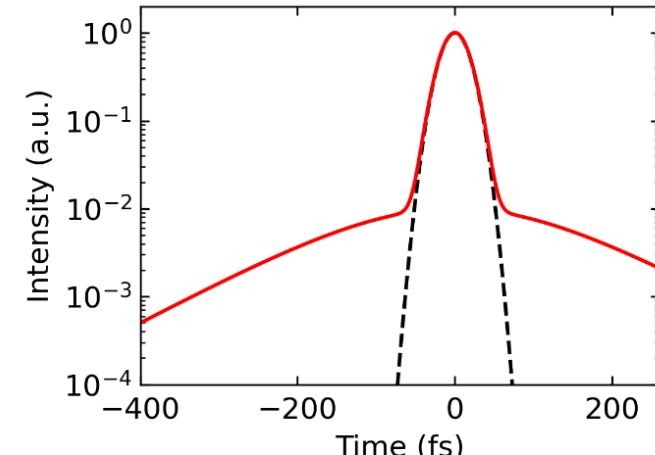
J Goodman *et al* New J. Phys. **24** 053016 (2022)



Increase in the optimum foil thickness, but energy still maximised when transparency occurs at the peak



Simulated laser rising edge profile



Lecture overview:

1. Introduction to high power lasers
2. Near critical density (NCD) plasma generation
3. Relativistic optics effects in NCD plasma
4. Relativistic plasma aperture
5. Electron and ion acceleration in NCD plasma
6. **Strong-field QED phenomena**
7. [Experimental considerations and methodology – if time permits]

Strong-field quantum electrodynamics (QED) processes

- Strong electric fields are those that approach or exceed the QED critical field strength, E_{cr} , in which interactions become highly nonlinear.
- High power laser–plasma interactions can provide the framework for the study of strong-field QED processes
- Laser fields provide a strong electromagnetic field and generate high-energy particles.
- 10 PW laser facilities should enable a new radiation dominated regime to be achieved experimentally

QED critical field (the field that classically would accelerate an electron to its rest mass energy in a Compton length): $E_{cr} = \frac{m_e^2 c^3}{e\hbar} = 1.3 \times 10^{18} V/m$

This field strength requires a laser intensity of the order of $5.65 \times 10^{29} W/cm^2$ and $a_0 = 4.1 \times 10^5$ for a 1 μm laser field.

Strong-field quantum electrodynamics (QED) processes

The parameter that characterizes the interaction of electrons, positrons, and photons with strong EM fields is:

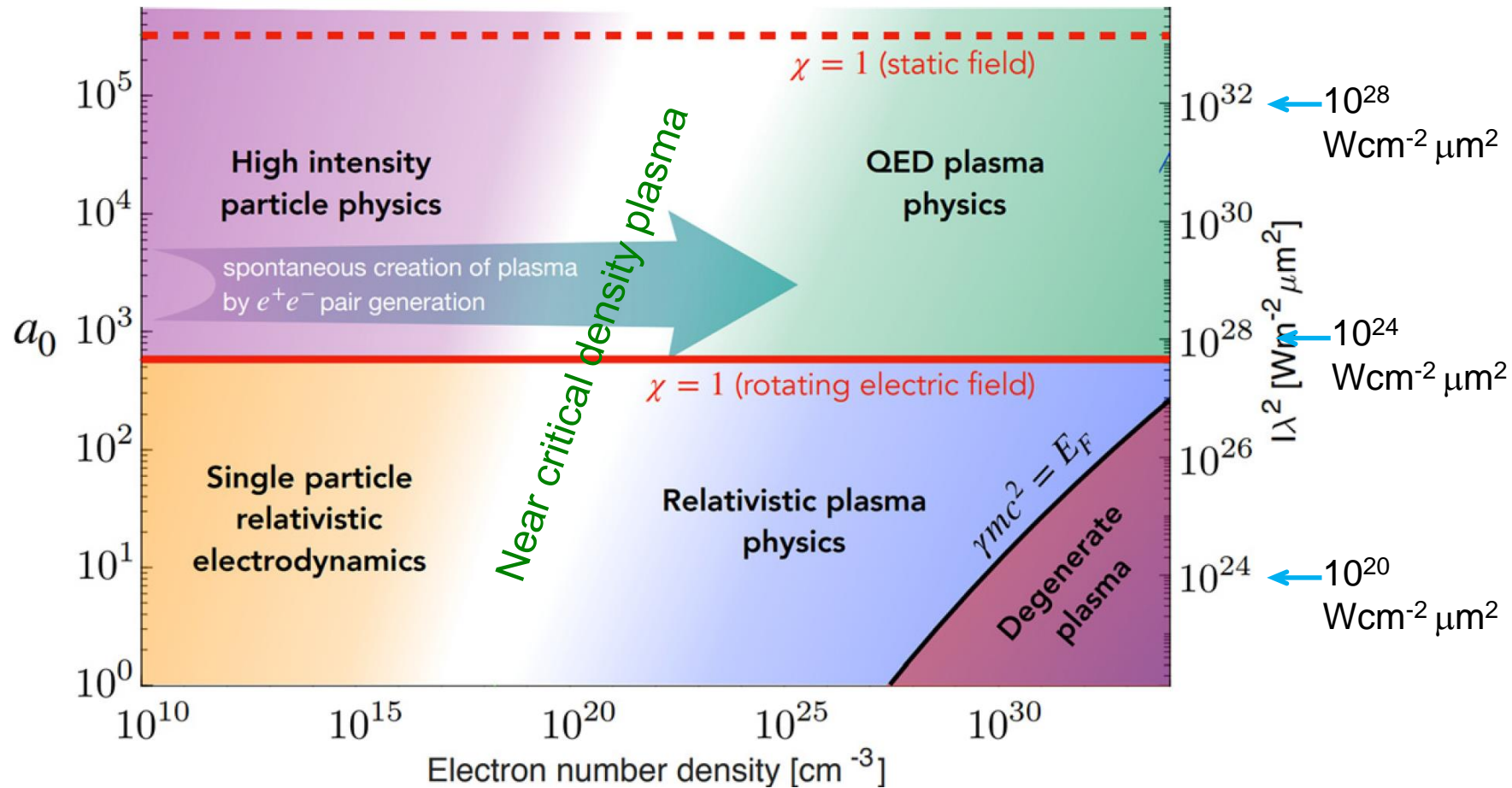
$$\chi = \left(\frac{\gamma E}{E_{cr}} \right) (1 - \beta \cos \theta)$$

Lorentz factor Electron velocity Angle between electron momentum and laser wave vector

χ maximised when:

- the electron counter-propagates with the laser
- for high γ (i.e. high energy electrons)
- when the electron momentum is perpendicular to the electric field, which can be achieved with colliding laser pulses - in circular polarization, the electric field and electron momentum in equilibrium motion (i.e., circulating) are (close to) perpendicular

Different regimes of strong field physics



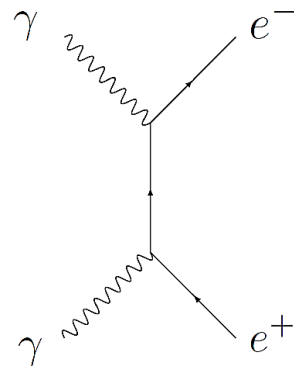
Adapted from Zhang et al., Phys. Plasmas 27, 050601 (2020)

Basic QED processes in strong fields

Breit–Wheeler pair-production

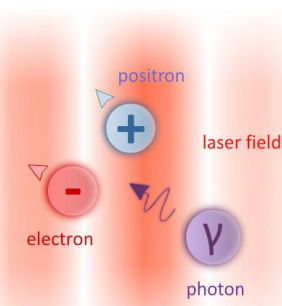
Breit–Wheeler pair production

$$\gamma + \gamma \rightarrow e^+ + e^-$$



Nonlinear or multi-photon Breit–Wheeler

$$\gamma + n\hbar\omega \rightarrow e^+ + e^-$$



Wikipedia.com

Radiation reaction

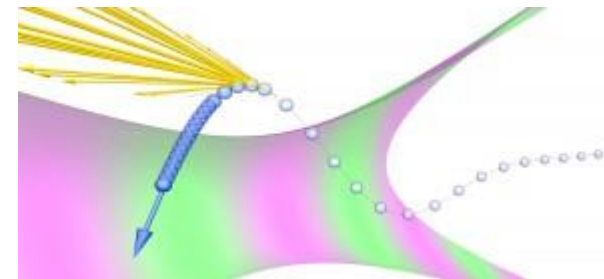
Accelerating charges radiate and thus must lose energy

How this occurs in very strong fields is not well understood

$$\frac{dp}{dt} = -e \cdot (\mathbf{E} + \mathbf{v} \times \mathbf{B}) + RR$$

Lorentz force

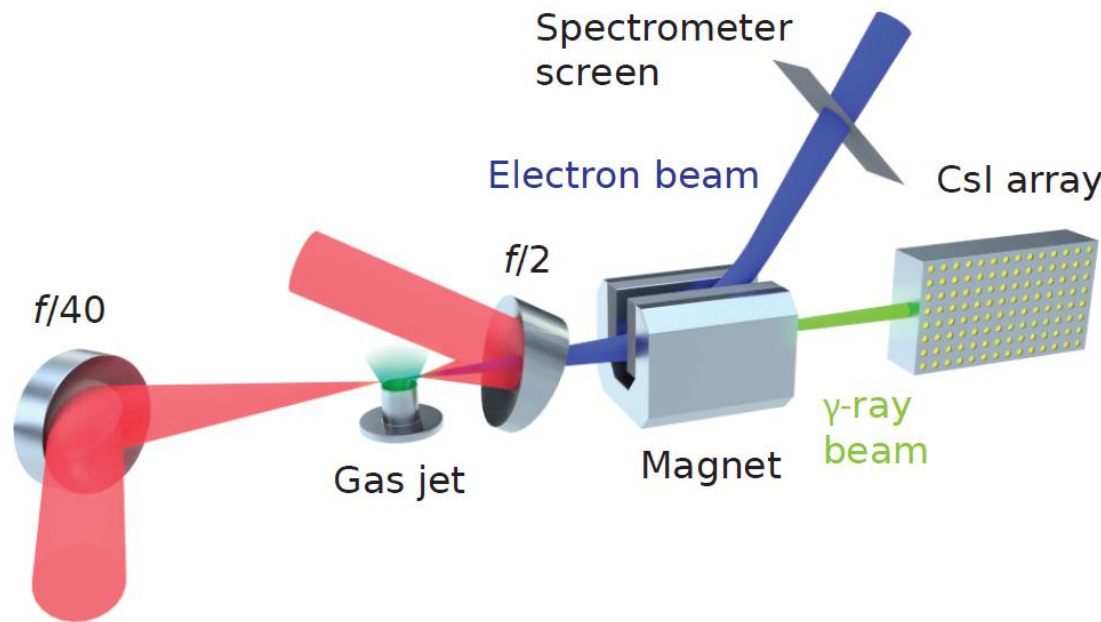
Radiation reaction force



novuslight.com

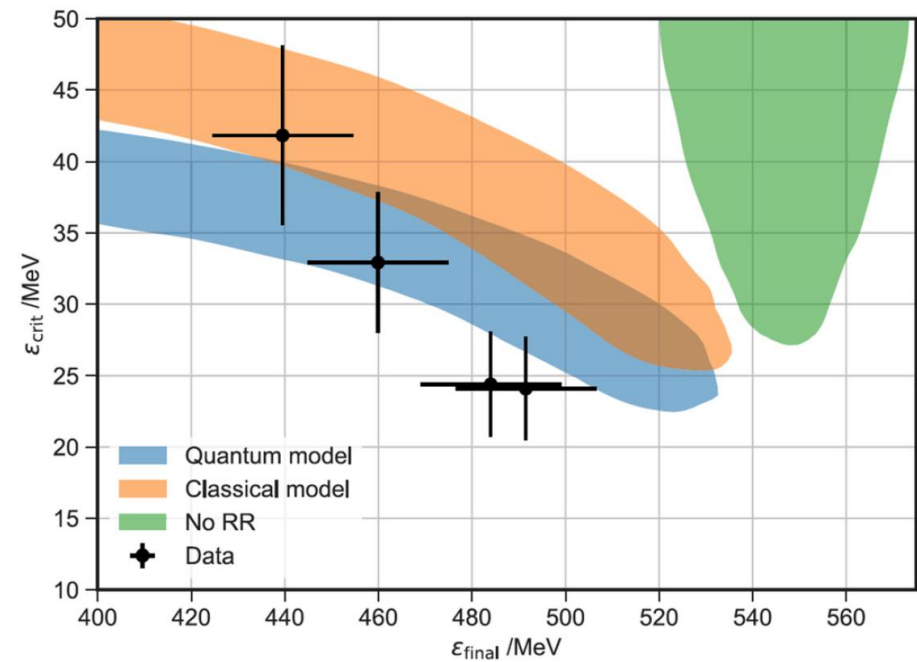
Experiments on radiation reaction physics

Can access strong fields in frame of relativistic beam
 – collide high intensity laser pulse with relativistic electron beam



Comparison of experimental data (points with error bars) and different models (shaded areas) for the critical energy ϵ_{crit} as a function of the post-collision energy of the electron beam ϵ_{final} .
 ϵ_{crit} is a characteristic energy of the photon spectrum, measuring the spectral shape

Cole et al., Phys. Rev. X 8, 011020 (2018)
 Poder et al., Phys. Rev. X 8, 031004 (2018)



Classical – emission continuous
 Quantum – emission is discrete (photons)

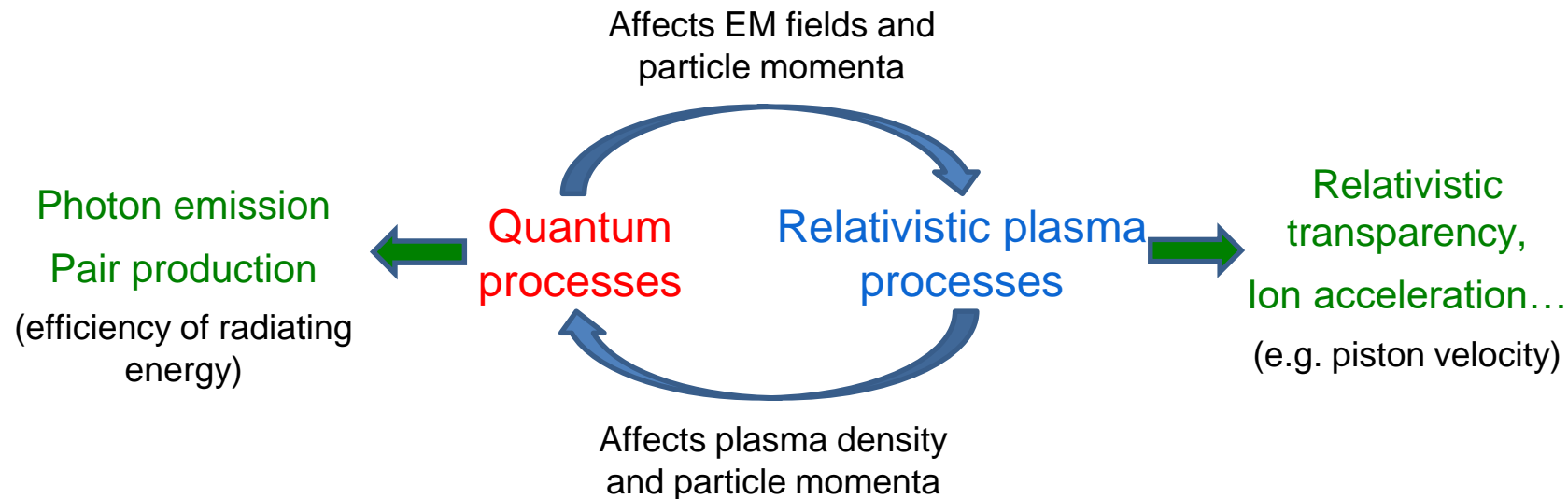
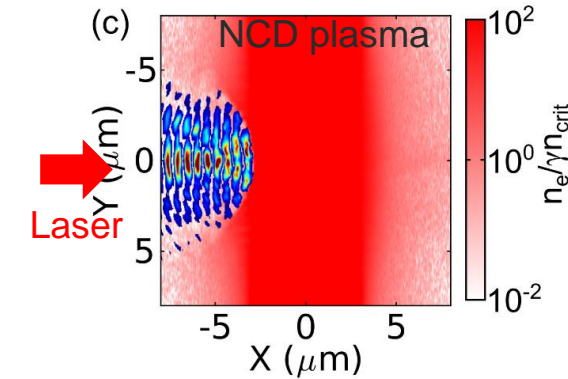
Collective effects: the QED-Plasma regime

Quantum effects continuously change the basic plasma parameters (e.g., plasma density, plasma temperature, and plasma frequency) during the interaction of light and matter.

As a result, the collective behaviour of QED plasmas would be very different from those of the classical plasmas.

Potentially important at intensities above 10^{22} Wcm^{-2}

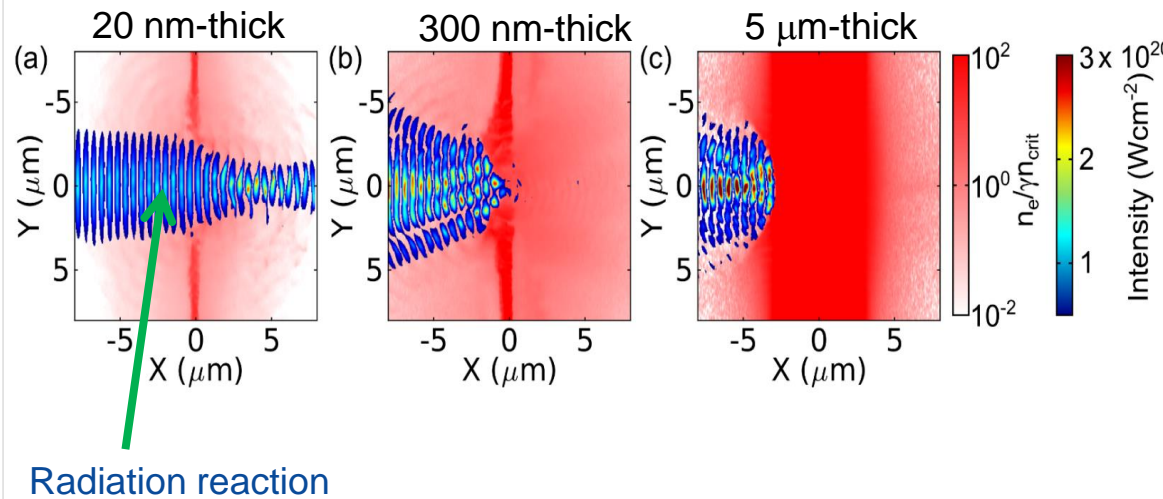
Of the order of 30%-40% of laser energy converted to radiation



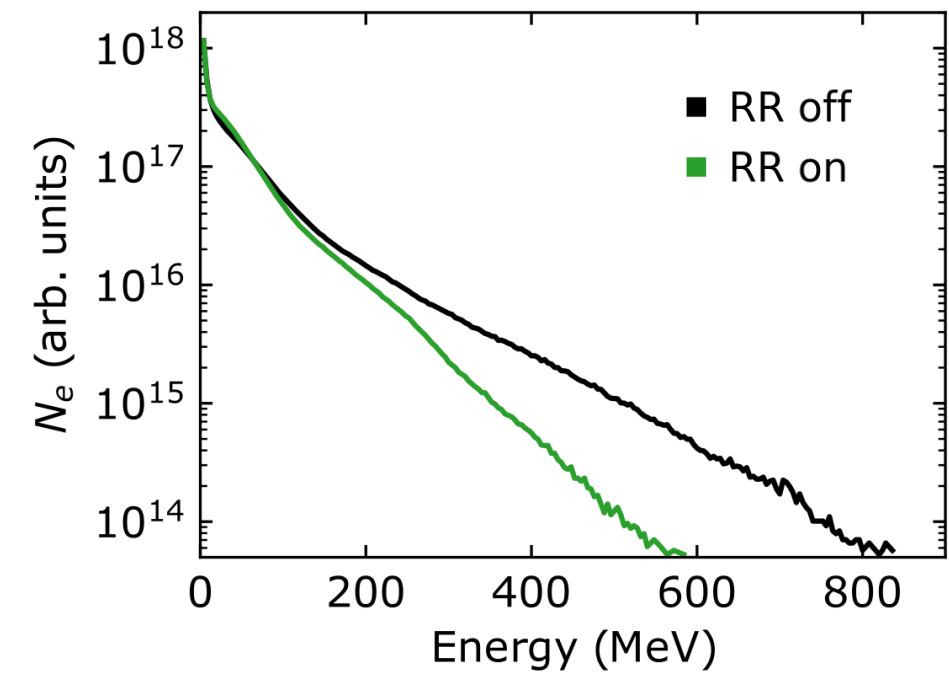
Radiation reaction affects ion acceleration at laser intensities $>10^{23} \text{ Wcm}^{-2}$

Radiation reaction will change the electron energy and laser propagation dynamics and thus ion acceleration in NCD plasma

This has been explored numerically in PIC simulations with and without radiation reaction included



Electron spectra at $2 \times 10^{23} \text{ W cm}^{-2}$ ($a_0 = 310$) with and without radiation reaction

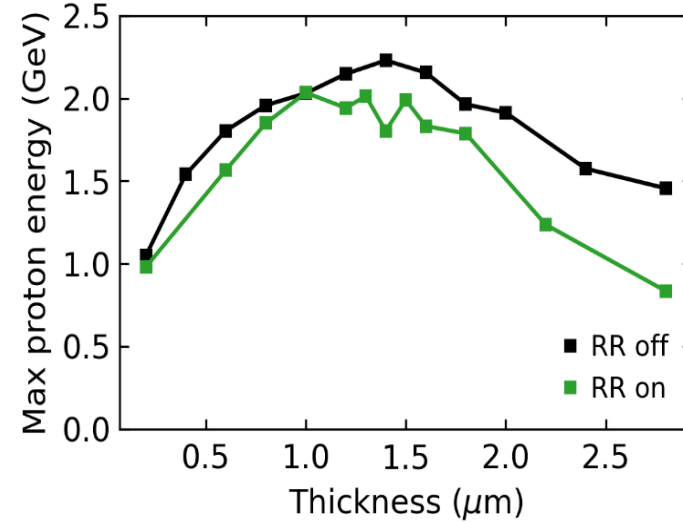


J Goodman et al 2022 New J. Phys. 24 053016

Radiation reaction affects ion acceleration at laser intensities $>10^{23} \text{ Wcm}^{-2}$

Radiation reaction turned off and on in the PIC code

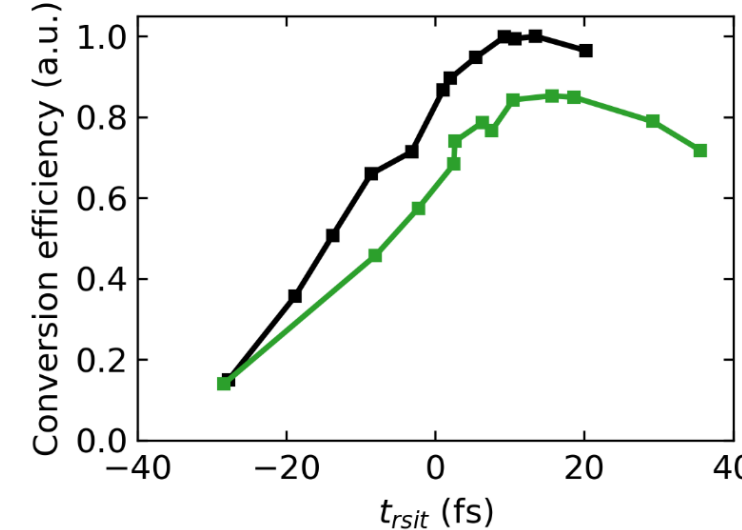
Lower proton energies



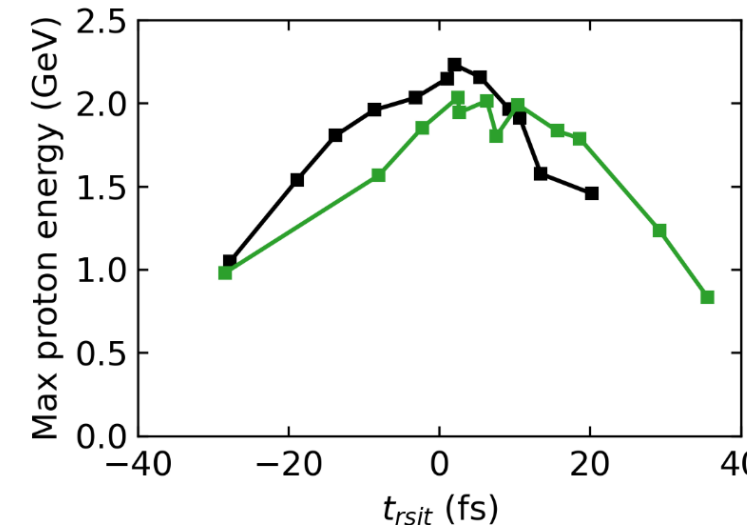
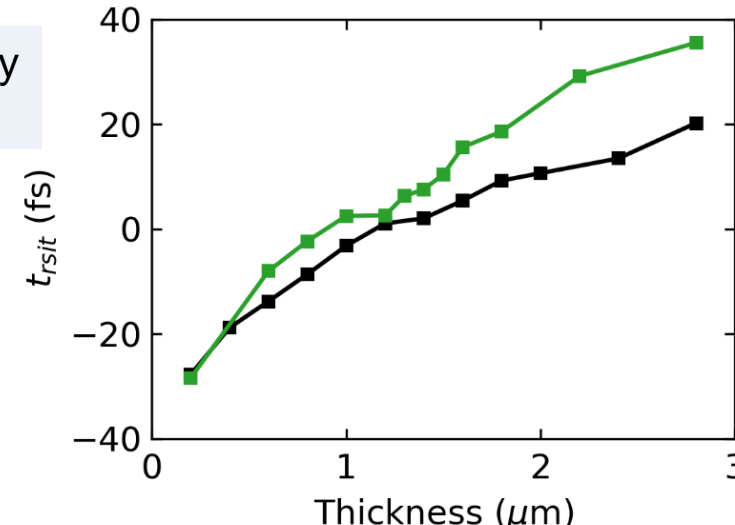
■ RR off
■ RR on

$2\times10^{23} \text{ W cm}^{-2} (a_0 = 310)$

Reduced conversion efficiency



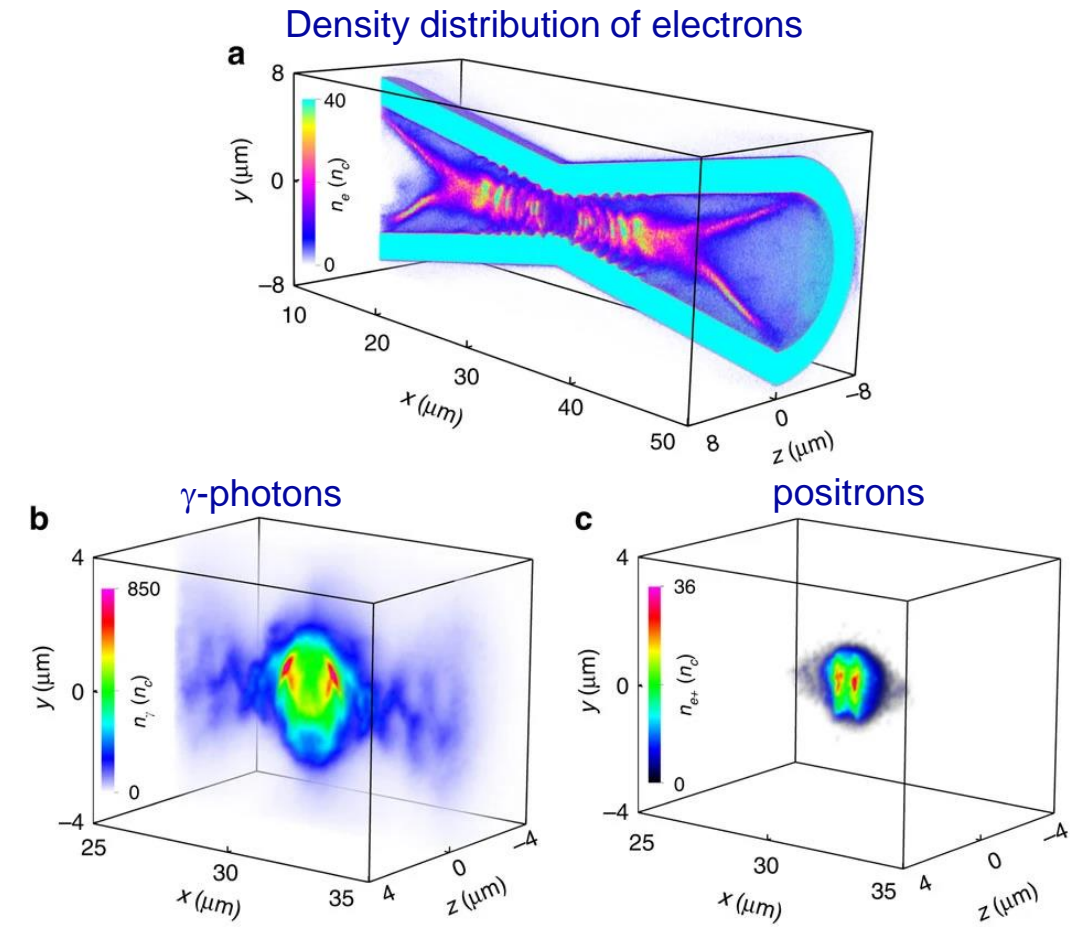
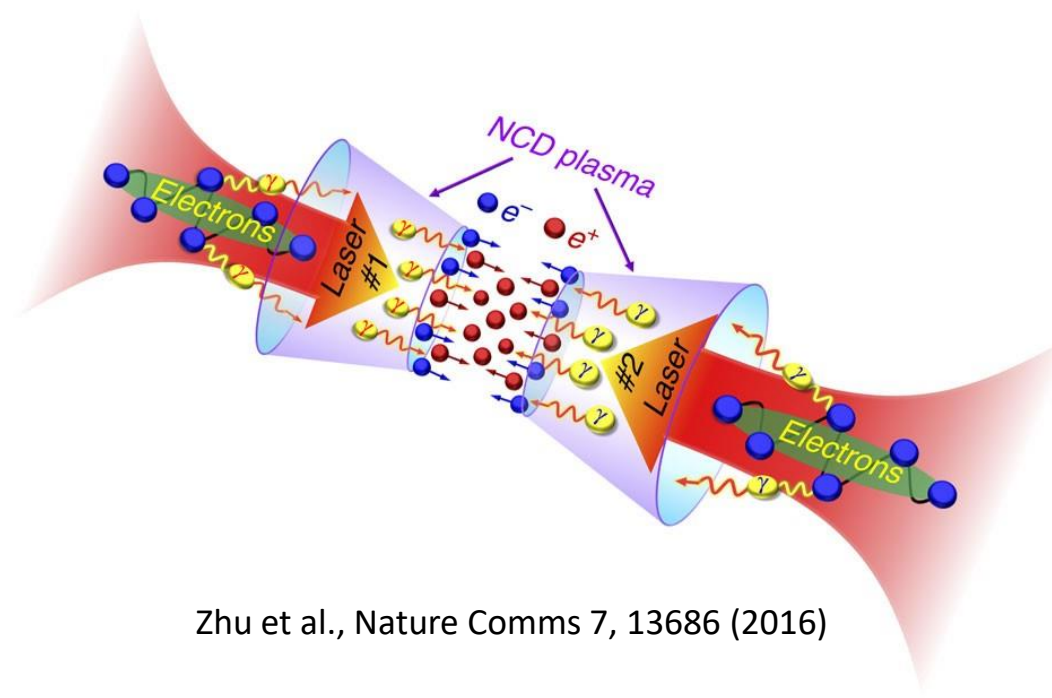
Transparency delayed



Max proton energies still highest for $t_{rsit} \approx 0$

Predictions of GeV electron–positron pairs generated by lasers in near-critical-density plasmas

Various schemes involving NCD plasma have been devised to generate copious electron-positron pair plasmas



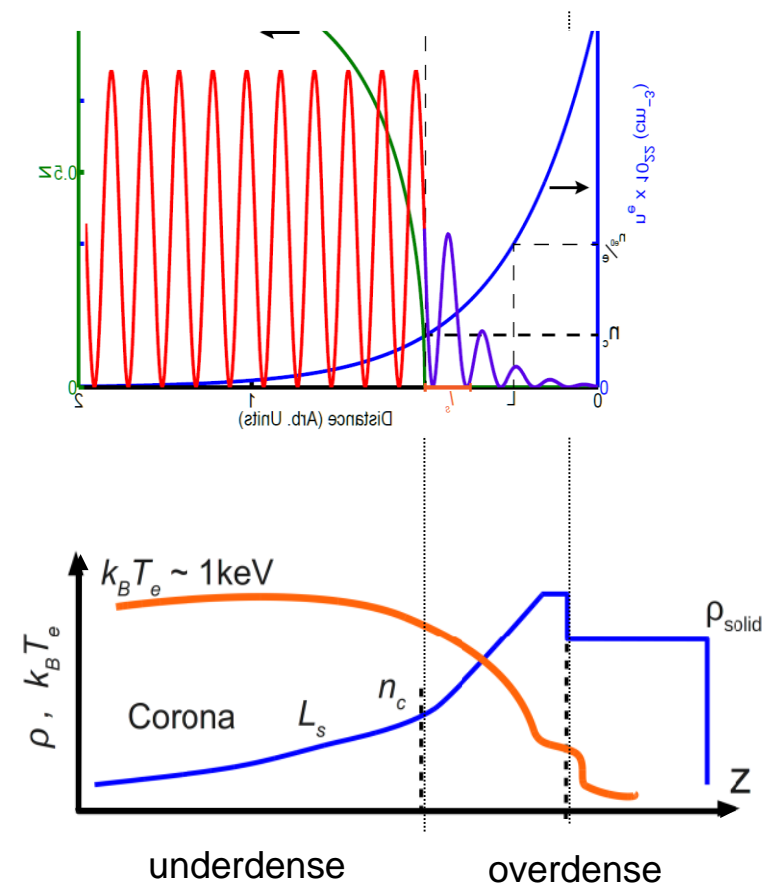
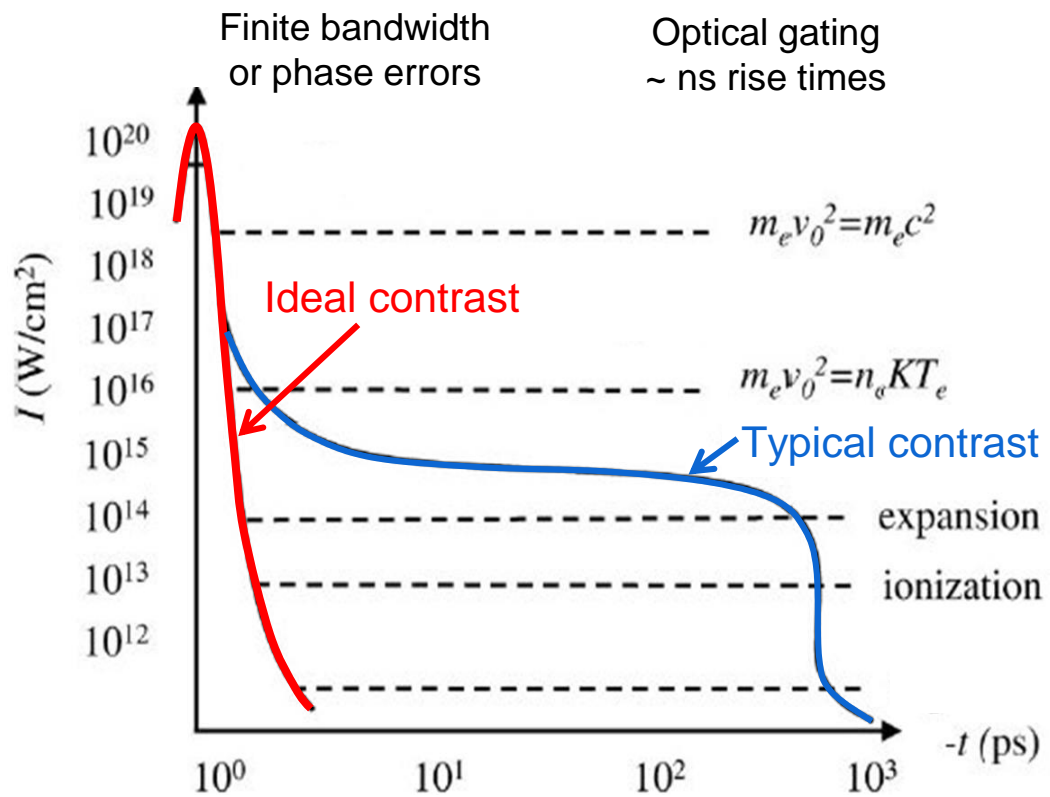
Questions?

Lecture overview:

1. Introduction to high power laser-plasmas
2. Near critical density (NCD) plasma generation
3. Relativistic optics effects in NCD plasma
4. Relativistic plasma aperture
5. Electron and ion acceleration in NCD plasma
6. Strong-field QED phenomena
7. Experimental considerations and methodology

Importance of laser pulse temporal-intensity contrast

Degree of plasma expansion prior to interaction with the main laser pulse depends on the pulse rising edge temporal profile

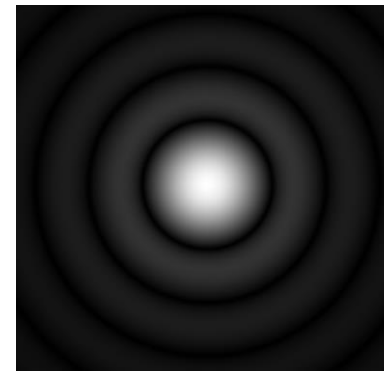


Exponential decrease in plasma density

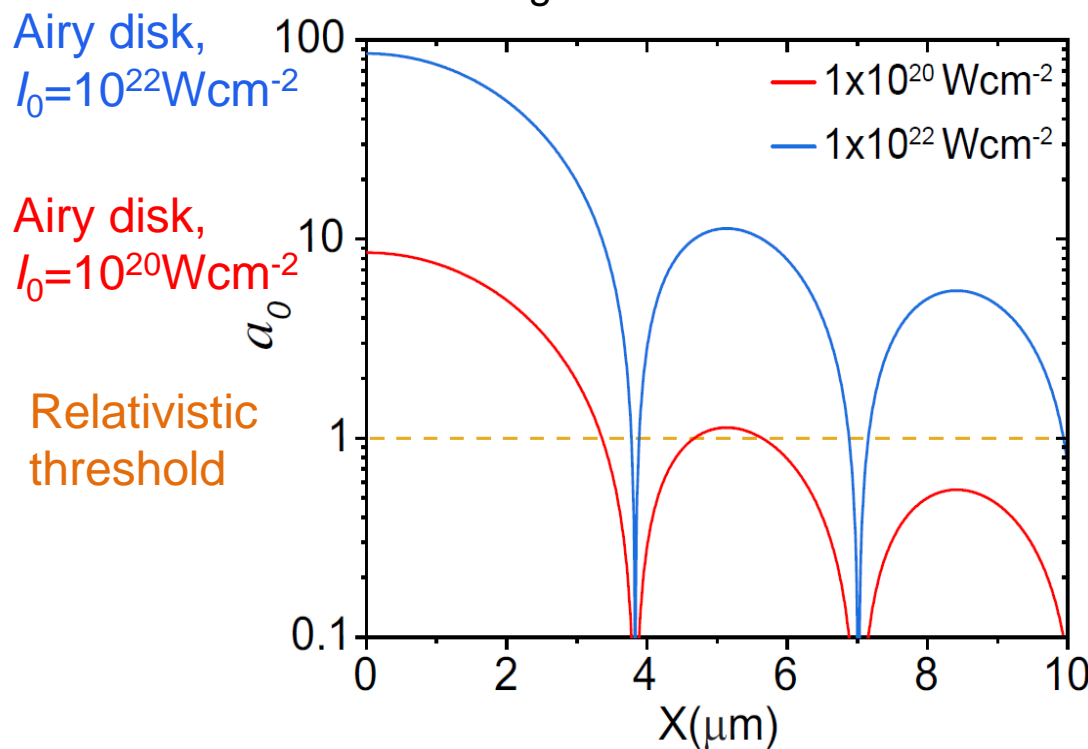
$$n_e(z) = n_0 \exp \left(-\frac{z}{L_s} \right)$$

Importance of laser pulse spatial-intensity contrast

Spatial-intensity contrast ratio: ratio of the intensity in the peak of the laser focal spot to the halo surrounding it (analogous to temporal-intensity contrast)

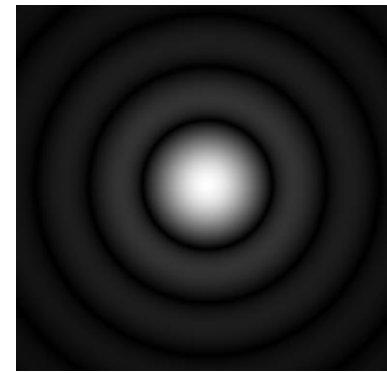
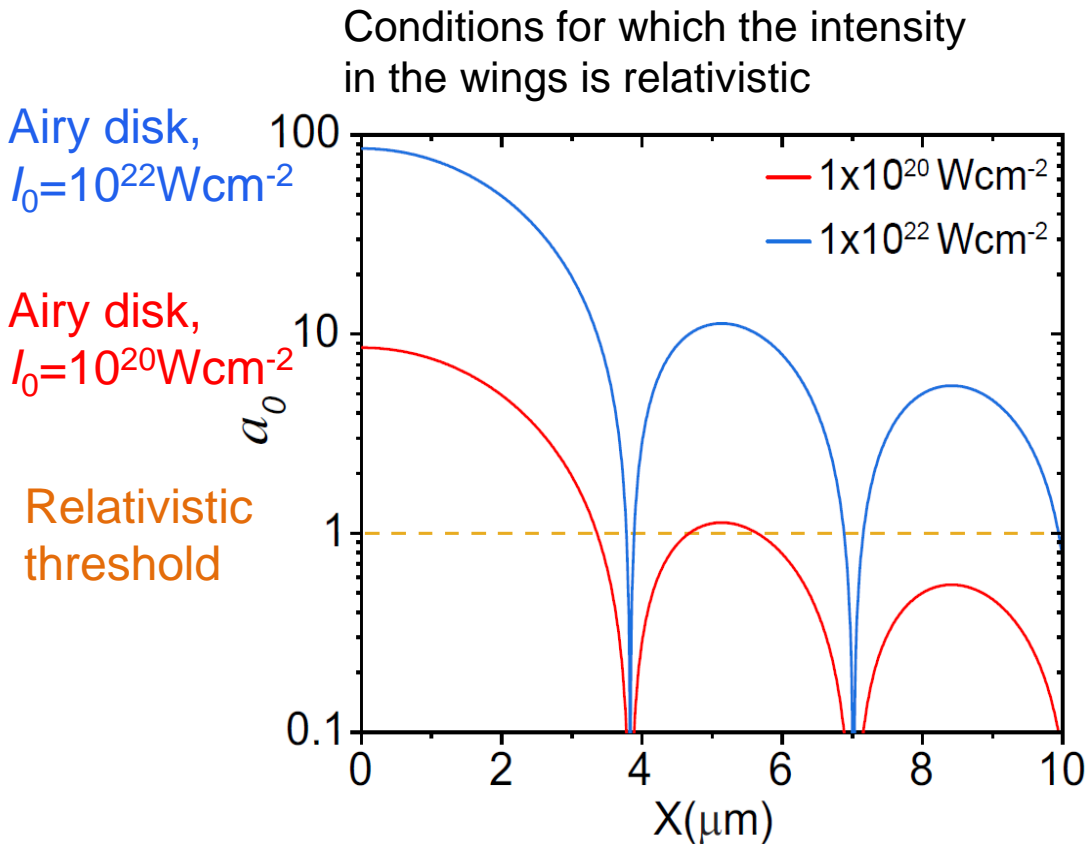


Conditions for which the intensity in the wings is relativistic

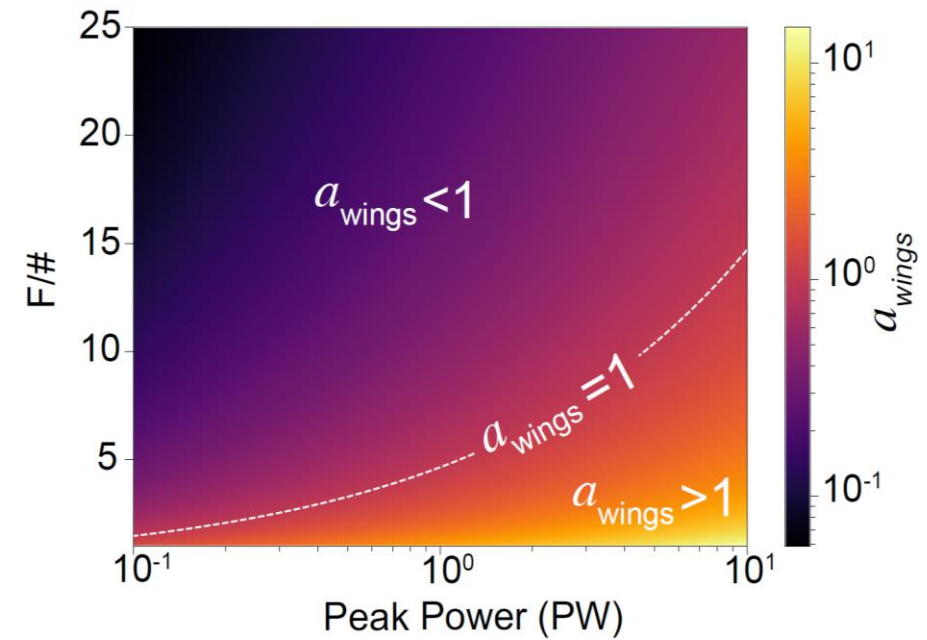


Importance of laser pulse spatial-intensity contrast

Spatial-intensity contrast ratio: ratio of the intensity in the peak of the laser focal spot to the halo surrounding it (analogous to temporal-intensity contrast)

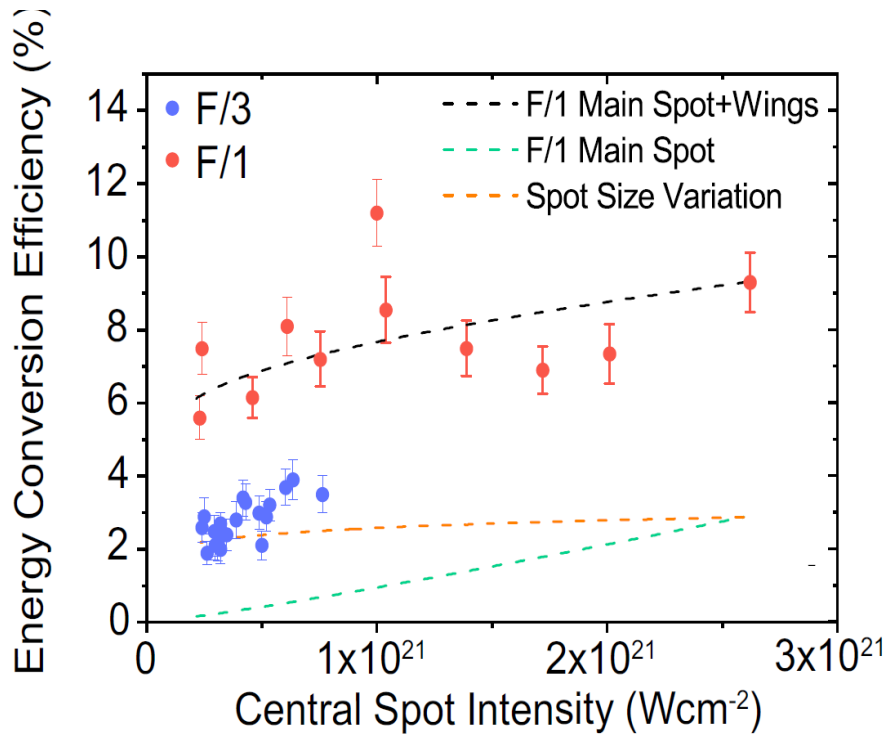


Normalised vector potential of the laser light in the wings, a_{wings} , as a function of laser pulse power and focusing geometry.

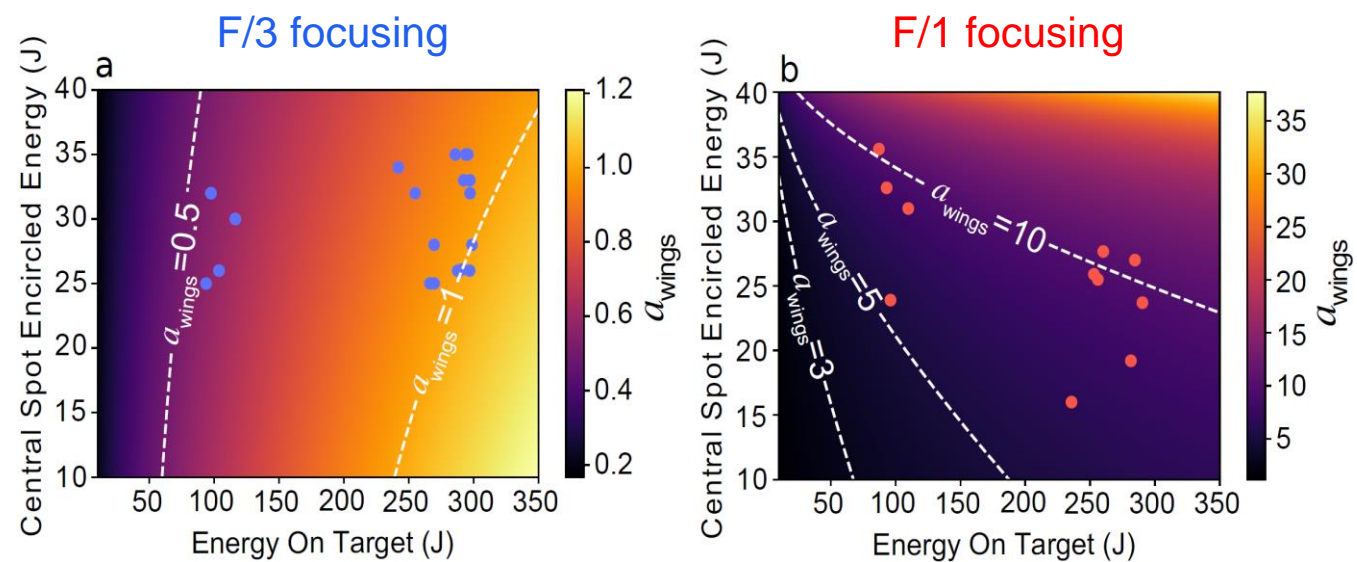


Experiment results on the scaling of TNSA proton beam properties with different focusing geometries

In all cases, 6 μm -thick Al foil targets were irradiated (p-polarization) under F1 or F3 focusing



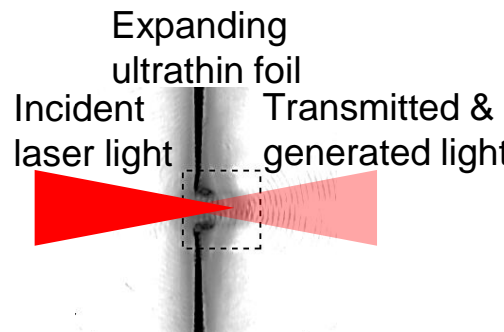
The key differences between F/3 and F/1 focusing are (1) the focal spot size, and (2) the intensity in the wings



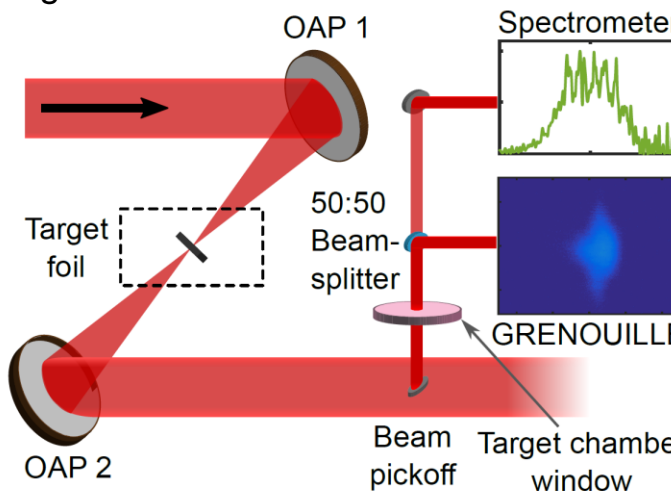
R. Wilson et al., Sci. Rep. 12, 1910 (2022)

Diagnosing the onset time of relativistic self-induced transparency

Experiment using the 40 fs Gemini laser at RAL



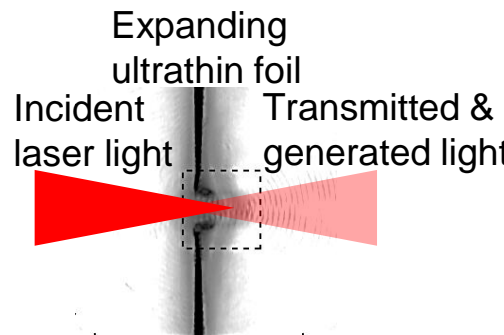
Measuring the temporal-spectral properties of the transmitted laser as diagnostic of RSIT



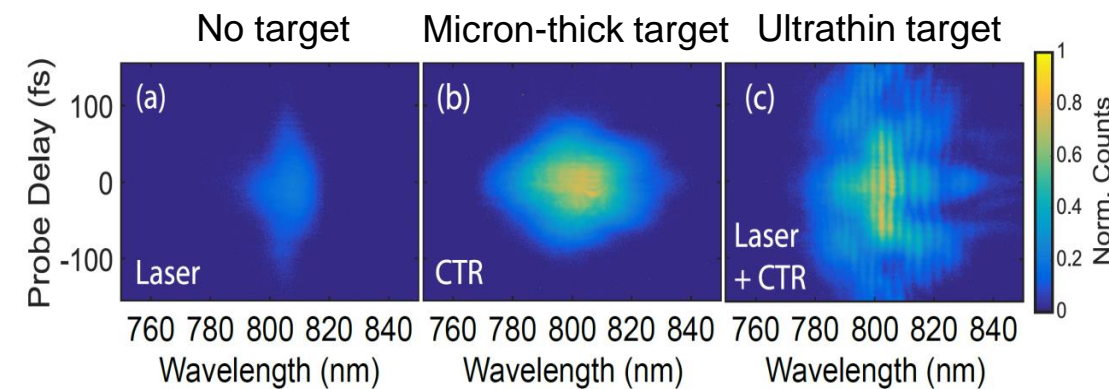
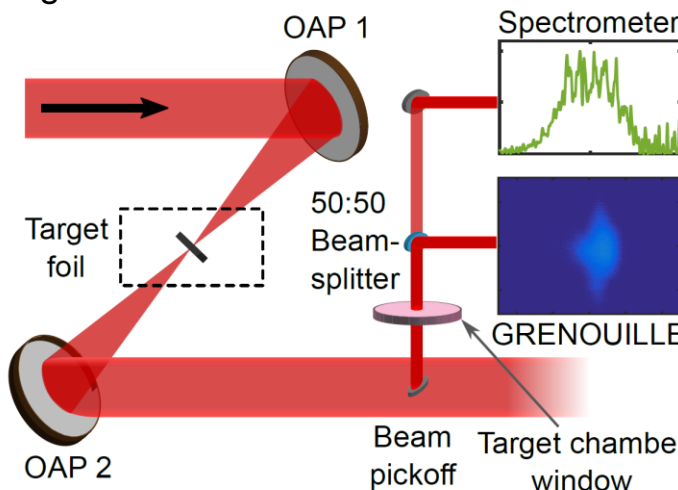
Williamson *et al*, Phys. Rev. Applied 14, 034018 (2020)

Diagnosing the onset time of relativistic self-induced transparency

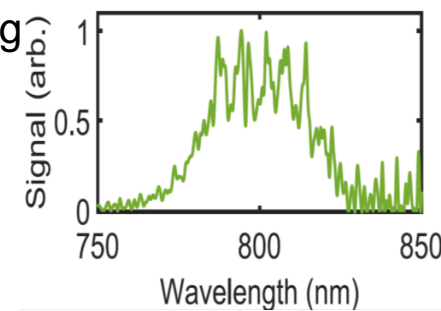
Experiment using the 40 fs Gemini laser at RAL



Measuring the temporal-spectral properties of the transmitted laser as diagnostic of RSIT

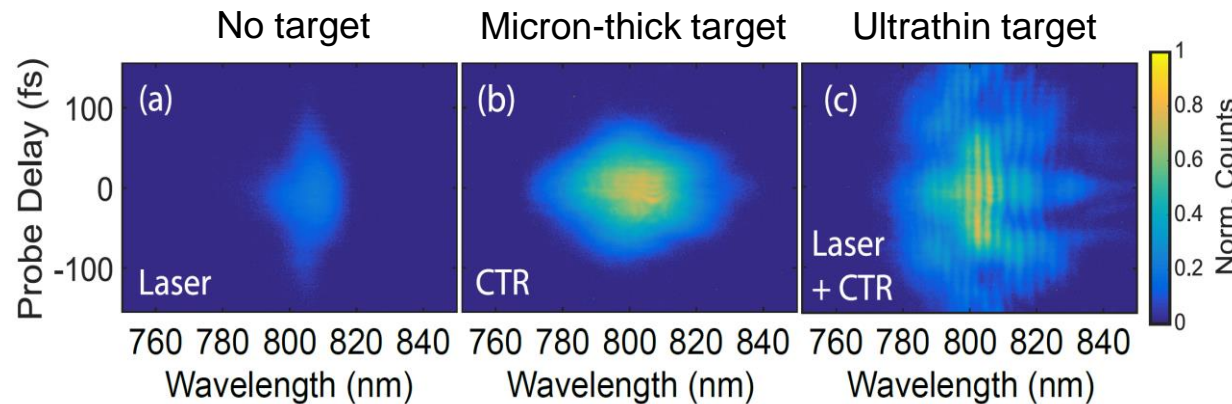


Frequency resolved optical gating (FROG) results and optical spectrum results both indicate there are two pulses in the detected light

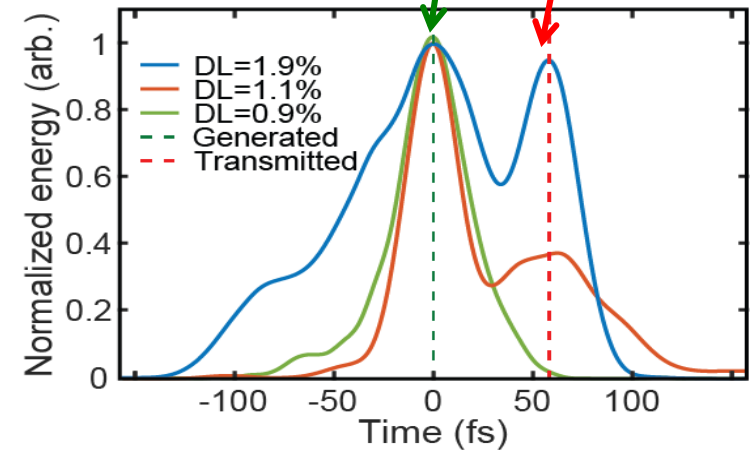
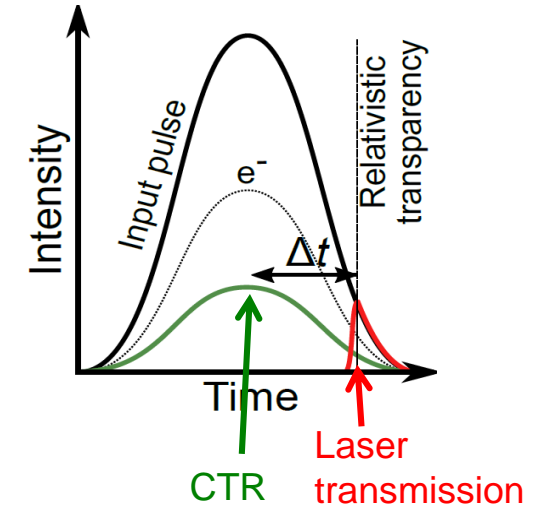
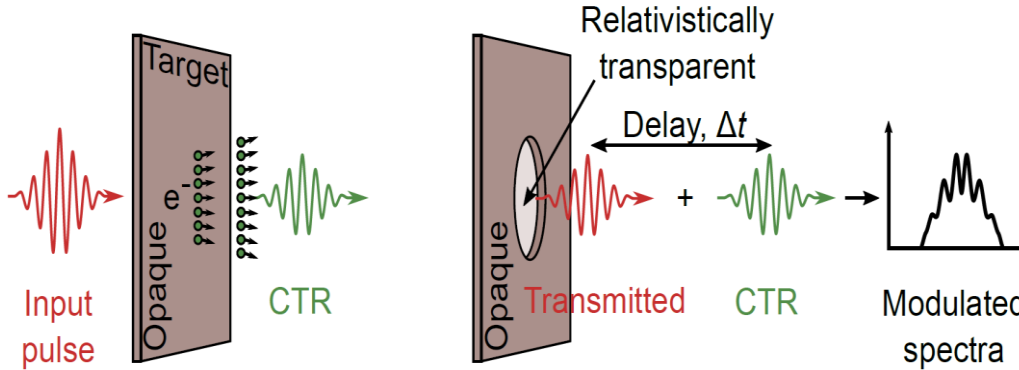
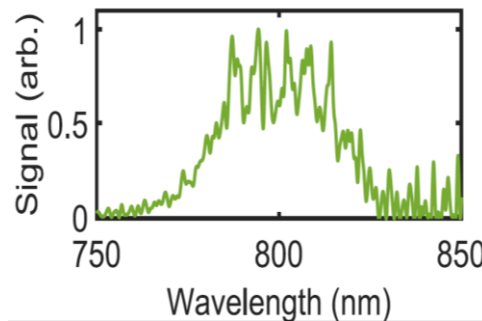


Williamson *et al*, Phys. Rev. Applied 14, 034018 (2020)

Diagnosing the onset time of relativistic self-induced transparency



Frequency resolved optical gating (FROG) results and optical spectrum results both indicate there are two pulses in the detected light

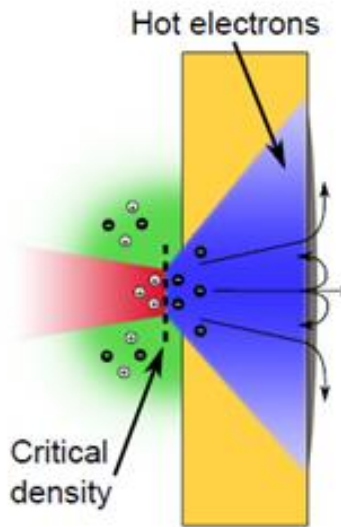


Williamson *et al*, Phys. Rev. Applied 14, 034018 (2020)

New tools for optimising laser-plasma processes

Consider for example laser-driven ion acceleration, which is influenced by:

- **Fast electron temperature and fast electron density and total number** at the rear surface drive proton **spectral** characteristics
- Transport physics defined by **material, target properties and self generated fields** drive proton **spatial** characteristics
- These are sensitive to a wide range of input parameters:



Laser:

- Intensity
- Energy
- Focal spot size
- Laser intensity contrast
- Polarisation
- ...

Plasma:

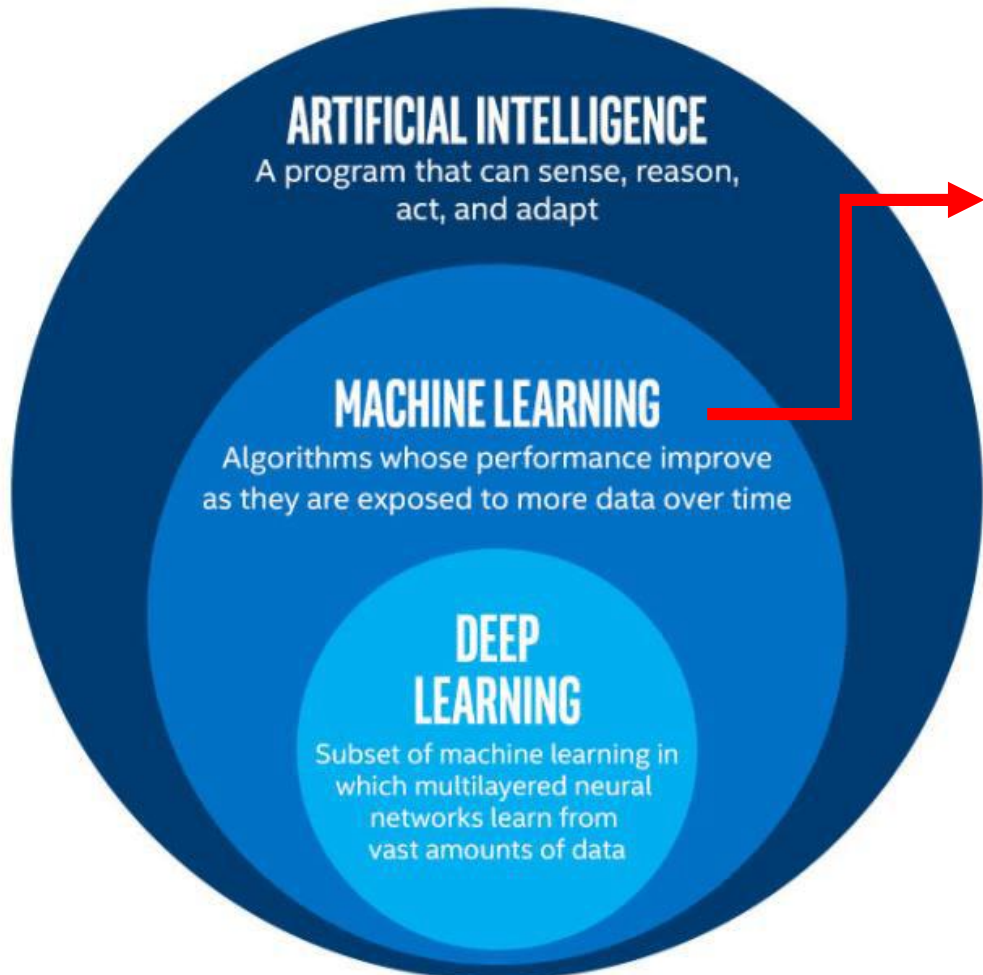
- Energy conversion efficiency
- Fast electron divergence angle
- Z (scattering, resistivity)
- Preplasma scale length
- Incidence angle
- ...



Very quickly this becomes a very high dimensional optimisation problem!

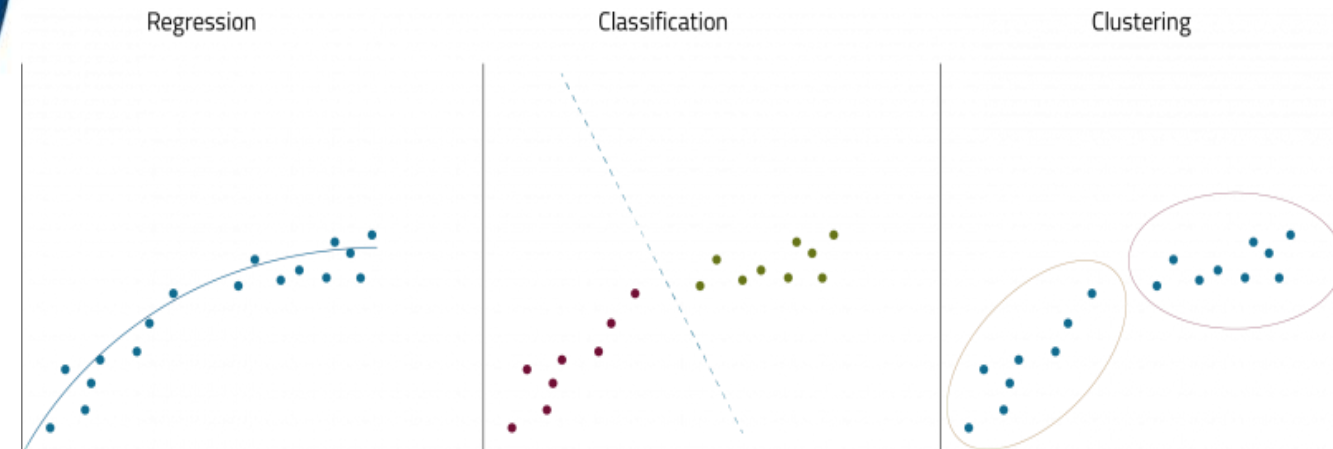
We can use **machine learning** to help

Machine Learning for Laser-Plasma Science

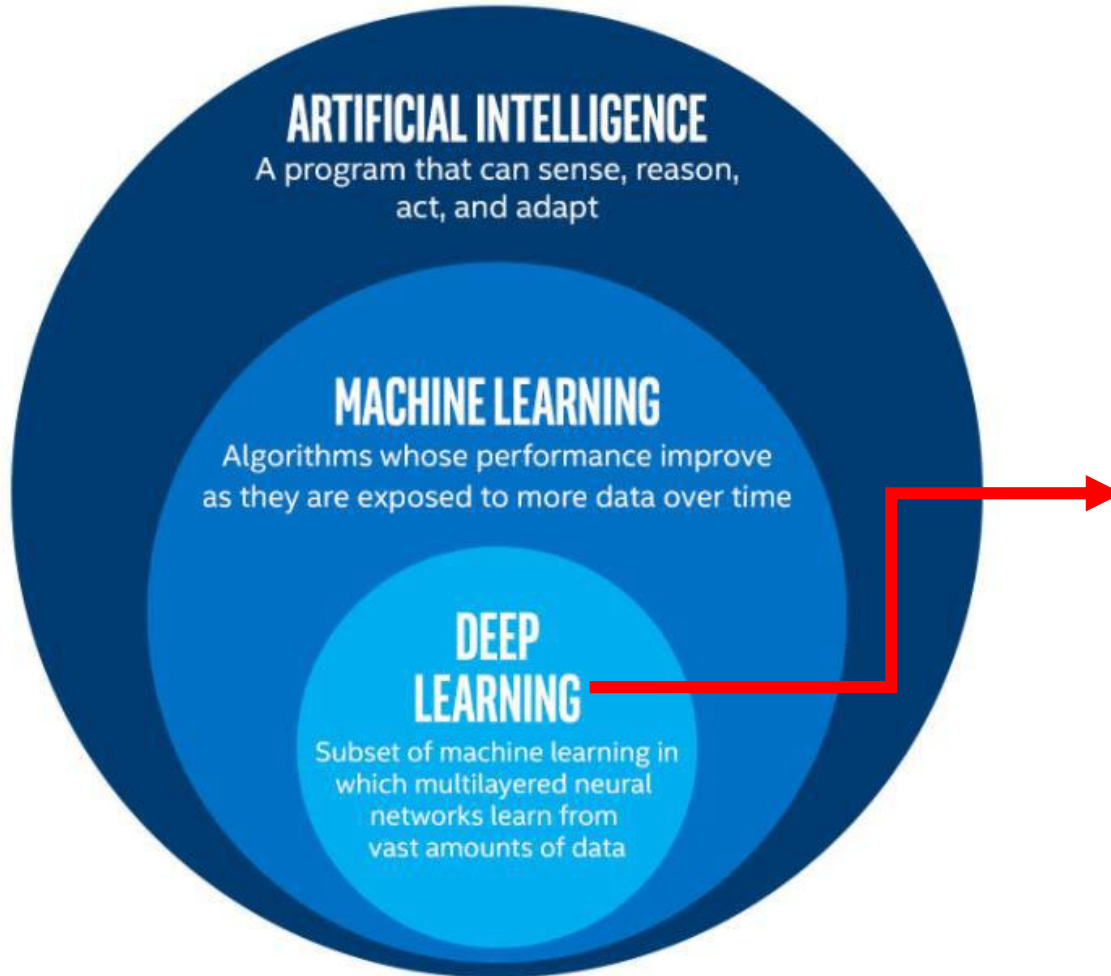


Many different data driven ML algorithms. 3 main types:

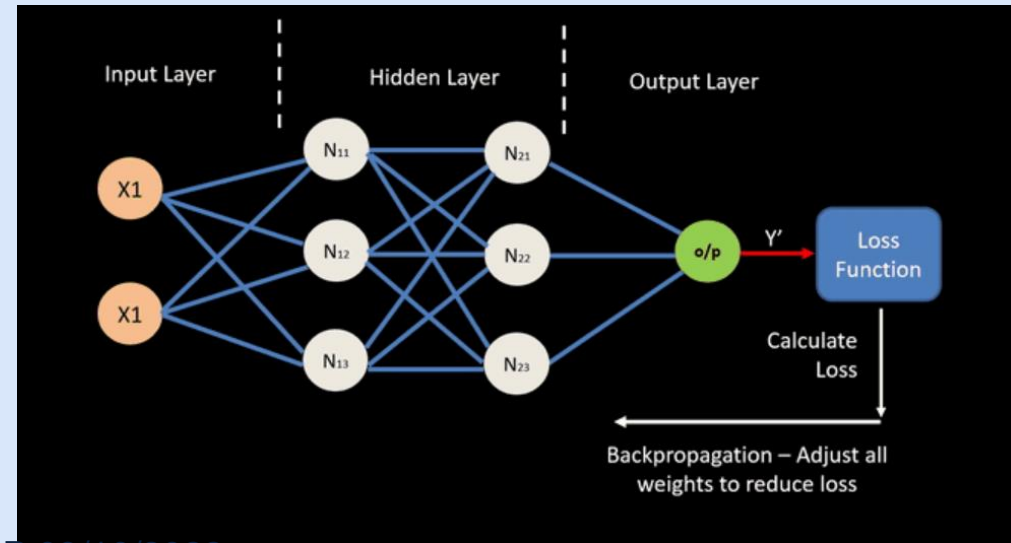
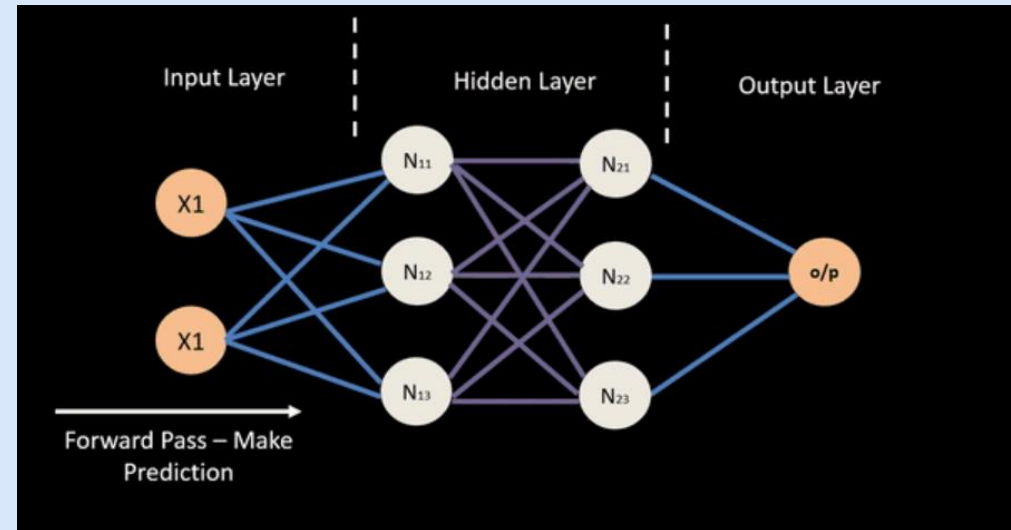
- **Unsupervised learning:** Clustering, k-means, principal component analysis, SVD etc.
- **Supervised Learning:** Classification, Random Forest, Naïve Bayes, Logistic Regression, Linear/non-linear regression etc.
- **Reinforcement Learning:** a machine learning training method based on rewarding desired behaviours and/or punishing undesired ones. Can involve aspects of supervised and unsupervised learning



Machine Learning for Laser-Plasma Science

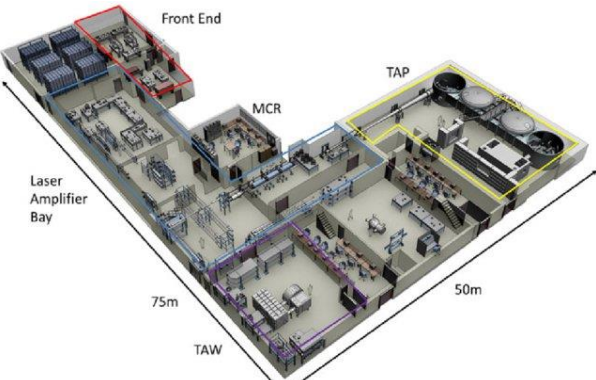


Complex, but a basic deep neural network is:



Why is Machine Learning now a feasible research direction in laser-plasma physics?

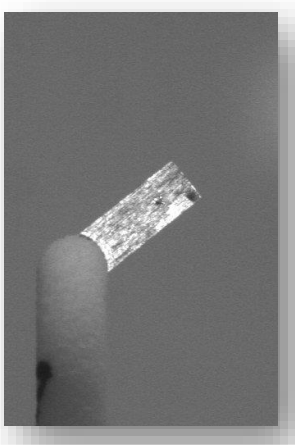
Lasers



1 pulse/ 30 mins

↓
10+ Hz

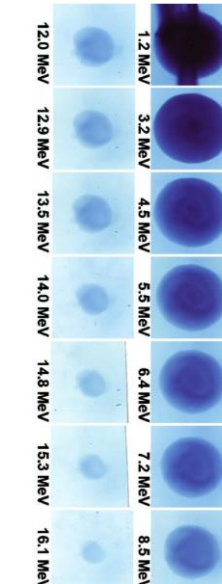
Targets



Hand made targets

↓
Mass manufacture,
tape targets, liquid
targets

Diagnostics



Film based/slow
readout diagnostics

↓
Scintillator based,
10+ Hz readout

Simulations/Computation

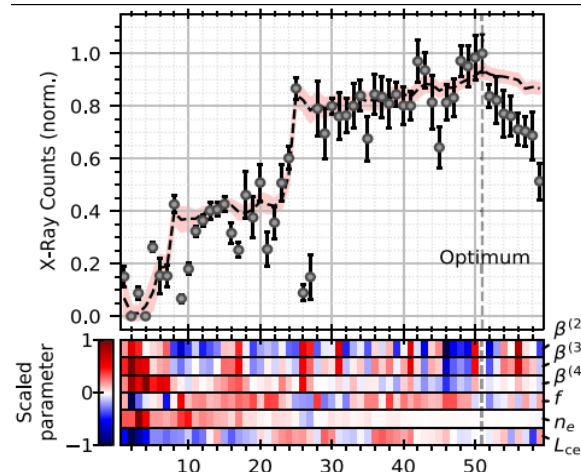


Physics/dimensionally
limited models/limited
access to HPC

↓
Improved, more
efficient models,
wider access to HPC

Machine Learning for Laser-Plasma Science

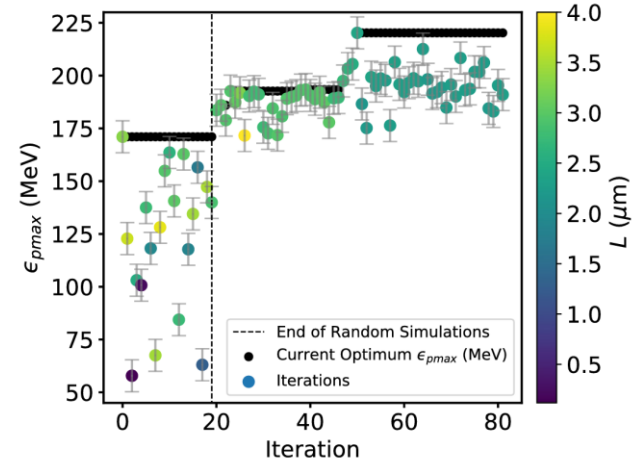
There have been a number of recent results in ML laser-plasma science



R.J Shaloo et al. Nature Comms 11, 6355 (2020)



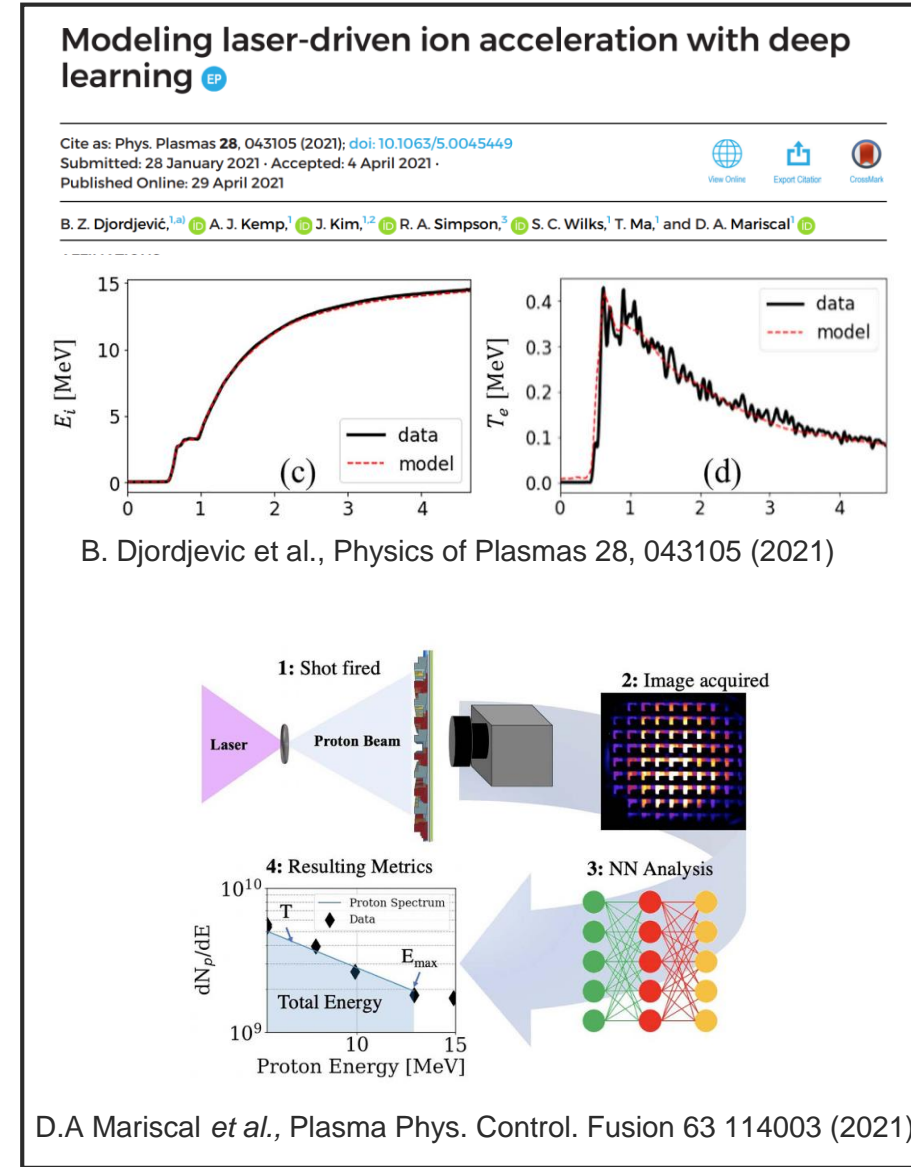
Bayesian Optimisation
using Gaussian
processes in experiments



E.J Dolier et al., New J. Phys. 24 073025 (2022)

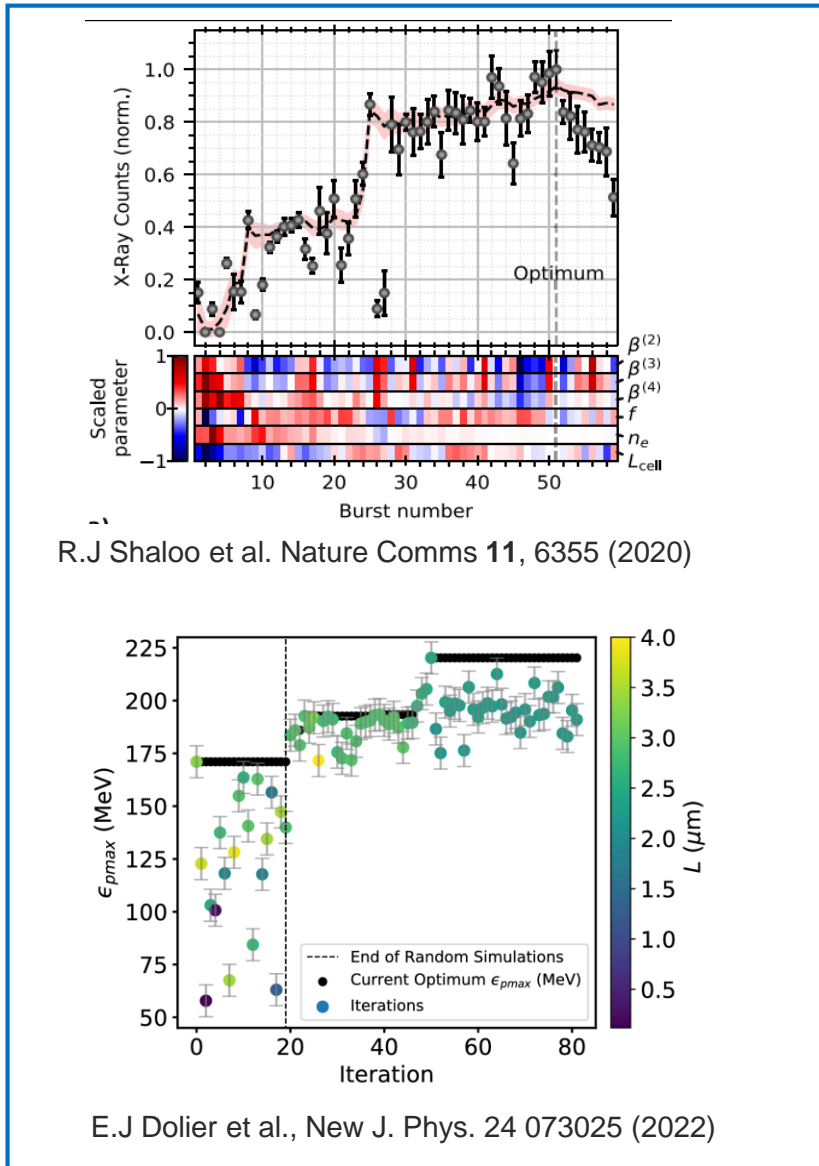


...and simulations

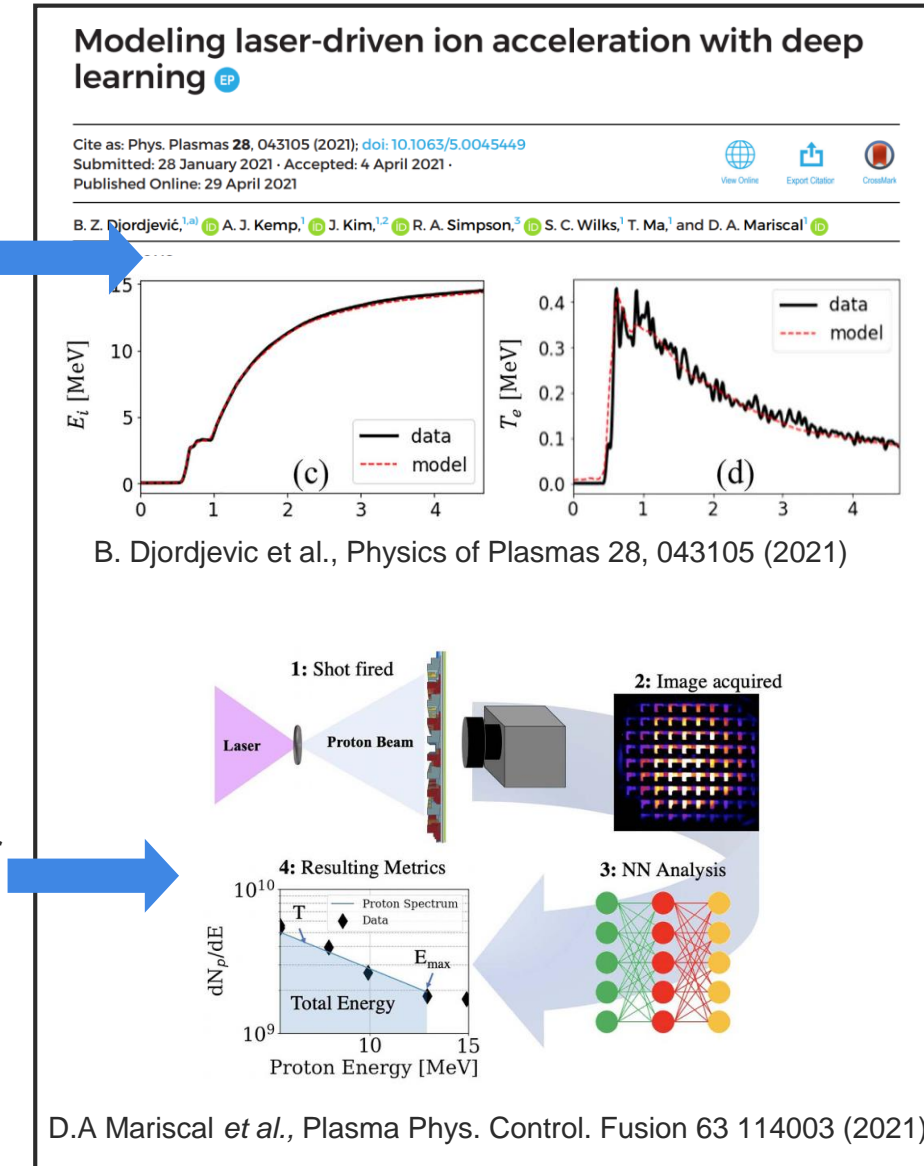


Machine Learning for Laser-Plasma Science

There have been a number of recent results in ML laser-plasma science

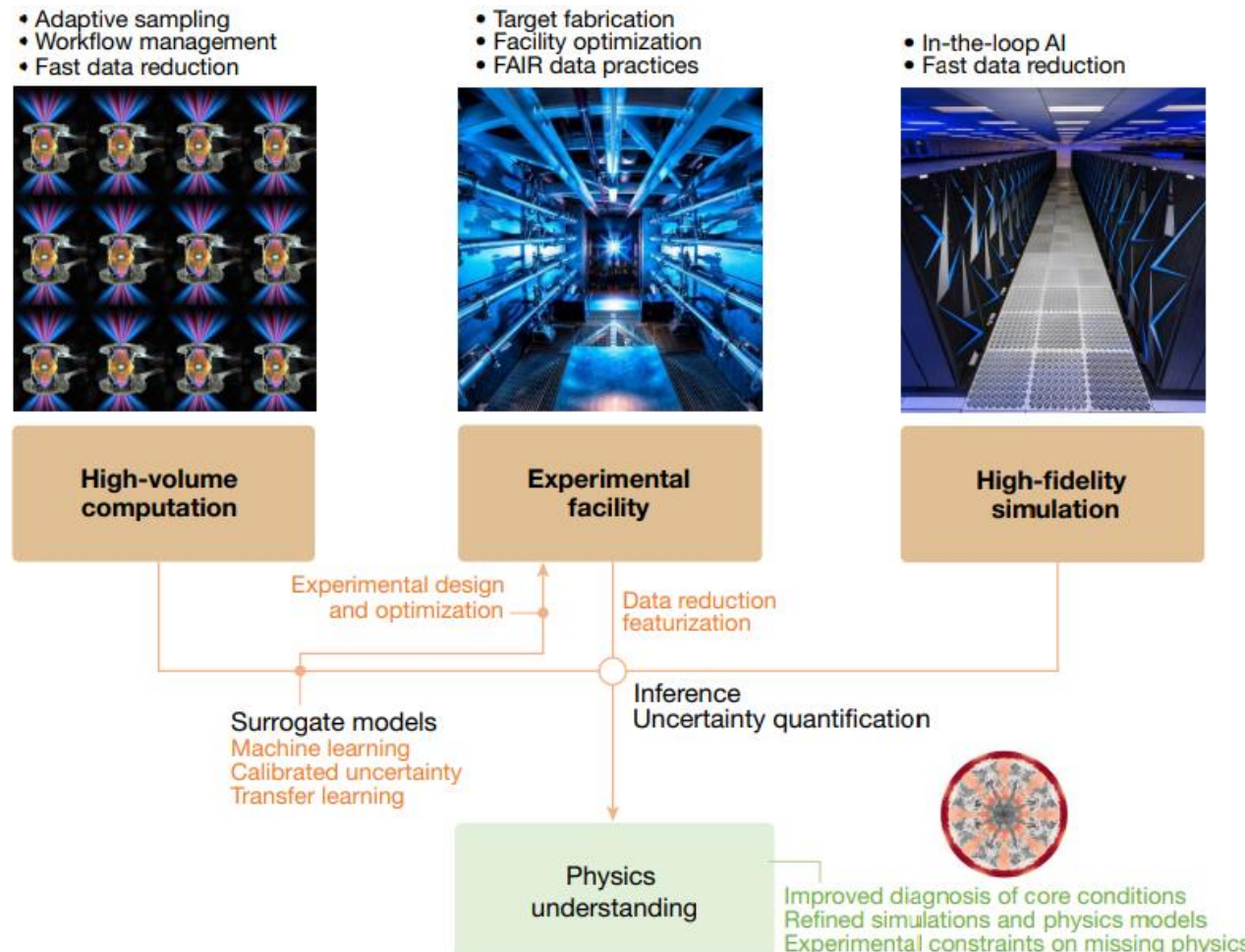


Deep neural networks
trained on simulation data



What is the future of Machine Learning for Laser-Plasma Science?

ML and deep learning enable the rapid integration of different sources of data for improved (and accelerated) physics understanding



Hatfield, P.W., Gaffney, J.A., Anderson, G.J. et al. *Nature* **593**, 351–361 (2021).

Thank you for your attention!

Acknowledgements:

- Contributions from R.J. Gray, M. King, R. Wilson, E. Dolier & J. Goodman (Uni. Strathclyde)
- The Central Laser Facility, UK
- Funding from EPSRC, STFC and Laserlab-Europe